

Research Report  
KTC-06-04/FRT116-02-1F

KENTUCKY  
TRANSPORTATION  
CENTER

*College of Engineering*

BASELINE MODELING OF THE OWENSBORO  
CABLE-STAYED BRIDGE OVER THE OHIO RIVER



UNIVERSITY OF KENTUCKY

**UK**  
**UNIVERSITY OF KENTUCKY**  
**College of Engineering**  
**Kentucky Transportation Center**

***Our Mission***

We provide services to the transportation community through research, technology transfer and education. We create and participate in partnerships to promote safe and effective transportation systems.

***We Value...***

Teamwork -- Listening and Communicating, Along with Courtesy and Respect for Others  
Honesty and Ethical Behavior  
Delivering the Highest Quality Products and Services  
Continuous Improvement in All That We Do

*For more information or a complete publication list, contact us*

**KENTUCKY TRANSPORTATION CENTER**

176 Raymond Building  
University of Kentucky  
Lexington, Kentucky 40506-0281

(859) 257-4513  
(859) 257-1815 (FAX)  
1-800-432-0719  
[www.ktc.uky.edu](http://www.ktc.uky.edu)  
[ktc@engr.uky.edu](mailto:ktc@engr.uky.edu)

*The University of Kentucky is an Equal Opportunity Organization*

Research Report  
KTC-06-04/FRT116-02-1F

# BASELINE MODELING OF THE OWENSBORO CABLE-STAYED BRIDGE OVER THE OHIO RIVER

by

**Jindong Hu**

Visiting Professor, Kentucky Transportation Center

**Issam E. Harik**

Professor of Civil Engineering and Head, Structures Section,  
Kentucky Transportation Center

**Suzanne Weaver Smith**

Associate Professor, Department of Mechanical Engineering

**Jeff Gagel**

Graduate Student, Department of Mechanical Engineering

**Jennie E. Campbell**

Graduate Student, Department of Mechanical Engineering

and

**R. Clark Graves**

Associate Program Manager, Pavements Section, Kentucky Transportation Center

Kentucky Transportation Center  
College of Engineering, University of Kentucky

In cooperation with

Transportation Cabinet  
Commonwealth of Kentucky

and

Federal Highway Administration  
U.S. Department of Transportation

The contents of this report reflect the views of the authors who are responsible for the facts and accuracy of the data presented herein. The contents do not necessarily reflect the official views or policies of the University of Kentucky, the Kentucky Transportation Cabinet, nor the Federal Highway Administration. This report does not constitute a standard, specification or regulation. The inclusions of manufacturer or trade names are for identification purposes and are not to be considered as endorsement.

March 2006

**Technical Report Documentation Page**

<b>1. Report No.</b> KTC-06-04/FRT116-02-1F	<b>2. Government Accession No.</b>	<b>3. Recipient's Catalog No.</b>	
<b>4. Title and Subtitle</b>  <p align="center"><b>BASELINE MODELING OF THE OWENSBORO CABLE-STAYED BRIDGE OVER THE OHIO RIVER</b></p>		<b>5. Report Date</b> March 2006	
		<b>6. Performing Organization Code</b>	
		<b>8. Performing Organization Report No.</b> KTC-06-04/FRT116-02-1F	
<b>7. Author(s):</b> J.D. Hu, Issam E. Harik, S.W. Smith, J. Gagel, J.E. Campbell and R.C. Graves		<b>10. Work Unit No. (TRAI5)</b>	
<b>9. Performing Organization Name and Address</b>  Kentucky Transportation Center College of Engineering University of Kentucky Lexington, Kentucky 40506-0281		<b>11. Contract or Grant No.</b> FRT116	
		<b>13. Type of Report and Period Covered</b>  Final	
		<b>14. Sponsoring Agency Code</b>	
<b>12. Sponsoring Agency Name and Address</b>  Kentucky Transportation Cabinet State Office Building Frankfort, Kentucky 40622		<b>15. Supplementary Notes</b> Prepared in cooperation with the Kentucky Transportation Cabinet and the U.S. Department of Transportation, Federal Highway Administration.	
<b>16. Abstract</b>  This report presents the baseline modeling of the Owensboro cable-stayed bridge which connects Owensboro, Kentucky and Rockport, Indiana over the Ohio River. The objective of this study is to establish the bridge baseline model via the dynamics-based technique and finite element method. The scope of research includes finite element modeling and modal analysis, field free vibration testing, finite element model calibration using field test results, and cable dynamic testing and modeling. It is demonstrated that a cable-stayed bridge is a highly pre-stressed structure. The stress stiffening of cable elements plays an important role in both static and dynamic analysis. The large deflection analysis has shown that large deflection has the limited effect on the member deflections. Dominate dynamic response modes in the low frequency range contain vertical and transverse directions. The free vibration modes of the bridge are complicated and coupled. A good agreement of frequencies has been found between finite element modeling and in field free vibration testing after calibrating the finite element model. But, the better matching for higher modes is not expected and not realistic, as the experimental model properties of the bridge come from the output-only measurement. The calibrated finite element model may be used as a baseline in the future structural analysis and monitoring of the Owensboro cable-stayed bridge.			
<b>17. Key Words</b> Cable-stayed bridge; Finite element model; Modal analysis; Free vibration testing; Natural frequency; Baseline model; Cable model; Kentucky.		<b>18. Distribution Statement</b> Unlimited with approval of Kentucky Transportation Cabinet	
<b>19. Security Classif. (of this report)</b> Unclassified	<b>20. Security Classif. (of this page)</b> Unclassified	<b>21. No. of Pages</b> 139	<b>22. Price</b>

# **EXECUTIVE SUMMARY**

## **Research Objectives**

Owensboro cable-stayed bridge, dedicated as the William H. Natcher Bridge, connects Owensboro (Daviess County), Kentucky and Rockport (Spencer County), Indiana over the Ohio River as seen in the photographs in Figures 1.1 and 1.2. The bridge was officially opened to traffic on October 21, 2002. The objective of this investigation is to analyze the dynamic characteristics of the bridge and establish a finite element model as a baseline in the structural analysis and monitoring of the Owensboro cable-stayed bridge.

To achieve the objective, this study contains the following four tasks:

- 1) On-site ambient vibration testing;
- 2) Finite element modeling and modal analysis;
- 3) Finite element model updating (calibration) using field test results;
- 4) Cable testing and modeling.

## **Background**

Cable-stayed bridges have become one of the most frequently used bridge systems throughout the world because of their aesthetic appeal, structural efficiency, enhanced stiffness compared with suspension bridges, ease of construction and small size of substructures. Over the past 40 years, rapid developments have been made on modern cable-stayed bridges. With the main span length increasing, more shallow and slender stiffness girders used in modern cable-stayed bridges, the safety of the whole bridge under service loadings and environmental dynamic loadings, such as impact, wind and earthquake loadings, presents increasingly important concerns in design, construction and service. It has become essential to synthetically understand and realistically predict their response to these loadings. The unique structural styles of cable-stayed bridges make the

span length longer and beautify the environment, but also add to the difficulties in accurate structural analysis. It is known that these long span and cable-stayed bridges constitute complex structural components with high geometric nonlinearity. In addition, the initial equilibrium configuration under dead loads has a significant effect on the structural behavior of cable-stayed bridges.

The discretized finite element method provides a convenient and reliable idealization of the structural continua and is particularly effective when using digital-computer analyses. The finite deformation theory with a discrete finite element model is the most powerful tool used in the nonlinear analysis of modern cable-stayed bridges. However, it is not an easy task to establish a real and reliable finite element model of such complex structures. The process requires the combination of the bridge field testing and analysis. The initial finite element model has to be updated or calibrated by the field test results.

## **Field Free Vibration Testing**

On-site dynamic testing of a bridge provides an accurate and reliable description of its dynamic characteristics. Matching the actual dynamic characteristics of bridges has become an integral part of dynamics-based structure evaluation in order to eliminate the uncertainties and assumptions involved in analytical modeling. The current dynamic characteristics (frequencies and mode shapes) of the Owensboro cable-stayed bridge were obtained from the field free vibration test results under the excitation due to running the loaded trucks. These dynamic characteristics were subsequently used as the basis for calibrating the finite element model to establish a baseline for the bridge.

## **Finite Element Modeling and Calibration**

A three-dimensional finite element model was constructed in the ANSYS, one of the most powerful engineering design and analysis commercial software packages. The established finite element model is then used to conduct both static and dynamic analysis

of the Owensboro cable-stayed bridge. Starting from the deformed equilibrium configuration, the modal analysis is performed. The modal analysis of the cable-stayed bridge is therefore a “pre-stressed” modal analysis. All possible frequencies and mode shapes can be calculated.

One of the advantages of finite element modeling and analysis is that parametric studies can be performed. The structural and material parameters that affect the modal properties of the bridge can be identified from such parametric studies. From the parametric studies, it is found that the key parameters affecting the vertical modal properties are the mass, cable sectional area, cable elastic modulus and deck vertical bending stiffness. The key parameters affecting the transverse and torsion modal properties are the mass, cable sectional area, cable elastic modulus and deck lateral bending stiffness. The parametric studies reported here not only prove the efficiency of the finite element methodology, but also demonstrate the variation in modal response caused by a variation in the input parameters.

Finite element model calibration was then carried out by adjusting its structural or material parameters, which affect the modal properties of the bridge, such that the FEM predicted frequencies and mode shape match the experimentally observed frequencies and mode shapes. The first eight frequencies determined through free vibration measurements in the system identified modes and FEM predictions are summarized in Tables E-1. This table shows that good agreement exist between the experimental and calibrated analytical results.

## **Cable Testing and Modeling**

Cable testing and modeling for the Owensboro Bridge included the following accomplishments:

- Two field tests of the cables were conducted (on October 15-16, 2002 and August 4-5, 2003), including tests with loaded trucks and with ambient (typical traffic and wind) excitation. Tests were conducted over a range of temperatures.

- Finite element models for the cables were developed using the as-built cable properties. Models included a set of twelve cables.
- Comparison of finite-element model results to field test results showed good correlation.

Notable results include the following:

- Field measurement of all cables can be performed in approximately 1.5 days using short time records and Cepstrum signal processing techniques. Periodic monitoring may be useful for the cables of the Owensboro bridge to understand tension changes as the bridge is in use.
- Field tests of the cables on both occasions resulted in consistent fundamental frequencies.
- Excessive motion of the cable cross ties (restrainers) was observed during both field tests. This raises concerns suggesting close inspection of the cross ties in case fatigue becomes a problem.
- No model refinement for the cable models was required for good correlation between model and field test results.

**Table E-1** Comparison of Frequencies

Mode	Test (Hz)	FE Model (Hz)	Mode classification
1	0.301667	0.293403	Vertical
2	0.388333	0.373609	Vertical
3	-	0.524643	Transverse + Torsion
4	0.601667	0.578998	Vertical
5	0.696667	0.675054	Vertical; Torsion for FEM
6	-	0.685296	Transverse + Torsion
7	0.74	0.710348	Vertical
8	-	0.758056	Torsion
9	-	0.766625	Transverse + Torsion
10	-	0.808145	Tower Sway + Torsion
11	-	0.816315	Tower Sway + Torsion
12	0.818333	0.821629	Vertical

## Conclusions and Recommendations

On site free vibration testing provides a fast way to obtain the real dynamic properties of a structure. The peak picking identification is very fast and efficient since no model has to be fitted to the data. For real applications, the peak picking method could be used on site to verify the quality of the measurements. But the mode shapes for the transverse direction did not match well since the bridge is very stiff in the transverse direction and the transverse excitation data could not be filtered from the noise data.

A good agreement of frequencies has been found between the results of the calibrated finite element model and in *situ* free vibration testing results. The identified frequencies from the high-speed measurements are quite stable. The better matching for higher modes is not expected and not realistic either, as the experimental modal properties of the bridge come from the output-only measurement. The calibrated finite element model may be used as a baseline in the future structural analysis and monitoring of the Owensboro cable-stayed bridge.

Related to cable modeling and testing, we conclude the following: 1) as-built information on the cable construction was used to develop verified finite-element models of the 96 cables which can be used as a baseline for future evaluation of cable stiffness and structural integrity, 2) field-survey testing of all cables can be accomplished with ambient (traffic) excitation in 1.5 days, so periodic monitoring of the cables is possible without permanent installation of a measurement system, 3) Excessive motion of the cable cross ties (restrainers) was observed during both field tests. This raises concerns suggesting close inspection of the cross ties in case fatigue becomes a problem and 4) periodic measurement of the cable response is recommended to monitor the continuing effectiveness of the restrainers and structural integrity of the cables.

## **ACKNOWLEDGEMENTS**

The financial support for this project was provided by the Kentucky Transportation Cabinet and Federal Highway Administration. The assistance of the staff in the Pavement Section in the Kentucky Transportation Center in coordinating and conducting the bridge testing is especially noteworthy. The authors are also grateful to the assistance provided by the engineers and the staff in Kentucky Highway District 9.

# TABLE OF CONTENTS

<b>EXECUTIVE SUMMARY.....</b>	<b>i</b>
<b>ACKNOWLEDGEMENTS.....</b>	<b>vi</b>
<b>TABLE OF CONTENTS.....</b>	<b>vii</b>
<b>LIST OF TABLES.....</b>	<b>ix</b>
<b>LIST OF FIGURES.....</b>	<b>x</b>
<b>1. INTRODUCTION</b>	
1.1. General.....	1
1.2. Bridge Description.....	3
1.3. On-Site Dynamic Testing.....	6
1.4. Finite Element Modeling and Calibration.....	7
1.5. Cable Testing and Modeling.....	9
1.6. Scope of Work.....	9
<b>2. FIELD DYNAMIC TESTING</b>	
2.1. General.....	11
2.2. Output-Only Dynamic Testing.....	13
2.3. Peak Picking (PP) System Identification.....	16
2.4. Remarks.....	21
<b>3. FINITE ELEMENT MODELING AND CALIBRATION</b>	
3.1. General.....	23
3.2. Initial Finite Element Model.....	26
3.3. Static Analysis under Dead Load.....	44
3.4. Modal Analysis.....	50
3.5. Parametric Studies.....	66
3.6. Finite Element Model Calibration.....	76
3.7. Remarks.....	82

**4. CABLE TESTING AND MODELING**

4.1. General.....86  
4.2. Field Testing of the Owensboro Bridge Stay Cables.....89  
4.3. Finite Element Analysis.....100  
4.4. Remarks.....113

**5. CONCLUSIONS AND RECOMMENDATIONS**

5.1. General.....115  
5.2. Finite Element Modeling and Dynamic Properties.....115  
5.3. Free Vibration Testing and Model Calibration.....117  
5.4. Cable Testing and Modeling.....117

**REFERENCES.....119**

## LIST OF TABLES

<b>Table No.</b>	<b>Description</b>	<b>Page No.</b>
E-1	Comparison of Frequencies	iv
2.1	Instrumentation Per Setup	16
2.2	Possible Frequencies for Testing (Hz)	20
2.3	Summary of Identified Frequencies (Hz)	21
3.1	Member Details Extracted from the Plan	27
3.2	Preliminary Material Properties	32
3.3	Preliminary Real Constants	33
3.4	Material Properties	36
3.5	Real Constants	37
3.6	Details of the Model	39
3.7	Initial Tension Forces in the Cables	45
3.8	Comparison of Maximum Deflections (absolute value, ft)	50
3.9	Comparison of Frequencies (Hz)	52
3.10	Natural Frequencies (Hz) and Mass Fraction	54
3.11	Natural Frequencies (Hz) and Participation Factors	54
3.12	Frequencies (Hz) for Different Deck Mass Densities	67
3.13	Frequencies (Hz) for Different Cable Areas	69
3.14	Frequencies (Hz) for Different Cable Moduli	71
3.15	Frequencies (Hz) for Different Deck Vertical Stiffness	73
3.16	Frequencies (Hz) for Different Lateral Deck Stiffness	75
3.17	Calibrated Real Constants	77
3.18	Calibrated Material Properties	79
3.19	Comparison of Frequencies	80
4.1	Cable Geometry and Material Properties of Upstream Cables 1-12	102
4.2	Finite Element Model Fundamental Frequency Results Compared with Test Frequencies and String Model Frequencies	103
4.3	Cable Geometry and Material Properties for Upstream Cables 1-48	106
4.4	Cable Geometry and Material Properties for Downstream Cables 1-24	107
4.5	Tension Adjustments for Model Correlation of Upstream Cables 1-12	111
4.6	Downstream Cable Frequency Results	111
4.7	Upstream Cable Frequency Results	112

## LIST OF FIGURES

<b>Fig. No.</b>	<b>Description</b>	<b>Page No.</b>
1.1	Aerial View of the Owensboro Cable-Stayed Bridge	4
1.2	Side View of the Owensboro Cable-Stayed Bridge	5
1.3	Plan and Elevation of the Owensboro Cable-Stayed Bridge	6
2.1	Measurement Instrumentation Plan	15
2.2	Typical Acceleration Time Histories	15
2.3	Full Data Averaged Vertical Response Spectra	19
2.4	Full Data Averaged Longitudinal Response Spectra	20
2.5	First Vertical Mode Shape of Owensboro Bridge ( $f = 0.301667$ Hz)	21
3.1	BEAM4 3-D Elastic Beam Element	28
3.2	3-D Tension-only Truss Element	30
3.3	Elevation of Finite Element Model	40
3.4	Plan of Finite Element Model	41
3.5	Isotropic Elevation of Finite Element Model	43
3.6	1st Mode Shape ( $f = 0.2934$ Hz, Vertical)	56
3.7	2nd Mode Shape ( $f = 0.3736$ Hz, Vertical)	57
3.8	3rd Mode Shape ( $f = 0.5246$ Hz, Transverse + Torsion)	58
3.9	4th Mode Shape ( $f = 0.5790$ Hz, Vertical)	59
3.10	5th Mode Shape ( $f = 0.6751$ Hz, Torsion)	60
3.11	6th Mode Shape ( $f = 0.6853$ Hz, Transverse + Torsion)	61
3.12	7th Mode Shape ( $f = 0.7103$ Hz, Vertical)	62
3.13	8th Mode Shape ( $f = 0.758$ Hz, Torsion)	63
3.14	9th Mode Shape ( $f = 0.7666$ Hz, Transverse + Torsion)	64
3.15	10th Mode Shape ( $f = 0.8081$ Hz, Tower Sway + Torsion)	65
3.16	Frequencies <i>vs</i> Deck Mass Density	68
3.17	Frequencies <i>vs</i> Cable Section Area	70
3.18	Frequencies <i>vs</i> Cable Elastic Modulus	72
3.19	Frequencies <i>vs</i> Deck Vertical Bending Stiffness	74
3.20	Frequencies <i>vs</i> Deck Lateral Bending Stiffness	76
3.21	Comparison of First Vertical Mode Shape	81
3.22	Comparison of Second Vertical Mode Shape	82
4.1	Aerial and Approach Views of the Owensboro Bridge	88
4.2	Elevation Drawing of the Owensboro Bridge	88
4.3	Recorded Changes to Design Tensions for Deck Alignment and Profile Adjustment	89
4.4	Field Tests of the Owensboro Bridge Conducted with Loaded Trucks	90

4.5	Typical Traffic Including Heavy Trucks During Test on August 4-5, 2003	90
4.6	Triaxial Accelerometer Placement and Coordinate Definition	91
4.7	Typical Anchor Accelerometer Mounting	92
4.8	Typical Cable Accelerometer Mounting	92
4.9	Cable Cross Ties (Restrainers)	93
4.10	Additional Images of October 2002 Testing	93
4.11	Additional Images of the Owensboro Bridge	93
4.12	Typical Cable Time-History Data, Corresponding Spectrum and Cepstrum	95
4.13	Typical Cable Spectrum and Three Possible FFT Lengths for Cepstrum	96
4.14	Resulting Cepstra Using Three FFT Lengths	97
4.15	Preliminary Frequency Results Compared to Taut String Model Frequencies	98
4.16	Typical Accelerometer Placement and Mounting for Second Field Survey Test	99
4.17	Cable to Anchor Comparison for Owensboro (left) and Maysville (right) for Anchor Y (In-Plane) to Cable Z (Out-of-Plane) Spectra	100
4.18	Cable Workpoints shown on the Bridge Plans	101
4.19	Finite Element Model of Twelve Unrestrained Cables of the Owensboro Bridge	102
4.20	Comparison of Finite Element Model Fundamental Frequency Results for Cables 1-12 E to Experimental and String Model Frequencies	103
4.21	Photograph of Restrainers on the Owensboro Bridge	104
4.22	Finite Element Model of Twelve Restrained Cables of the Owensboro Bridge	105
4.23	Comparison of Finite Element Frequency Results and Field Test Results	107
4.24	Cable Frequency Trend vs. Anchor Stiffness and Definition of Critical Stiffness	108
4.25	FE model of the Owensboro anchor along side anchor picture	109
4.26	Deflected FE Model with Transverse Loading Applied from Cable	109
4.27	Anchor Force-Deflection Plots for Selected Owensboro Anchor Geometries: In-Plane (left) and Out-of-Plane (right)	110

# **1. INTRODUCTION**

## **1.1. General**

Cable-stayed bridges have become one of the most frequently used bridge systems throughout the world because of their aesthetic appeal, structural efficiency, enhanced stiffness compared with suspension bridges, ease of construction and small size of substructures. Over the past 40 years, rapid developments have been made in modern cable-stayed bridges. With the main span length increased and more shallow and slender stiffness girders used in modern cable-stayed bridges, their safety of the whole bridges under service loadings and environmental dynamic loadings, such as impact, wind and earthquake loadings, presents increasingly important concerns in design, construction and service. It has become essential to synthetically understand and realistically predict their response to these loadings. The unique structural styles of cable-stayed bridges make the span length longer and beautify the environment, but also add to the difficulties in accurate structural analysis. It is known that these long span and cable-stayed bridges constitute complex structural components with high geometric nonlinearity. In addition, the initial equilibrium configuration under dead loads has a significant effect on the structural behavior of cable-stayed bridges.

A long span cable-stayed bridge exhibits nonlinear characteristics under any load conditions. These nonlinear sources may come from

- The sag effect of inclined stay cables;
- The combined axial load and bending moment interaction effect of the girders and towers;
- The large displacement effect;
- The nonlinear stress-strain behavior of materials.

The discretized finite element method provides a convenient and reliable idealization of the structural continua and is particularly effective when using digital-computer analyses. The finite deformation theory with a discrete finite element model is the most powerful tool used in the nonlinear analysis of modern cable-stayed bridges.

However, it is not an easy task to establish a real and reliable finite element model of such complex structures. The process requires the combination of bridge field test results and analyses. The initial finite element model has to be updated or calibrated by field test results.

For a long span bridge, it is useful to establish both the analytical dynamic characteristics from the finite element predictions and the measured dynamic characteristics from the field testing. Many investigations of the dynamic characteristics of the cable-stayed bridge have been conducted over the years (Fleming and Egeseli 1980, Wilson and Gravelle 1991, Wilson and Liu 1991, Yang and Fonder 1998, Ren and Obata 1999, Zhu et al. 2000, Chang et al. 2001, Zhang et al., Cunha et al. 2001, Au et al. 2001 and Harik et al. 2005). In these works, the ambient structural response due to wind and/or traffic loads has been proven to be useful for determining the dynamic characteristics of bridges. The structural model updating as a form of calibration is a rapidly developing technology, and provides a “global” way to evaluate the structural state. Detailed literature reviews have been performed by Doebling et al. (1996), Salawu (1997) and Stubbs et al. (1999). While its applications have been diverse and scattered (Casas and Aparicio 1994, Chen et al. 1995, Hearn and Testa 1991, Harik et al. 1997, Harik et al. 1999, Juneja et al. 1997, Liu 1995, Mazurek and Dewolf 1990). Once a finite element model is calibrated according to the measured dynamic characteristics, the model can then be used for aerodynamic and /or seismic response predictions. Furthermore, the calibrated finite element model can be used as a baseline for health assessments of a bridge structure in the future.

The present work focuses on the comprehensive research to conceive a three-dimensional finite element model of the Owensboro cable-stayed bridge. Therefore, a three-dimensional finite element model has been created in the ANSYS, one general purpose commercial finite element software. All geometrically nonlinear sources are included such as cable sags, large deflections and axial force and bending moment interactions. The initial equilibrium configuration is achieved to account for the effect of dead loads. The finite element model is further updated through the use of free vibration field test results. The analytical model calibrated with experimental results is used to

study both static and dynamic responses of the bridge to various parametric changes. This calibrated finite element model can be utilized as a baseline in the structural analysis and monitoring of the Owensboro cable-stayed bridge. Cable testing and modeling for the Owensboro cable-stayed bridge are performed separately. They included field tests and finite element modeling of the cables. The outcomes of this research could be applied to provide useful information and data for the development of more refined design and analysis tools with future long span cable-stayed bridges.

## **1.2. Bridge Description**

Owensboro cable-stayed bridge, dedicated as the William H. Natcher Bridge, connects Owensboro (Daviess County), Kentucky and Rockport (Spencer County), Indiana over the Ohio River as seen in the photographs in Figures 1.1 and 1.2. It is one of the longest cable-stayed spans over a U.S. inland waterway system. The main bridge with a total length of 4,505 ft. includes the main span being 1200 ft. in length, two side spans with each being 500 ft. long, Kentucky approach being 1345 ft. long, and Indiana approach being 960 ft. long. Whole bridge width of 67 feet from parapet to parapet includes four 12 foot traffic lanes and four 4 foot shoulders. The main cable-stayed superstructure consists of a concrete deck supported by two main 12 foot deep steel plate girders with floor beams spaced at 30 feet. The deck consists of pre-cast deck sections with cast-in-place joints and post-tensioning in both longitudinal and transverse directions. The elevation drawing is shown in Figure 1.3. The bridge officially opened to traffic on October 21, 2002.



**Figure 1.1** Aerial View of the Owensboro Cable-Stayed Bridge



**Figure 1.2** Side View of the Owensboro Cable-Stayed Bridge

Steel stay cables are arranged in a two plane semi harped system along each edge of the deck. The ninety-six cables are nominally four sets of twenty-four cables. All cable-stayed bridges have had problems with stay wind gallop when the right combination of light rain and wind occur. However, the stay cable system of the Owensboro cable-stayed bridge is state-of-the-art. A co-extruded high density polyethylene pipe has been used which has a brilliant white outer layer eliminating the necessity to use a tape wrap. The outer layer has a small spiral bead around the pipe to break up air flow when there is light rain and wind to help prevent cable gallop. In addition, stay damping cables are connected between the stay cables with soft neoprene collars to further dampen galloping.

Two diamond-shaped main towers increase superstructure's stiff and add stability against wind and seismic loads. The towers are 345 feet above the surface of the river and are supported on concrete filled drilled shafts. Abutments are conventional concrete units supported by steel H piles.

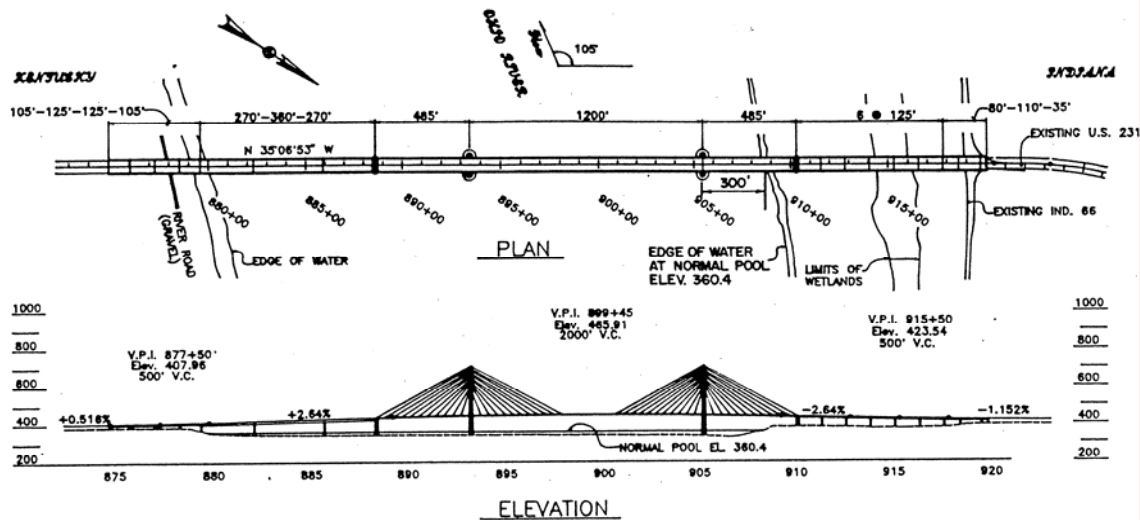


Figure 1.3 Plan and Elevation of the Owensboro Cable-Stayed Bridge

### 1.3. On-Site Dynamic Testing

On-site dynamic testing of a bridge provides an accurate and reliable description of its dynamic characteristics. In the civil engineering, structures such as bridges or buildings are considered systems and the system identification (experimental modal analysis) means the extraction of modal parameters (frequencies, damping ratios and mode shapes) from dynamic measurements. These modal parameters were utilized as a basis in the finite element model updating, structural damage detection, structural safety evaluation, and structural health monitoring on service.

There are three main types of bridge dynamic testing: (1) forced vibration testing; (2) free vibration testing; and (3) ambient vibration testing. In forced vibration testing and free vibration testing, the structure is excited by artificial means such as shakers, drop weights or test vehicle. By suddenly dropping a load on the structure, a condition of free vibration is induced. The disadvantage of this method is that traffic has to be shut down for an extended period of time. It is clear that this can be a serious problem for bridges that carry significant vehicular traffic.

In contrast, ambient vibration testing does not affect the traffic on the bridge because it uses existing vehicular traffic and natural wind loading to excite the bridge. This method is obviously cheaper than forced vibration testing since no extra equipment is needed to excite the structure. However, relatively long records of response measurements are required and the measured data are more stochastic. Consequently, the system identification results may be less reliable than such results obtained from a known forced vibration.

For the Owensboro cable-stayed bridge, on-site dynamic testing was performed using the free vibration testing method. Dynamic characteristics (frequencies and mode shapes) of the Owensboro cable-stayed bridge were extracted from the peak of the average normalized power spectral densities (ANPSDs). These vibration properties are subsequently used as a basis for updating the finite element model of the bridge.

#### **1.4. Finite Element Modeling and Calibration**

With modern commercial finite element programs it is possible to accurately predict both static and dynamic structural behavior of cable-stayed bridges. The discretized finite element model provides a convenient and reliable idealization of the structure. Thanks to rapid computer developments and the wealth of matrix analysis studies on nonlinear problems available, finite deformation theory with a discrete finite element model is one of the most powerful tools used in the analysis and design of cable-stayed bridges. An important advantage of the finite element method is that structural complexities can be considered effectively. Application of the finite deformation theory can include the effect of all nonlinear cable-stayed bridge sources such as cable sags, large deflections, and axial force and bending moment interactions. Another advantage of the finite element method lies in the capability of in-depth dynamic analysis.

A complete three-dimensional finite element model of the Owensboro cable-stayed bridge has been developed for the ANSYS (ANSYS 6.1) commercial finite element program. The ANSYS has been chosen because of the program's significant

capability to account for cable stress stiffening and pre-stressed modal analysis capability. The finite element model of the Owensboro cable-stayed bridge is composed of two element types: 3-D elastic beam elements and 3-D tension-only truss elements. The model consists of 668 nodes and 1087 finite elements with a total of 3960 active degrees of freedom (DOF).

In the design of cable-stayed bridges, the dead load often contributes most of bridge load. In the finite element analysis, the dead load influence is included through static analysis under dead loads before the live load or dynamic analysis is carried out. The objective of the static analysis process is to achieve the deformed equilibrium configuration of the bridge due to dead loads where the structural members are “pre-stressed”. The initial tension in the cables due to the dead load is determined by on-site testing. In addition, the geometric nonlinear effect has been studied by including the stress stiffening and large deflection.

A cable-stayed bridge is a highly pre-stressed structure. Starting from the deformed equilibrium configuration, the modal analysis is performed. Therefore, the dead load effect to the stiffness is included in the modal analysis through the specification of the pre-stress forces in the cables. The modal analysis is consequently a “pre-stressed” modal analysis, from which possible frequencies and mode shapes can be calculated. A coupled mode can be included, which gives a comprehensive understanding of the dynamic behavior of cable-stayed bridges. Parametric studies can also be performed by using the following parameters: deck self-weight, cable stiffness, and edge girder and sub-stringer bending stiffness.

Due to deviations in the structure’s original geometric or material properties it is difficult to establish the initial finite element model for structural evaluation. The original finite element model has to be updated or calibrated using field testing results in order to approximate the current conditions of the bridge. Finite element model updating is carried out until the finite element analytic frequencies and mode shapes match the field

testing results, maintaining physically realistic material properties. The updated finite element model is used as the baseline model for future evaluations of the bridge.

## **1.5. Cable Testing and Modeling**

Separate consideration of the cable response is motivated by the occurrence of wind-induced vibrations of bridge stay cables worldwide. Observed and documented since the mid-1980's, a particularly troublesome vibration has been observed in light-to-moderate wind combined with light rain. "Rain-wind" vibrations led to failure of anchor details on many bridges. Researchers worldwide continue to study factors affecting wind-induced stay cable vibration toward the goal of developing design approaches for prevention and mitigation.

The ninety-six cables of the Owensboro cable-stayed bridge are unique flexible structures whose dynamic response characteristics depend on material properties, tension, and possibly temperature. To bring the bridge deck into alignment side-to-side as the constructed sections met in the center and to smooth the vertical deck profile, cable design tensions were adjusted from those in the original plans. Cable testing and modeling for the Owensboro cable-stayed bridge included two field tests of the cables. The first of these was just before the bridge opened with excitation provided by loaded trucks. The second test used ambient (typical traffic and wind) excitation. Signal processing analysis of the recorded acceleration time histories identified fundamental frequencies of the cables. Finite element models were developed for all cables using the as-built cable properties and compared to field test results showing good correlation.

## **1.6. Scope of Work**

The primary aim of this investigation is to evaluate the structural dynamic characteristics of the Owensboro cable-stayed bridge and to establish the baseline model of the bridge. Dynamics-based structural evaluation will be used. To achieve the goal, the scope of work will be divided into the following five parts:

- (1). Conduct finite element modeling and modal analysis;
- (2). Extract the dynamic characteristics from on-site free vibration testing;
- (3). Calibrate the finite element model by the results of the field testing;
- (4). Conduct field tests of stay cables and finite element modeling of them;
- (5). Understand the structural behavior under service loadings and environmental dynamic loadings.

## **2. FIELD DYNAMIC TESTING**

### **2.1. General**

On-site dynamic testing of a bridge provides an accurate and reliable description of its real dynamic characteristics. There are three main types of dynamic bridge testing:

- *Forced Vibration Test*
- *Free Vibration Test*
- *Ambient Vibration Test*

In the first two methods, the structure is excited by artificial means such as shakers, drop weights or testing vehicle. By suddenly dropping a load on the structure, a condition of free vibration is induced. The disadvantage of these methods is that traffic has to be shut down for a rather long time, especially for large structures such as long-span bridges, and requires numerous test setups. It is clear that this can be a serious problem for bridges that have high traffic volumes. In contrast, ambient vibration testing does not affect the traffic on the bridge because it uses the traffic and wind as natural excitation. This method is obviously cheaper than forced vibration testing since no extra equipment is needed to excite the structure. However, relatively long records of response measurements are required and the measured data are more stochastic. Consequently, accurately identifying the system response modes is less accurate.

Basically, the system identification procedure is carried out according to both input and output measurement data through the frequency response functions (FRFs) in the frequency domain or impulse response functions (IRFs) in the time domain. For civil engineering structures, the dynamic responses (output) are the direct records of the sensors that are installed at several locations. However, the input or excitation of the real structure in the operational condition often can be hardly realized. It is extremely difficult to measure the input excitation forces acting on a large-scale structure. Although forced excitations (such as heavy shakers and drop weights) and correlated input-output

measurements are sometime available, testing or structural complexity and achievable data quality restrict these approaches to dedicated applications.

The output data-only dynamic testing has the advantage of being inexpensive since no equipment is needed to excite the structure. The ambient vibration is a kind of output data-only dynamic testing. The service state does not have to be interrupted by using this technique. The output data-only dynamic testing has been successfully applied to many large scale cable-supported bridges such as the Golden Gate Bridge (Abdel-Ghaffer and Scanlan 1985), the Quincy Bayview Bridge (Wilson and Gravelle 1991), the Fatih Sultan Mehmet Suspension Bridge (Brownjohn et al. 1992), the Tsing Ma Suspension Bridge (Xu et al. 1997), the Hitsuishijima Bridge, one of the Honshu-Shikoku Bridge (Okauchi et al. 1997), the Vasco da Gama Cable-Stayed Bridge (Cunha et al. 2001), the Kap Shui Mun Cable-Stayed Bridge (Chang et al. 2001), and the Roebling Suspension Bridge (Ren et al. 2001). In the case of output data-only dynamic testing, only response data are measured while actual loading conditions are unknown. A system identification procedure will therefore need to base itself on output-only data.

System Identification using output-only measurements presents a challenge requiring the use of special identification techniques, which can deal with very small magnitudes of ambient vibration contaminated by noise without the knowledge of input forces. There have been several output-only data system identification techniques available that were developed by different investigators or for different uses such as: peak-picking from the power spectral densities (Bendat and Piersol 1993), auto regressive-moving average (ARMA) model based on discrete-time data (Andersen et al. 1996), natural excitation technique (NExT) (James et al. 1995), and stochastic subspace identification (Van Overschee and De Moor 1996; Peeters and De Roeck 2000). The mathematical background for many of these methods is often very similar, differing only from implementation aspects (data reduction, type of equation solvers, sequence of matrix operations, etc.). The benchmark study was carried out to compare system identification techniques for evaluating the dynamic characteristics of a real building on operation conditions from ambient vibration data (De Roeck et al. 2000).

For the Owensboro cable-stayed bridge, on-site free vibration tests have been conducted. The Owensboro cable-stayed bridge consists of a 1200' main span, two 500' side spans, 1345' Kentucky approach and 960' Indiana approach. The bridge has the width of 67' with four 12' traffic lanes and four 4' shoulders. The output data-only dynamic testing and system identification of the Owensboro cable-stayed bridge are performed. The field dynamic testing was carried out just prior to opening the bridge in order to obtain the baseline dynamic characteristics of the bridge. Loaded trucks were run to excite dynamic responses from the bridge. The acceleration responses of 96 deck stations were recorded as trucks drove a high-speed pass. The modal characteristics of the bridge are extracted from the peak picking of the average normalized power spectral densities (ANPSDs) in frequency domain. The dynamic test results will be used to calibrate the finite element model and then to establish the baseline finite element model that reflects the built-up structural conditions for the long-term structural evaluation, damage identification and health monitoring of the bridge.

## **2.2. Output-Only Dynamic Testing**

Just prior to opening the bridge, loaded trucks were run to excite dynamic responses from the bridge and the cables. Two loaded truck cases were used. The high-speed test is the case where two loaded trucks, weighing 52,780 and 52,940 lbs drove a fast pass.

The equipment used to measure the acceleration-time responses of instrumentation consisted of tri-axial accelerometers linked to its own data acquisition system. The system contained a Keithly MetraByte 1800HC digital recording strong motion accelerograph. Two units contained internal accelerometers, while the two remaining units were connected to Columbia Research Labs, SA-107 force balance accelerometers. The accelerometers are capable of measuring accelerations up to 2g's at frequencies up to DC-50Hz. The data was stored in a personal computer for further processing.

Sets of three accelerometers were mounted to aluminum blocks in orthogonal directions to form a tri-axial accelerometer station. A block was positioned at each station

with the accelerometers oriented in the vertical, transverse and longitudinal directions. To prevent any shifting of the accelerometers during testing, 25-pound bags of lead shot were laid on top of the accelerometer blocks once in position. To ensure the blocks were placed in level, adjustable feet and carpenters level were attached to each block. Accelerometers were connected to the data acquisition system by shielded cables.

Measurement stations were chosen to be between two cable planes. Instruments were placed on the pavement due to the limited access to the actual floor beams. As a result, a total of 96 locations (48 points per side) were measured. A view on the measurement instrumentations is shown in Figure 2.1. Twenty four test setups are conceived to cover the planned testing area of the cable-stayed span of the bridge. A reference location, hereinafter referred as the base station, is selected based on the mode shapes from the preliminary finite element model. Each setup is composed of three base tri-axial accelerometer stations and four moveable tri-axial accelerometer stations. Each setup yields a total of twelve sets of data from moveable stations and nine sets of base station data. Table 2.1 shows the distribution of the different stations per setup.

Testing began at the Owensboro side and progressed to the Rockport side. In each test set up, response data were measured for the high-speed test. Once the data were collected in one set up, the four moveable stations were then relocated to the next positions while the base stations remained stationary. This sequence was repeated twenty four times to get output-only measurements on all stations. The sampling frequency on site is chosen to be as high as 200 Hz to capture the short-time transient signals of the free vibration in full detail. The output-only measurement is simultaneously recorded for 600 seconds at all accelerometers, which results in a total of 120,000 data points per channel. The typical acceleration records are as shown in Figure 2.2 for the high-speed test.

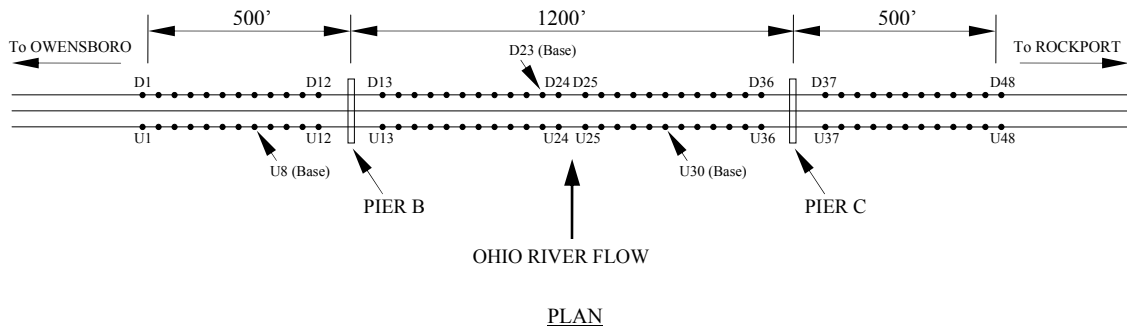


Figure 2.1 Measurement Instrumentation Plan

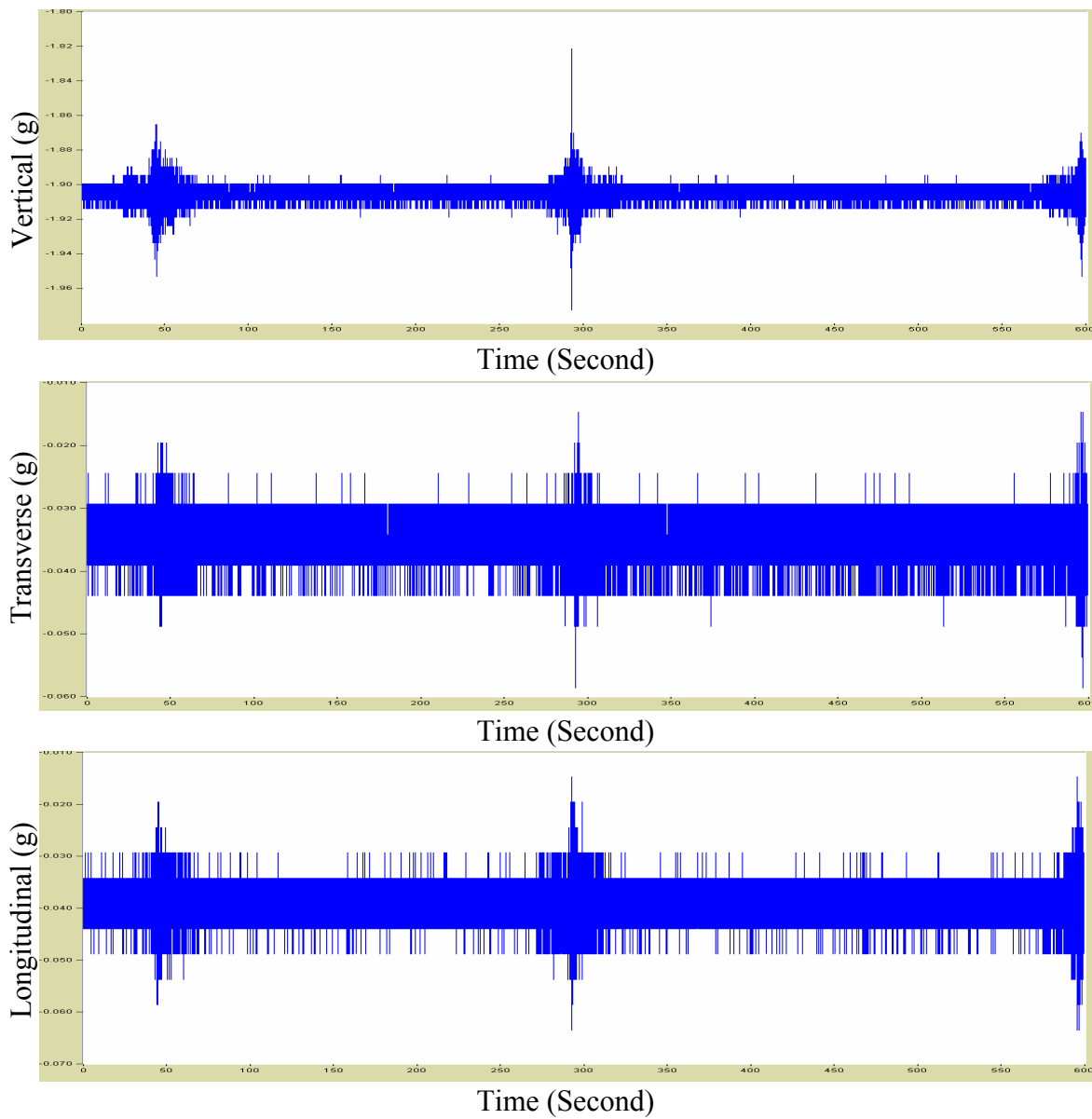


Figure 2.2 Typical Acceleration Time Histories

**Table 2.1** Instrumentation Per Setup

Setup	Points measured
1	D1, D2, U1, U2, U8, D23, U30
2	D3, D4, U3, U4, U8, D23, U30
3	D5, D6, U5, U6, U8, D23, U30
4	D7, D8, U7, U8, U8, D23, U30
5	D9, D10, U9, U10, U8, D23, U30
6	D11, D12, U11, U12, U8, D23, U30
7	D13, D14, U13, U14, U8, D23, U30
8	D15, D16, U15, U16, U8, D23, U30
9	D17, D18, U17, U18, U8, D23, U30
10	D19, D20, U19, U20, U8, D23, U30
11	D21, D22, U21, U22, U8, D23, U30
12	D23, D24, U23, U24, U8, D23, U30
13	D25, D26, U25, U26, U8, D23, U30
14	D27, D28, U27, U28, U8, D23, U30
15	D29, D30, U29, U30, U8, D23, U30
16	D31, D32, U31, U32, U8, D23, U30
17	D33, D34, U33, U34, U8, D23, U30
18	D35, D36, U35, U36, U8, D23, U30
19	D37, D38, U37, U38, U8, D23, U30
20	D39, D40, U39, U40, U8, D23, U30
21	D41, D42, U41, U42, U8, D23, U30
22	D43, D44, U43, U44, U8, D23, U30
23	D45, D46, U45, U46, U8, D23, U30
24	D47, D48, U47, U48, U8, D23, U30

U refers to upstream and D stands for downstream.

### 2.3. Peak Picking (PP) System Identification

The raw data from the output only testing displays a series of data that show the acceleration of the bridge in one of the three axial directions with respect to time, creating a time-history record of accelerations for the bridge. The raw data is not particularly useful for the dynamic analysis of the bridge and therefore must be transformed from the time domain into the frequency domain. The manner by which this was accomplished was the implementation of the Fourier Transform, which is mathematically defined using the transform equation:

$$F(\omega) = \int_{-\infty}^{\infty} f(t)e^{i\omega t} dt$$

where  $f(t)$  is a function of time,  $F(\omega)$  is amplitude as a function of frequency, and  $\omega$  is circular frequency (radians per second). The inverse of the Fourier Transform is defined by the equation:

$$f(t) = \frac{1}{2\pi} \int_{-\infty}^{\infty} F(\omega) e^{-i\omega t} d\omega.$$

Using the equations above, any function that is a function of time can be converted into a function of frequency or vice versa. The only drawback associated with using these equations is that  $f(t)$  must be a continuous function, which does not fit the description of the piecewise nature of digitally sampled data such as obtained in the bridge testing. For this reason, a different form of Fourier Transform must be used, known as the Discrete Fourier Transform (DFT), which is useful when data point values are known at regularly spaced intervals, which lends itself nicely to the problem at hand. The Discrete Fourier Transform is defined by the equation:

$$F_n = \sum_{k=0}^{N-1} f_k e^{2\pi i k n / N} \quad (n = 0, 1 \dots N - 1).$$

where  $N$  is the number of sampled points and  $f_k$  is a set of  $N$  sampled points. The inverse form of the Discrete Fourier Transform is given by the equation:

$$f_k = \frac{1}{N} \sum_{n=0}^{N-1} F_n e^{-2\pi i k n / N} \quad (k = 0, 1 \dots N - 1).$$

This set of equations is extremely useful for engineering applications such as this, but there are still some problems. These equations require  $N^2$  complex mathematical operations which, even with modern computing power, can take quite some time even for small data sets. There is one other method that can reduce the computing time significantly.

The Fast Fourier Transform (FFT), a numerical operation, can exploit the periodic and symmetric nature of trigonometric functions to greatly improve efficiency in comparison to the Discrete Fourier Transform. The number of computations for the Fast

Fourier Transform is reduced to  $N \log_2(N)$ , which is approximately 100 times faster than the Discrete Fourier Transform for a set of 1000 data points.

The peak picking method is initially based on the fact that the frequency response function (FRF) goes through an extreme around the natural frequencies. In the context of vibration measurements, only the FRF is replaced by the auto spectra of the output-only data. In this way the natural frequencies are simply determined from the observation of the peaks on the graphs of the average response spectra. The average response spectra are basically obtained by converting the measured accelerations to the frequency domain by a Discrete Fourier Transform (DFT). The coherence function computed for two simultaneously recorded output signals has values close to one at the natural frequency. This fact also helps to decide which frequencies can be considered as natural.

The peak picking algorithm, however, involves averaging temporal information, thus discarding most of their details. It has some theoretical drawbacks such as (1) picking the peaks is always a subjective task, (2) operational deflection shapes are obtained instead of mode shapes, (3) only real modes or proportionally damped structures can be deduced by the method, and (4) damping estimates are unreliable. In spite of these drawbacks, this method is most often used in civil engineering practice for ambient or free vibration measurements because it is fast and easy to apply.

The data processing and modal identification are carried out by a piece of software known as DADiSP (Data Analysis and Display Software) version 2000 by DSP Development Corporation, Cambridge, Massachusetts, (DADiSP 2000). The time-history data was imported into the software. This software is useful for displaying, analyzing and manipulating large pieces of data, such as the 120,000+ points contained in each of the data files obtained. The software was also used to perform Fast Fourier Transforms on the imported data files.

After picking the peaks from the combined spectral plot, the magnitudes of the FFT spectra from the moveable stations were divided by the magnitudes of the FFT

spectra from the base stations at each frequency to create a relative-magnitude plot for the bridge, relating the magnitudes at the moveable stations to those at the base station. The relative magnitudes for each point along the bridge were plotted at each of the picked-peak frequencies to determine the mode shapes of the bridges. The mode shapes predicted by the field data were then compared to a preliminary finite-element model for verification. This sequence was repeated for all records in each of the vertical, transverse, and longitudinal direction.

The average response spectra for all measurement data of the vertical and longitudinal directions are shown in Figures 2.3-2.4. The possible frequencies (peaks) of the vertical data and longitudinal data are summarized in Table 2.2 for the test.

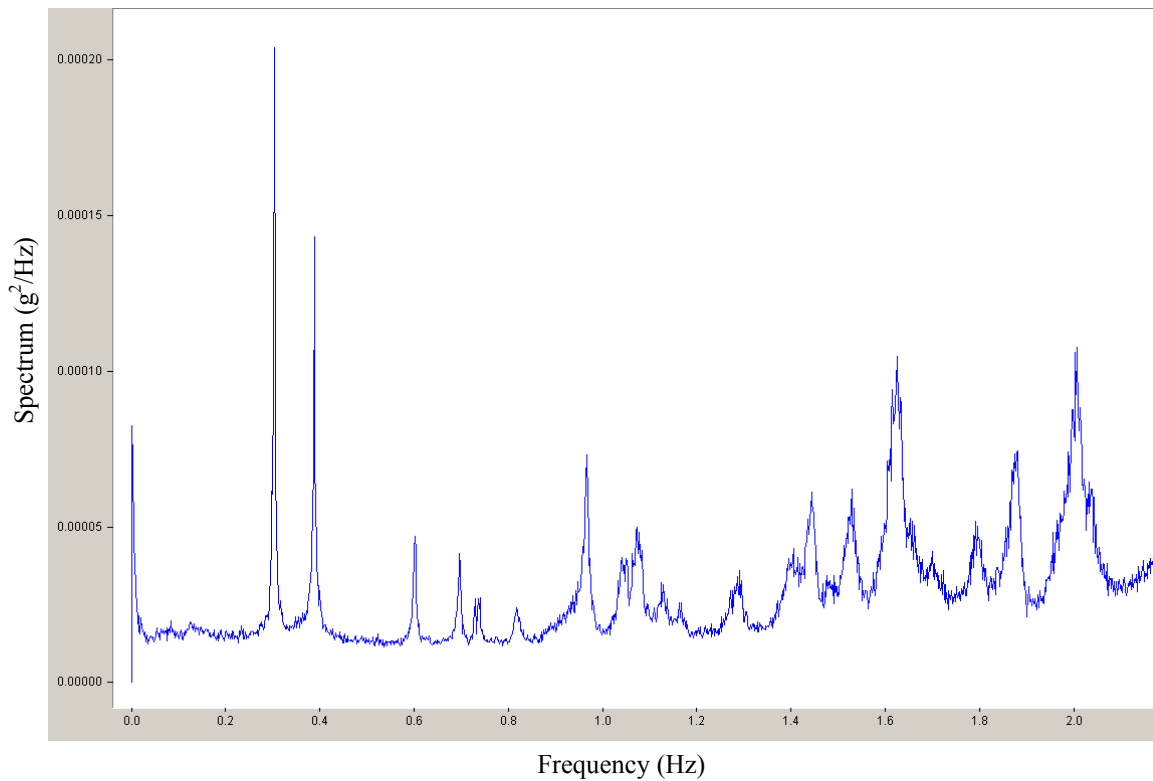


**Figure 2.3** Full Data Averaged Vertical Response Spectra

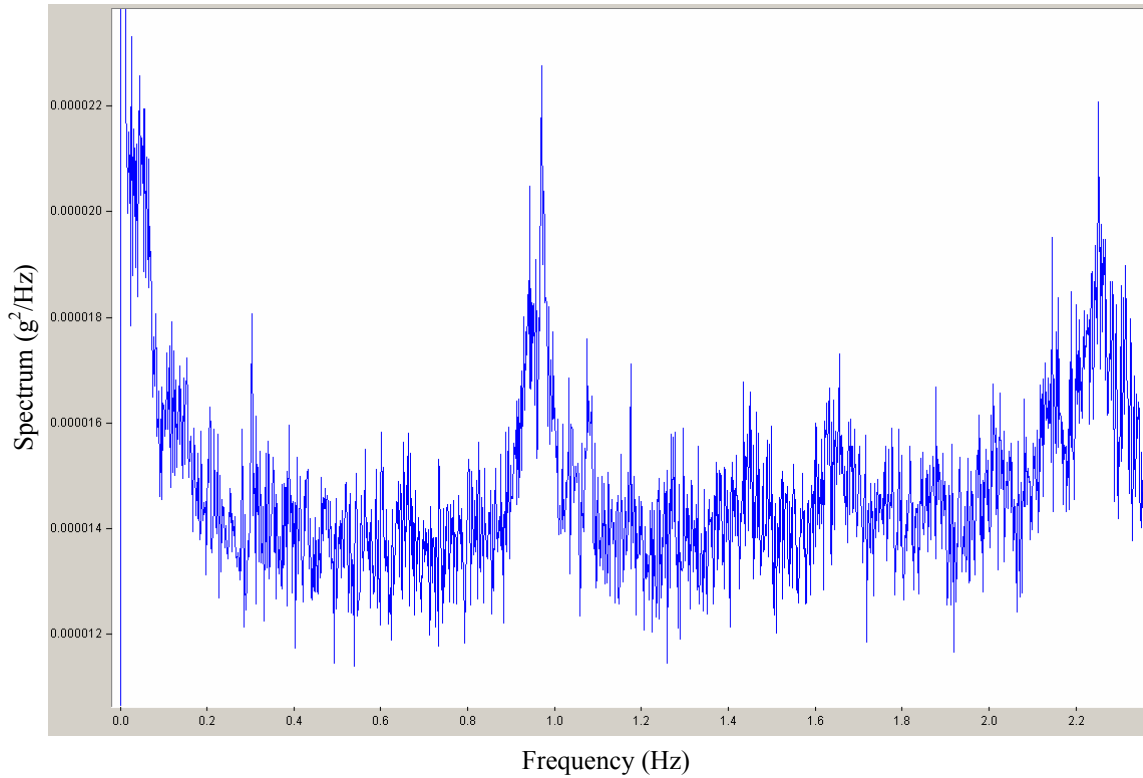


**Figure 2.4** Full Data Averaged Longitudinal Response Spectra

**Table 2.2** Possible Frequencies for Testing (Hz)

Vertical	Longitudinal
0.301667	0.301667
0.388333	0.97
0.601667	1.07833
0.696667	1.175
0.74	2.2533
0.818333	
0.966667	
1.07167	
1.125	
1.165	
1.28333	
1.52667	
1.87167	
2.00833	

The identified frequencies are summarized in Table 2.3 for the high-speed test. Good mode shapes have also been extracted by the peak picking system identification method. The first vertical mode shapes are given in Figures 2.5.

**Table 2.3** Summary of Identified Frequencies (Hz)

Frequencies	Modes
0.301667	Vertical
0.388333	Vertical
0.601667	Vertical
0.696667	Vertical
0.74	Vertical
0.818333	Vertical
0.966667	Vertical + Longitudinal
1.07167	Vertical

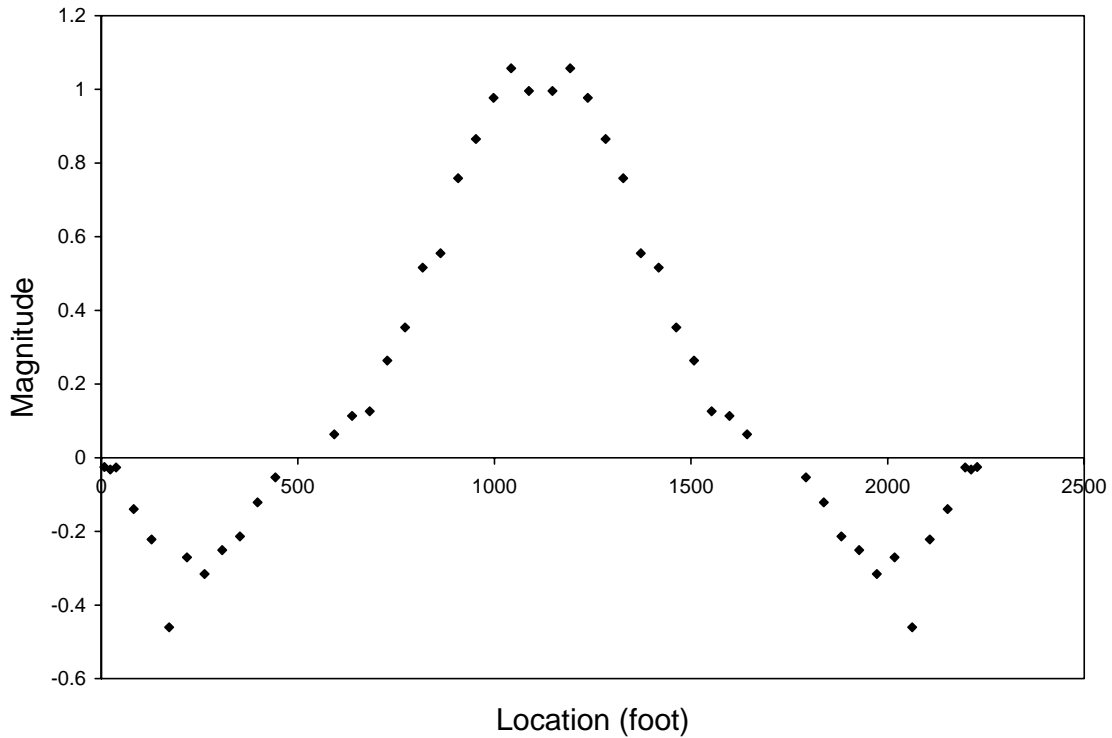


**Figure 2.5** First Vertical Mode Shape of Owensboro Bridge  
( $f = 0.301667$  Hz)

## 2.4. Remarks

The following remarks can be made from the output-only dynamic testing of the Owensboro cable-stayed bridge:

1. The modal parameters can be effectively extracted from output-only dynamic testing by using the frequency domain based peak picking (PP) method.

2. The peak picking identification is very fast and efficient since no model has to be fitted to the data. For real applications, the peak picking method could be used on site to verify the quality of the measurements.
3. Ambient or free vibration testing provides a convenient, fast and cheap way to perform the bridge dynamic testing.

### **3. FINITE ELEMENT MODELING AND CALIBRATION**

#### **3.1. General**

Modern cable-stayed bridges have been experiencing a revival since the mid-1950s, while the concept of supporting a bridge girder by inclined tension stays can be traced back to the seventh century (Podolny and Fleming 1972). The increasing popularity of contemporary cable-stayed bridges among bridge engineers can be attributed to: (1) the appealing aesthetics; (2) the full and efficient utilization of structural materials; (3) the increased stiffness over suspension bridges; (4) the efficient and fast mode of construction; and (5) the relatively small size of the bridge elements.

For the cable-stayed bridges, it was difficult to do accurate structural analysis. The commonly used classical theories for static analysis of cable-stayed bridges are the elastic theory and the deflection theory. The elastic theory is basically a linearized approximate theory, as it does not take into account the deformed configuration of the structure. Though the values of bending moment and shear yielded by the elastic theory are too high, it satisfies more safe design but not economy. This method is quite expeditious and convenient for preliminary designs and estimates. Basically, the elastic theory is sufficiently accurate for shorter spans or for designing relatively deep rigid stiffening systems that limit the deflections to small amounts. However, the elastic theory does not suit the designing of cable-stayed bridges with long spans, or large dead loads. The deflection theory, in contrast, is a more “exact” theory that takes into account the deformed configuration of the structure and results in a more economical and slender bridge.

Nowadays, it is no longer a problem to accurately predict both the static and dynamic structural behavior of cable-stayed bridges. The finite element method of structural continua provides a convenient and reliable idealization of the structure and is particularly effective in digital-computer analysis. The finite element type of idealization is applicable to structures of all types. Thanks to rapid computer developments and the

accumulation of matrix analysis studies on nonlinear problems. The finite deformation theory with a discrete finite element model has been the most powerful tool used in the nonlinear analysis of cable-supported bridges. The applications of the finite deformation theory can include the effect of all nonlinear sources of cable-stayed bridges such as cables, large deflections, axial force and bending moment interaction.

An important advantage of the finite element method is that structural complexities such as tower movements, cable extensibility, and support conditions, etc. can be considered effectively. The finite element method can also be used to analyze the effect of changes in different parameters, i.e., the parameter design. Two- or three-dimensional finite element models with beam and truss elements are often used to model both the superstructure and the substructure of cable-supported bridges (Nazmy and Abdel-Ghaffar 1990, Wilson and Gravelle 1991, Lall 1992, Ren 1999, Spyrakos et al. 1999). Another advantage of the finite element method lies in its capability to do in-depth dynamic analysis. The dynamic characteristics of cable-supported bridges have been of particular interest since the collapse of the Tacoma Narrows Bridge in the State of Washington on November 7, 1940, as a result of wind action. Parametric studies on natural frequencies and modes (West et al. 1984) using a finite element formulation demonstrate the variation of the modal parameters of stiffened cable-supported bridges. The finite element method has been a unique way to do the dynamic response analysis of cable-supported bridges under the loadings of winds, traffics and earthquakes (Boonyapinyo et al. 1999, Abdel-Ghaffar and Rubin 1983, Abdel-Ghaffar and Nazmy 1991, Ren and Obata 1999).

This chapter describes the structural evaluation effort for the Owensboro cable-stayed bridge by using finite element method. Details of a three-dimensional finite element model are presented. The analytical model of the Owensboro cable-stayed bridge is constructed in ANSYS, which is one of the most powerful engineering design and analysis software (ANSYS 6.1). The ANSYS is chosen because of the program's significant capability to account for the cable stress stiffening and the pre-stressed modal

analysis capability. This model will be used for both static and dynamic analyses of the Owensboro cable-stayed bridge.

In the finite element analysis, the influence of the dead load is considered by the static analysis under dead loads prior to application of the live loads or a dynamic analysis is carried out. The objective of the static analysis process is to achieve the deformed equilibrium configuration of the bridge under dead loads where the structural members are “pre-stressed”. A cable-stayed bridge is indeed a highly pre-stressed structure. Starting from the deformed equilibrium configuration, the modal analysis is followed. Consequently, the dead load effect on the stiffness can be included in the modal analysis; thereby, the modal analysis will be a “pre-stressed” modal analysis.

Hence, the modal analysis of a cable-stayed bridge must include two steps: static analysis due to dead load and “pre-stressed” modal analysis. For a completed cable-stayed bridge, the initial position of the cable and bridge is unknown. Only the final geometry of the bridge due to the dead load can be known by referring to the bridge plans. The initial geometry of the ideal finite element model of a cable-stayed bridge should be such that the geometry of a bridge does not change when a dead load is applied, since this is indeed the final geometry of the bridge as it stands. In other words, the deformed configuration of the bridge under the self-weight dead load should be close to the initial geometry input. In addition, the geometric nonlinear effect has been studied by including the stress stiffening and large deflection. All possible frequencies and mode shapes can be provided performing the pre-stressed modal analysis. A coupled mode can be included to give a comprehensive understanding of the dynamic behavior of the cable-stayed bridges. Finite element (FE) model calibration, i.e., parametric studies, is also performed. The parameters include self-weight of the deck, the stiffness of cables, and bending stiffness of edge girders and center beams. The results of the modal analysis will be compared later with *in-situ* free vibration measurements to calibrate or update the initial finite element model.

## **3.2. Initial Finite Element Model**

Since modern cable-stayed bridges involve a variety of decks, towers and cables that are connected together in different ways, the finite element method (FEM) is generally regarded as the most proper way for conducting the dynamic analysis. In FEM connection, the single-girder beam element model, the double-girder beam element model, the triple-girder beam element model, the shell element model and the thin-walled element model have been developed to model the bridge deck (Yang and McGuire 1986a, Yang and McGuire 1986b, Boonyapinyo et al.1994, Wilson and Gravelle 1991 and Zhu et al. 2000). Referring to Zhu et al.'s work, we choose the triple-girder beam element model to model the bridge deck.

### **3.2.1. Primary Assumption**

A completely three-dimensional finite element model was established by using the finite element analysis software ANSYS version 6.1. The software ANSYS was able to account for the cable stress stiffening and the pre-stressed modal analysis. This model would be used for static and dynamic analyses of the Owensboro cable-stayed bridge. Due to the complexity and variations of such a cable-stayed bridge, there are too many uncertainties in both geometry and material. Some primary assumptions are made to establish the initial finite element model of the Owensboro cable-stayed bridge:

- Towers: Assumed that the tower head consists of twelve beams, although the tower head is actually a continuous part along its height.
- Edge girders: Assumed that two edge girders are completely continuous, although they are composed of eighteen different section properties.

### **3.2.2. The Geometry of the Bridge**

After selecting an appropriate modeling methodology, serious considerations must be given to proper representation of the bridge geometry. These geometric issues

are directly related to the structural behavior. The consideration must include not only the global geometry of the bridge, but also local geometric characteristics of individual bridge members. The geometry and member details are extracted from the plan of the Owensboro cable-stayed bridge. The plan referred is Kentucky Department of Highways, Indiana Department of Transportation; Daviess County, Kentucky – Spencer County, Indiana; U.S. 231 over the Ohio River and Indiana 66; Owensboro, Kentucky to Rockport, Indiana prepared by the Haworth, Meyer & Boleyn Consulting Engineers (1991). The drawing number is 22535. Table 3.1 shows the member details extracted from the plan.

**Table 3.1** Member Details Extracted from the Plan

Member	Reference
Towers	Sheets 90-110
Cables	Sheets 160-164
Edge Girders	Sheets 138-149
Center beam	Sheet 159
Floor beams	Sheets 158-158A
Decks	Sheets 165-186

### **3.2.3. Element Types**

A cable-stayed bridge is a complex structural system. Each member of the bridge plays a different role. Different element types are therefore needed. In this FE model, two types of elements were chosen for modeling the different structural members. They are the 3-D elastic beam element (BEAM4), and 3-D tension-only truss element (LINK10). The theoretical background of each type of elements is briefly described below.

#### **3.2.3.1. BEAM4 Element**

BEAM4 element is a uniaxial 3-D elastic beam element with tension, compression, torsion and bending capabilities. The element has six degrees of freedom at each node: translations in x, y and z directions of the nodal and rotations about x, y and z axes of the nodal. BEAM4 element is defined by the cross-sectional geometrical





### 3.2.3.2. LINK10 Element

LINK10 element is a uniaxial 3-D elastic truss element with tension-only (or compression-only) capability. With the tension-only option used here, the stiffness is removed if the element goes into compression (simulating a slack cable or slack chain condition). The feature is unique to model the cables of the Maysville cable-stayed bridge. The element has three degrees of freedom at each node: translations in x, y and z directions of the nodal. No bending of the element is considered. LINK10 3-D truss element is defined by the cross-sectional area, initial strain and material property of two nodes. The geometry, node locations and the coordinate system for this element are shown in Figure 3.2.

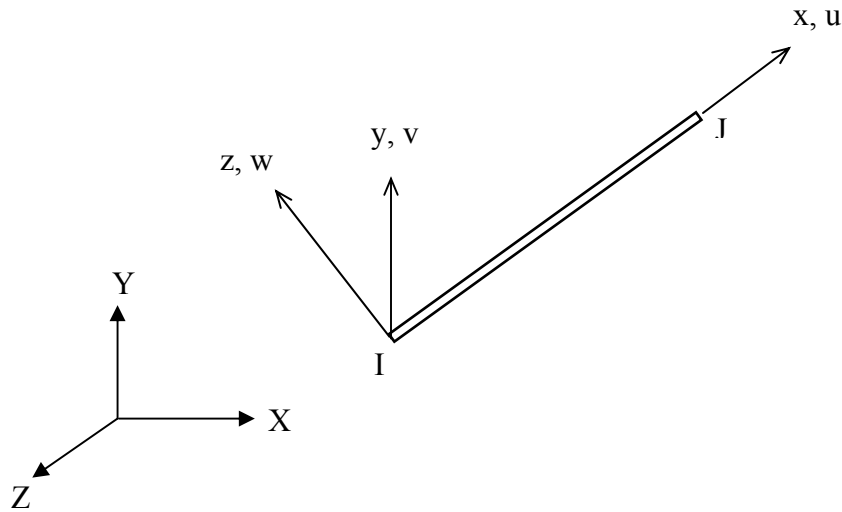


**Figure 3.2** 3-D Tension-only Truss Element

The stiffness matrix of tension-only truss element in the local coordinate system is

$$[k_l] = \frac{AE}{L} \begin{bmatrix} C_1 & 0 & 0 & -C_1 & 0 & 0 \\ 0 & 0 & 0 & 0 & 0 & 0 \\ 0 & 0 & 0 & 0 & 0 & 0 \\ -C_1 & 0 & 0 & C_1 & 0 & 0 \\ 0 & 0 & 0 & 0 & 0 & 0 \\ 0 & 0 & 0 & 0 & 0 & 0 \end{bmatrix}$$

where

$A$  = element cross-sectional area

$E$  = Young's modulus

$L$  = element length

$C_1 = 1.0$  when tension;  $1.0 \times 10^6$  when compression.

The consistent mass matrix of LINK10 element in the local coordinate system is

$$[m_l] = \frac{\rho AL(1 - \varepsilon^{in})}{6} \begin{bmatrix} 2 & 0 & 0 & 1 & 0 & 0 \\ 0 & 2 & 0 & 0 & 1 & 0 \\ 0 & 0 & 2 & 0 & 0 & 1 \\ 1 & 0 & 0 & 2 & 0 & 0 \\ 0 & 1 & 0 & 1 & 2 & 0 \\ 0 & 0 & 1 & 0 & 0 & 2 \end{bmatrix}$$

where

$\rho$  = mass density

$\varepsilon^{in}$  = initial strain (as an input)

An important input property of the LINK10 elements that are aimed at modeling cable behavior is the initial strain. The initial strain is used for calculating the stress stiffness matrix for the first cumulative iteration. Stress stiffening should always be used for cable problems to provide numerical stability. The initial strain in the element is given by  $\delta / L$ , where  $\delta$  is the difference between the element length  $L$  and the zero strain length  $L_0$ .

### 3.2.4. Material Properties and Real Constants

The basic materials used in the Owensboro cable-stayed bridge are the structural steel, concrete and high strength steel. The preliminary material constants used in the finite element model are shown in Table 3.2; furthermore, they follow the typical values of ASMT standards.

**Table 3.2** Preliminary Material Properties

Group No.	Young's modulus (lb/ft <sup>2</sup> )	Poisson's ratio	Mass density (lb/ft <sup>3</sup> )	Structural member
1	$4.176 \times 10^9$	0.3	490	Edge girders, Floor beams
2	$4.176 \times 10^9$	0.3	490	Center beam
3	$4.176 \times 10^9$	0.3	490	Cables
4	$6.358 \times 10^8$	0.2	150	Towers
5	$6.867 \times 10^8$	0.2	150	Decks

The real constants consist of all necessary geometric properties of the cross-section and initial strain if necessary. Depending on the element type, different real constants are considered as the input. All preliminary real constants used in the current model are summarized in Table 3.3. Real constants are based on the following facts of the main structural members.

### **Edge Girder**

The edge girders are of the continuous type with an expansion bearing at each end, one fixed bearings at pier B, and one expansion bearing at pier C. Each edge girder consists of type I beams of eighteen different cross-sections. There are floor beams between two edge girders.

### **Cables**

The cables are composed of 18 - 58 strands of high strength steel wire, each strand being 0.6 inches in diameter. These strands are parallel to each other, which are surrounded by PE pipe forming a single cable. The initial strains are obtained from the axial force of the bridge plans.

### **Towers**

The towers are composed of shaft, lower legs, upper legs, tie strut and tower head. The tie strut is connected with the edge girders by two bearings.

**Floor Beams and Center Beam**

In the cable-stayed spans, the reinforced concrete grid decks are supported by the frames which are composed of edge girders, floor beams and center beam. The floor beams are the type I structures with variable cross-sections. The center beam is a type I cross-sectional beam.

**Table 3.3** Preliminary Real Constants

Type	Cross-section Area: (ft <sup>2</sup> )	Inertia moment: (ft <sup>4</sup> )		Initial strain	Structural member
		I <sub>zz</sub>	I <sub>yy</sub>		
1	1.5234	30.9475	0.25233	-	Edge girder
2	1.7734	33.983	0.25288	-	Edge girder
3	0.9922	4.3274	0.25209	-	Edge girder
4	1.04427	4.4394	0.25222	-	Edge girder
5	0.9401	4.215	0.25199	-	Edge girder
6	1.0964	4.55105	0.25238	-	Edge girder
7	1.1198	4.7361	0.26226	-	Edge girder
8	0.96354	4.4046	0.26188	-	Edge girder
9	1.0677	4.62575	0.26211	-	Edge girder
10	1.01562	4.51527	0.26198	-	Edge girder
11	1.11979	5.08067	0.31623	-	Edge girder
12	1.27083	6.0398	0.39026	-	Edge girder
13	0.91667	4.01716	0.24211	-	Edge girder
14	0.96875	4.13183	0.24221	-	Edge girder
15	1.02083	4.2459	0.24233	-	Edge girder
16	1.0729	4.3594	0.24249	-	Edge girder
17	1.01562	4.6952	0.28901	-	Edge girder
18	1.11979	4.92278	0.28924	-	Edge girder
19	0.18758	0.03094	0.0015	-	Center beam
20	0.3919	0.02483	1.6034	-	Floor beam
21	83	2486.3	2870.25	-	Tower (lower)
22	64.5	1894.4	638.6	-	Tower (upper)
23	58.5	613.9	1829.2	-	Tower (tie strut)
24	159.36	3399.7	1317.4	-	Tower (head)
25	142.72	3044.7	946.3	-	Tower (head)
26	128	2730.67	682.67	-	Tower (head)
27	126.72	2703.36	662.4	-	Tower (head)
28	122	2602.67	591.1	-	Tower (head)
29	121.28	2587.3	580.7	-	Tower (head)
30	52	69	732	-	Tower-edge girder
31	0.059722	-	-	3.613E-03	Cables 1 & 48
32	0.058229	-	-	3.5285E-03	Cables 2 & 47

**Table 3.3 Continued** Preliminary Real Constants

Type	Cross-section Area: (ft <sup>2</sup> )	Inertia moment: (ft <sup>4</sup> )		Initial strain	Structural member
		I <sub>zz</sub>	I <sub>yy</sub>		
33	0.086597	-	-	3.7096E-03	Cables 3 & 46
34	0.044792	-	-	3.5552E-03	Cables 4 & 45
35	0.050764	-	-	3.6605E-03	Cables 5 & 44
36	0.047778	-	-	3.744E-03	Cables 6 & 43
37	0.044792	-	-	3.6995E-03	Cables 7 & 42
38	0.041806	-	-	2.2396E-03	Cables 8 & 41
39	0.038819	-	-	1.8568E-03	Cables 9 & 40
40	0.035833	-	-	1.9514E-03	Cables 10 & 39
41	0.026875	-	-	2.0494E-03	Cables 11 & 38
42	0.037326	-	-	1.0586E-03	Cables 12 & 37
43	0.037326	-	-	1.1035E-03	Cables 13 & 36
44	0.026875	-	-	2.0226E-03	Cables 14 & 35
45	0.035833	-	-	2.0115E-03	Cables 15 & 34
46	0.037326	-	-	2.1107E-03	Cables 16 & 33
47	0.040313	-	-	2.1563E-03	Cables 17 & 32
48	0.043299	-	-	2.179E-03	Cables 18 & 31
49	0.047778	-	-	2.4008E-03	Cables 19 & 30
50	0.050764	-	-	2.3303E-03	Cables 20 & 29
51	0.05375	-	-	2.0271E-03	Cables 21 & 28
52	0.058229	-	-	2.5415E-03	Cables 22 & 27
53	0.056736	-	-	3.3491E-03	Cables 23 & 26
54	0.074653	-	-	3.4066E-03	Cables 24 & 25

**3.2.5. Details of the Model**

A detailed 3-D finite element model of the bridge is developed. This model was used for both the static and dynamic analysis of the bridge. The main structural members of the Owensboro cable-stayed bridge are the edge girders, cables, floor beams, center beam, decks and towers that are discretized by different finite elements. The finite elements used for modeling the bridge are described below.

Modeling of the cable is possible in the ANSYS by employing the tension-only truss elements and utilizing its stress stiffening capability. The element is nonlinear and requires an iteration solution. All cable members of the Owensboro cable-stayed bridge are designed to sustain the tension force only and hence modeled by 3-D tension-only

truss elements (LINK10) but the section properties are different. Each cable between the edge girder and the tower are modeled as a single finite element. The stiffness is removed with this element if the element goes into compression. Both stress stiffening and large displacement capability are available. The stress stiffening capability is needed for analysis of structures with a low or non-existing bending stiffness as is the case with cables. Hence, an important feature input for this element is the initial strain in the element. This initial strain is used in calculating the stress stiffness matrix for the first cumulative iteration. In the model, initial strains are the final stay tension that is from the part 4 in this report.

The columns, heads and struts of the towers are modeled as 3-D elastic beam elements (BEAM4). The large deflection capability of 3-D elastic beam elements is available.

The edge girders and center beams are modeled as 3-D elastic beam elements (BEAM4) because of their continuous natural across many panels. The floor beams are also modeled as 3-D elastic beam elements (BEAM4) to provide tension, compression, bending and torsion stiffness.

The aforementioned bridge deck is presented with a triple-girder model. In the triple-girder model, a central girder, i.e. the center beam, is located at the centroid of the original bridge deck. Two side girders, i.e., the edge girders, of the same section properties are symmetrically located at the corresponding cable planes. The decks may be distributed over these three girders in the model. For the triple-girder model, we may obtain the equivalent mass and stiffness of the central girder and two side girders by referring to Zhu et al.'s work (2000). In the triple-girder model, the transverse connection between the central girder and the side girder is generally simplified as the rigid link. In the current model, the stiffness of the floor beam may be properly raised by increasing the elastic modulus.

In addition, the fixed bearings and expansion bearings that connect the edge girders and towers are modeled as 3-D elastic beam elements (BEAM4) with larger bending stiffness. For the purpose of latter parametric study and model calibration through *in-situ* dynamic testing, all material properties and real constants that reflect effectively the properties of individual structural members are listed in Tables 3.4 and 3.5, respectively. The initial strains in Table 3.5 are obtained by considering the initial tension forces in the cables listed in Table 3.7.

**Table 3.4** Material Properties

Group No.	Young's modulus (lb/ft <sup>2</sup> )	Poisson's ratio	Mass density (lb/ft <sup>3</sup> )	Structural member
1	$6.358 \times 10^8$	0.2	150	Towers
2	$4.176 \times 10^9$	0.3	490	Cables
3	$4.176 \times 10^9$	0.3	710.5	Edge girders
4	$4.176 \times 10^9$	0.3	695.1	Edge girders
5	$4.176 \times 10^9$	0.3	752.3	Edge girders
6	$4.176 \times 10^9$	0.3	747.5	Edge girders
7	$4.176 \times 10^9$	0.3	757.3	Edge girders
8	$4.176 \times 10^9$	0.3	742.9	Edge girders
9	$4.176 \times 10^9$	0.3	740.9	Edge girders
10	$4.176 \times 10^9$	0.3	755.1	Edge girders
11	$4.176 \times 10^9$	0.3	745.4	Edge girders
12	$4.176 \times 10^9$	0.3	750.2	Edge girders
13	$4.176 \times 10^9$	0.3	740.9	Edge girders
14	$4.176 \times 10^9$	0.3	728.6	Edge girders
15	$4.176 \times 10^9$	0.3	759.6	Edge girders
16	$4.176 \times 10^9$	0.3	754.5	Edge girders
17	$4.176 \times 10^9$	0.3	749.7	Edge girders
18	$4.176 \times 10^9$	0.3	745	Edge girders
19	$4.176 \times 10^9$	0.3	750.2	Edge girders
20	$4.176 \times 10^9$	0.3	740.9	Edge girders
21	$4.176 \times 10^9$	0.3	886.2	Center beam
22	$4.176 \times 10^{12}$	0.3	490	Floor beams
23	$4.176 \times 10^9$	0.3	490	Bearings

**Table 3.5** Real Constants

Type	Cross-section Area: (ft <sup>2</sup> )	Inertia moment: (ft <sup>4</sup> )		Initial strain	Structural member
		I <sub>zz</sub>	I <sub>yy</sub>		
1	3.33	35.031	0.25233	-	Edge girder
2	3.58	38.066	0.25288	-	Edge girder
3	2.7988	8.4107	0.25209	-	Edge girder
4	2.8508	8.5227	0.25222	-	Edge girder
5	2.7467	8.2983	0.25199	-	Edge girder
6	2.903	8.6344	0.25238	-	Edge girder
7	2.9264	8.8194	0.26226	-	Edge girder
8	2.7701	8.4879	0.26188	-	Edge girder
9	2.8743	8.7091	0.26211	-	Edge girder
10	2.8222	8.5986	0.26198	-	Edge girder
11	2.9264	9.164	0.31623	-	Edge girder
12	3.0774	10.123	0.39026	-	Edge girder
13	2.7232	8.1005	0.24211	-	Edge girder
14	2.7753	8.2152	0.24221	-	Edge girder
15	2.8274	8.3292	0.24233	-	Edge girder
16	2.8795	8.4427	0.24249	-	Edge girder
17	2.8222	8.7785	0.28901	-	Edge girder
18	2.9264	9.0061	0.28924	-	Edge girder
19	7.4139	98.031	5448.7	-	Center beam
20	0.3919	0.02483	1.6034	-	Floor beam
21	83	2486.3	2870.2	-	Tower (lower)
22	64.5	1894.4	638.6	-	Tower (upper)
23	58.5	613.9	1829.2	-	Tower (strut)
24	159.36	3399.7	1317.4	-	Tower (head)
25	142.72	3044.7	946.31	-	Tower (head)
26	128	2730.7	682.67	-	Tower (head)
27	126.72	2703.4	662.4	-	Tower (head)
28	122	2602.7	591.1	-	Tower (head)
29	121.28	2587.3	580.7	-	Tower (head)
30	52	69	732	-	Bearing
31	0.059722	-	-	3.6130E-03	Cables 1 & 49
32	0.058229	-	-	3.5285E-03	Cables 2 & 50
33	0.086597	-	-	3.7096E-03	Cables 3 & 51
34	0.044792	-	-	3.5552E-03	Cables 4 & 52
35	0.050764	-	-	3.6605E-03	Cables 5 & 53
36	0.047778	-	-	3.7440E-03	Cables 6 & 54
37	0.044792	-	-	3.6995E-03	Cables 7 & 55
38	0.041806	-	-	2.2396E-03	Cables 8 & 56
39	0.038819	-	-	1.8568E-03	Cables 9 & 57
40	0.035833	-	-	1.9514E-03	Cables 10 & 58

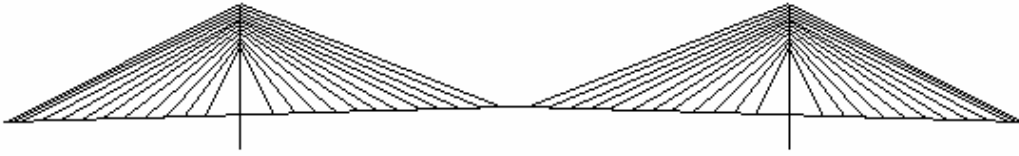
**Table 3.5 Continued** Real Constants

Type	Cross-section Area: (ft <sup>2</sup> )	Inertia moment: (ft <sup>4</sup> )		Initial strain	Structural member
		I <sub>zz</sub>	I <sub>yy</sub>		
41	0.026875	-	-	2.0494E-03	Cables 11 & 59
42	0.037326	-	-	1.0586E-03	Cables 12 & 60
43	0.037326	-	-	1.1035E-03	Cables 13 & 61
44	0.026875	-	-	2.0226E-03	Cables 14 & 62
45	0.035833	-	-	2.0115E-03	Cables 15 & 63
46	0.037326	-	-	2.1107E-03	Cables 16 & 64
47	0.040313	-	-	2.1563E-03	Cables 17 & 65
48	0.043299	-	-	2.1790E-03	Cables 18 & 66
49	0.047778	-	-	2.4008E-03	Cables 19 & 67
50	0.050764	-	-	2.3303E-03	Cables 20 & 68
51	0.053750	-	-	2.0271E-03	Cables 21 & 69
52	0.058229	-	-	2.5415E-03	Cables 22 & 70
53	0.056736	-	-	3.3491E-03	Cables 23 & 71
54	0.074653	-	-	3.4066E-03	Cables 24 & 72
55	0.074653	-	-	3.4066E-03	Cables 25 & 73
56	0.056736	-	-	3.3491E-03	Cables 26 & 74
57	0.058229	-	-	2.5415E-03	Cables 27 & 75
58	0.053750	-	-	2.0271E-03	Cables 28 & 76
59	0.050764	-	-	2.3303E-03	Cables 29 & 77
60	0.047778	-	-	2.4008E-03	Cables 30 & 78
61	0.043299	-	-	2.1790E-03	Cables 31 & 79
62	0.040313	-	-	2.1563E-03	Cables 32 & 80
63	0.037326	-	-	2.1107E-03	Cables 33 & 81
64	0.035833	-	-	2.0115E-03	Cables 34 & 82
65	0.026875	-	-	2.0226E-03	Cables 35 & 83
66	0.037326	-	-	1.1035E-03	Cables 36 & 84
67	0.037326	-	-	1.0586E-03	Cables 37 & 85
68	0.026875	-	-	2.0494E-03	Cables 38 & 86
69	0.035833	-	-	1.9514E-03	Cables 39 & 87
70	0.038819	-	-	1.8568E-03	Cables 40 & 88
71	0.041806	-	-	2.2396E-03	Cables 41 & 89
72	0.044792	-	-	3.6995E-03	Cables 42 & 90
73	0.047778	-	-	3.7440E-03	Cables 43 & 91
74	0.050764	-	-	3.6605E-03	Cables 44 & 92
75	0.044792	-	-	3.5552E-03	Cables 45 & 93
76	0.086597	-	-	3.7096E-03	Cables 46 & 94
77	0.058229	-	-	3.5285E-03	Cables 47 & 95
78	0.059722	-	-	3.6130E-03	Cables 48 & 96

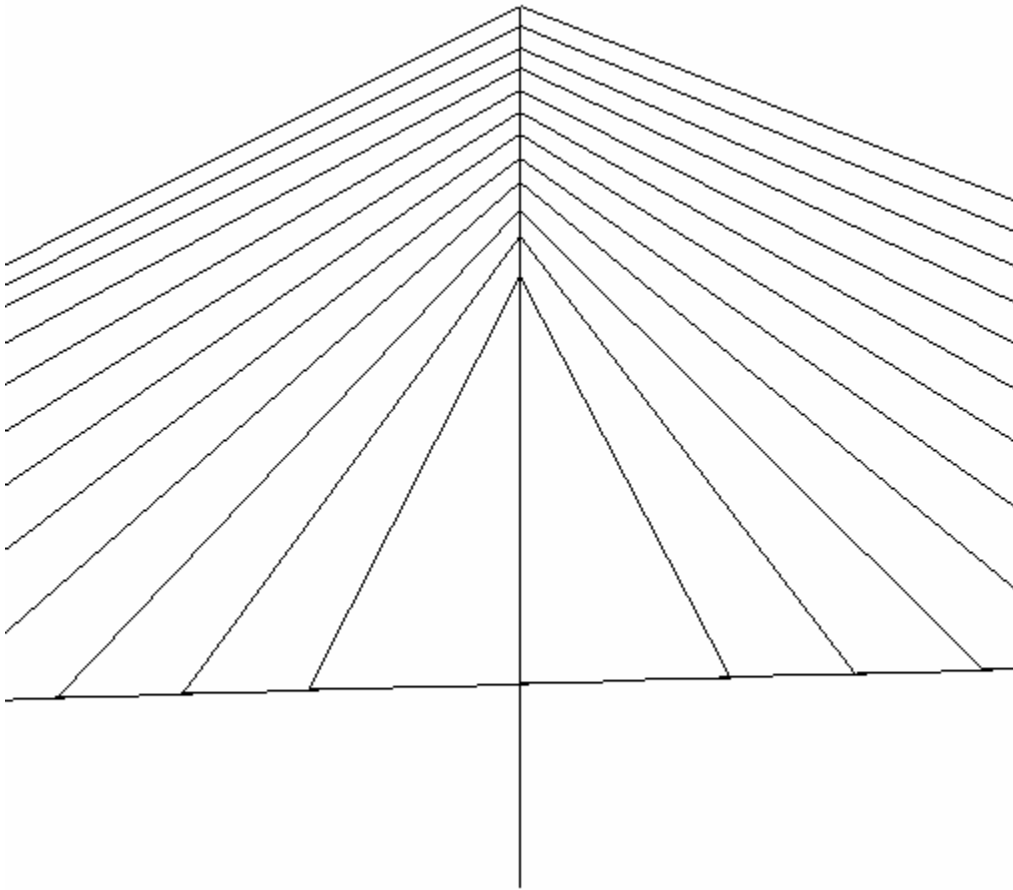
The finite element model of the Owensboro cable-stayed bridge totally consists of 668 nodes and 1087 finite elements that include 991 BEAM4 elements and 96 LINK10 elements. As a result, the number of active degree of freedom (DOF) is 3960. The details of the model such as element types, material types and real constant types are summarized in Table 3.6 for individual structural members. The detailed 3-D finite element models are shown in Figures 3.3-3.5.

**Table 3.6** Details of the Model

Member	Element Type	Material Type	Real Constant Type
Edge girder	BEAM4	3-20	1 - 18
Floor beam	BEAM4	22	20
Center beam	BEAM4	21	19
Tower upper leg	BEAM4	1	22
Tower lower leg	BEAM4	1	21
Tower tie strut	BEAM4	1	23
Tower head	BEAM4	1	24-29
Cable	LINK10	2	31 - 78
Bearing	BEAM4	23	30

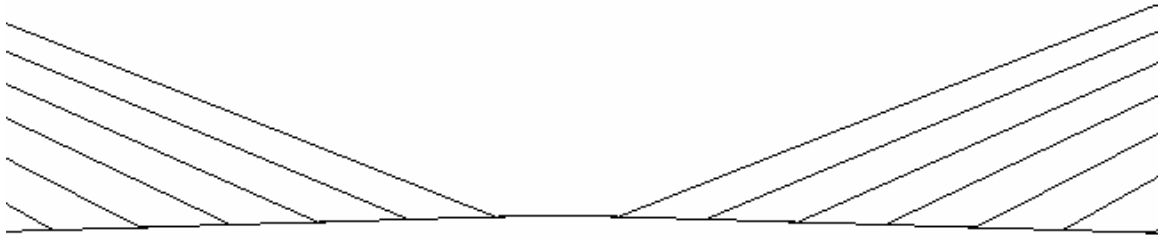


Full Elevation



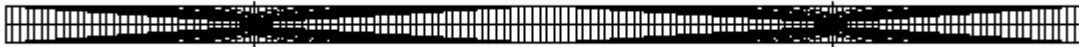
Part Elevation – Tower and Cables

**Figure 3.3** Elevation of Finite Element Model

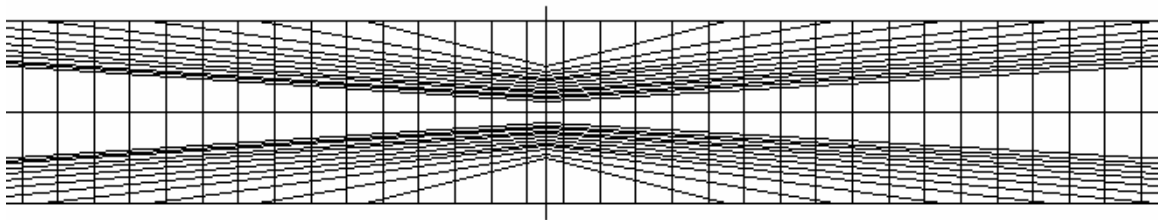


Part Elevation – Central Span

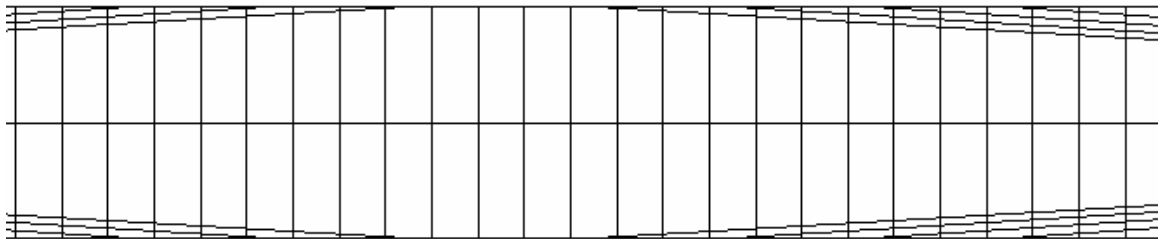
**Figure 3.3 Continued** Elevation of Finite Element Model



Full Plan

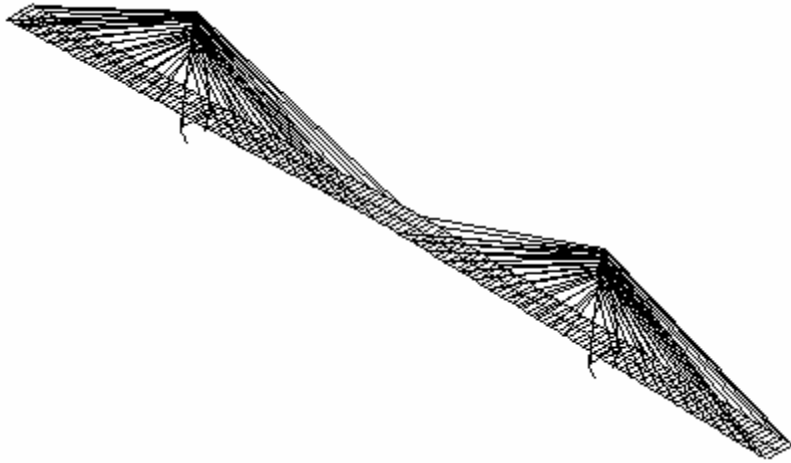


Part Plan – Tower, Edge Girders, Center Beam and Floor Beams

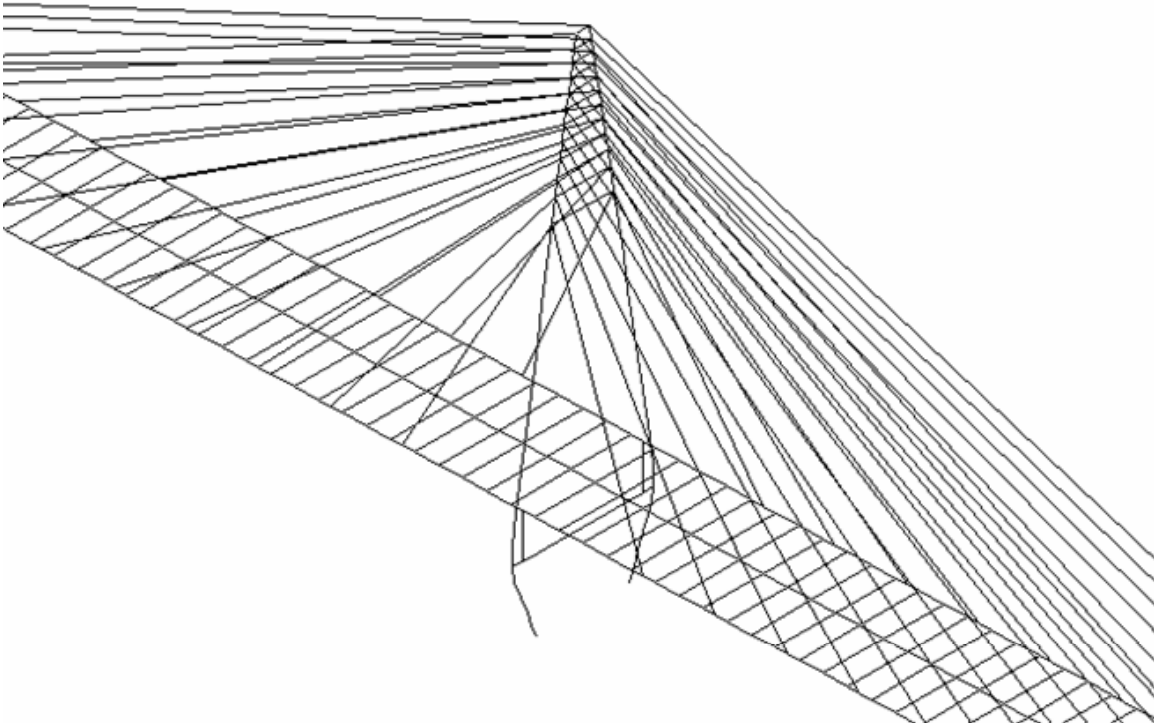


Part Plan – Central Span, Edge Girders, Center Beam and Floor Beams

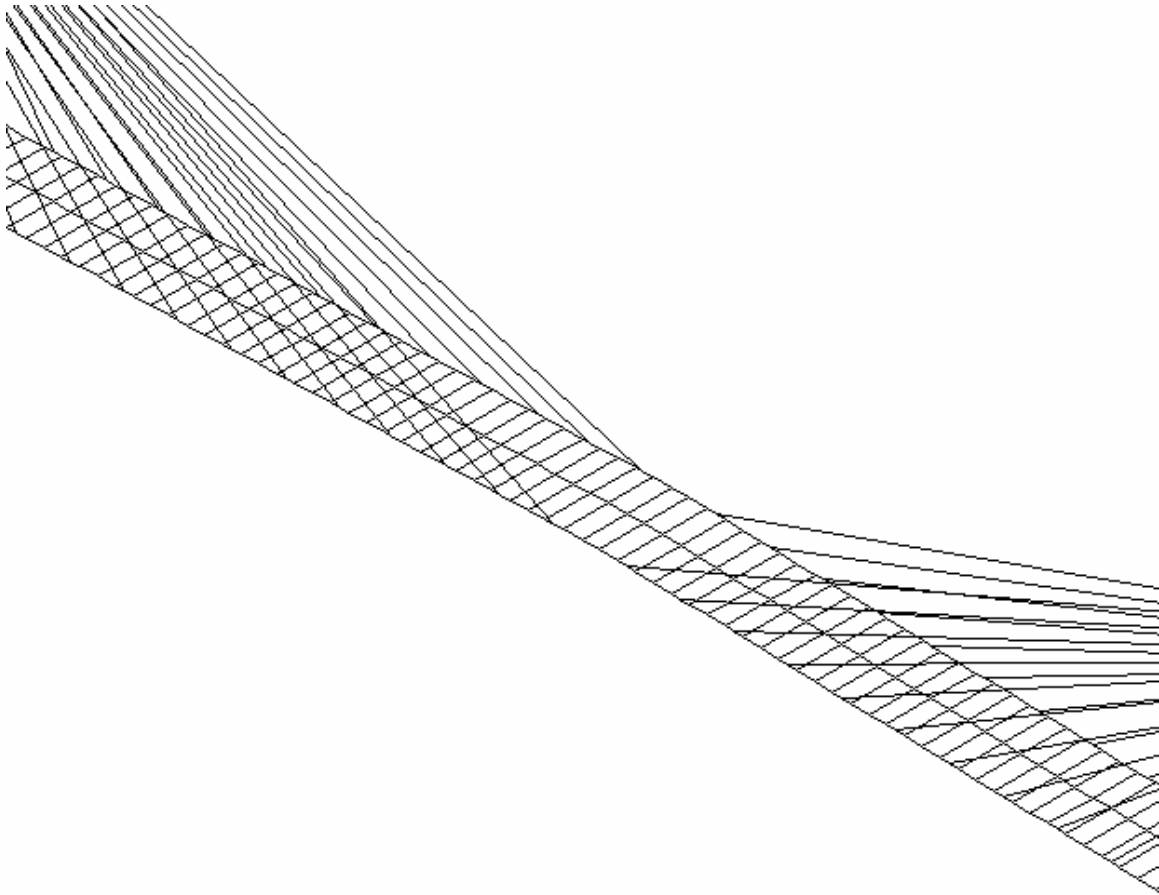
**Figure 3.4** Plan of Finite Element Model



Full Elevation – Isotropic



Part Elevation – Tower and Cables



Part Elevation – Central Span

**Figure 3.5** Isotropic Elevation of Finite Element Model

### **3.2.6. Boundary Conditions**

The boundary conditions of an actual bridge are always complex but are often idealized as fixes, hinges and rollers in the analytical model. In current model, the towers of the Owensboro cable-stayed bridge are treated as being fixed in all degrees-of-freedom at the bases. The north and south ends of the deck are connected to the approaches by a tension-link mechanism that permits the end of the deck to rotate freely about the vertical (y) and transverse (z) axes. Rotation about the longitudinal axis (x) and all three translational degree of freedom are modeled as fixed at each end of the deck.

The connection of the deck to the towers presented a special challenge to the development of the finite element model. For the connection of the deck to the towers,

the deck-tower bearings are simulated using two rigid vertical links. These two links are used to connect two edge girders to the tower tie strut. In order to restrain the relative motions between deck and tower, the relative three translational motions and two rotations about longitudinal (x) and vertical (y) axes between deck and tower are coupled; the only relative motion possible is a free rotation of the deck with respect to the tower cross-beam, about the z axis.

### **3.3. Static Analysis under Dead Load**

In the design of cable-stayed bridges, the dead load often contributes most of bridge loads. The dead load has a significant influence on the stiffness of a cable-stayed bridge. In the finite element analysis, this influence can be considered by the static analysis under dead loads before the live load or dynamic analysis is carried out. The objective of the static analysis process is intended to achieve the deformed equilibrium configuration of the bridge due to dead loads in which the structural members are “pre-stressed”. After doing the deformed equilibrium configuration, the real analysis is followed. Consequently, the dead load effect on the stiffness is included in the analysis.

For the static analysis of the Owensboro cable-stayed bridge under dead loads, the dead load value of the deck can be given by considering the volume of the deck and the density of the concrete. Actually, the deck loads are transferred from the edge girders, center beams and floor-beams to the stayed cables and towers. Thus in the finite element analysis, the dead load is equivalently distributed to the center beam and the two edge girders.

The capabilities of the static analysis procedure in the ANSYS include large deflections (geometrically nonlinear analysis) and stress stiffening. Since the structure involves non-linearity, an iterative solution associated with the Newton-Raphson solution procedure is required.

**3.3.1. Initial Tension in the Cables**

A cable-stayed bridge directly derives its stiffness from the cable tension. The final geometry of the bridge due to the dead load is known from the drawing of the Owensboro cable-stayed bridge plans. Referring to the drawing, we have modeled the initial geometry of the bridge, which is really the shape of the bridge under the dead load. Actually, the bridge deck was stayed piece by piece from the cable. And thus the cable stretched and deflected down until almost all of the deck was stayed from the cables, resting on each end on the towers.

It turns out that the ideal finite element model of a cable-stayed bridge should be such that on application of the dead load, the geometry of the bridge does not change; this is indeed the final geometry of the bridge. In other words, the deformed configuration of the bridge under the self-weight should be as close to the initial geometry. This can be approximately realized by manipulating the initial tension force in the cables that is specified as an input quantity (pre-strain) in the cable elements. Hence, the bridge can be modeled in the final geometry with a pre-tension force in the cables. In such a way, the initial tension force in the cables plays an important role. The initial tension force in the cables can be obtained by the testing. The initial tension forces in the cables of the model are listed in the table 3.7 from the chapter 4, Cable Testing and Modeling.

**Table 3.7** Initial Tension Forces in the Cables

Cable Number	Cable Designs' Axial Force (kips)	Final Stay Tension Dead Load Only Upstream Cable (kips)	Final Stay Tension Dead Load Only Downstream Cable (kips)
1	901	N/A	N/A
2	881	845	871
3	1316	1366	1317
4	612	659	671
5	713	714	838
6	654	768	726
7	591	713	671
8	388	391	N/A
9	388	301	N/A
10	305	301	283
11	230	N/A	N/A

**Table 3.7 Continued** Initial Tension Forces in the Cables

Cable Number	Cable Designs' Axial Force (kips)	Final Stay Tension Dead Load Only Upstream Cable (kips)	Final Stay Tension Dead Load Only Downstream Cable (kips)
12	152	146	165
13	150	164	172
14	227	N/A	N/A
15	298	301	213
16	330	329	311
17	370	363	311
18	413	384	394
19	471	479	449
20	506	494	449
21	523	447	455
22	604	618	596
23	624	737	850
24	957	1062	1062
25	550	458	452
26	623	613	639
27	601	585	560
28	519	468	498
29	502	466	422
30	483	500	435
31	417	422	407
32	366	N/A	411
33	327	N/A	N/A
34	300	219	260
35	227	255	283
36	150	143	184
37	152	156	156
38	236	255	255
39	305	246	N/A
40	383	477	477
41	390	394	338
42	478	425	394
43	474	466	477
44	653	597	602
45	615	658	616
46	1311	1290	1313
47	888	846	910
48	901	N/A	N/A

### **3.3.2. Geometric Non-linearity**

For the static analysis, it is well known that a long span cable-stayed bridge exhibits geometrically nonlinear characteristics that are reflected in the nonlinear load-deflection behavior under any load conditions. These geometrically nonlinear sources may come from

- The large deflection effect due to changes in geometry;
- The combined axial load and bending moment interaction effect;
- The sag effect due to changes in cable tension load levels.

In the structural analysis for small deflection, the geometric change of the structure is always assumed to be small and can be neglected so that all quantities, such as force and deformation, are determined by the original configuration of the structure. In such a case, the overall stiffness of the structure in the deformed configuration is assumed to be equal to the stiffness of the un-deformed configuration, in order to make the analysis simpler. However, a large deflection solution is required whenever the displacements are large enough so that the structural stiffness matrix based on the initial geometry does not characterize the deformed structure. Since cable-stayed bridges are highly flexible structural system, the displacements under normal working loads are deemed to be large enough to warrant a nonlinear analysis that accounts for the rigid body motion of the structure. The geometric change can be no longer neglected. In this case, the bridge stiffness must be always updated in the simultaneous deformed configuration. Due to this simultaneous deformed configuration is also an unknown, the iteration techniques should be used.

In the ANSYS, the capability for large deflection analysis is available for most of the structural element types. The large deflection is accounted for by reorienting the stiffness into its new configuration through updating the nodal locations. In the geometrically nonlinear analysis, the deformations are characterized by the large displacements and large rotations, but small strains. This is consistent with the fact that

most of structures behave. The total Lagrange (T.L.) formulation is employed in which the basic working variable is the total displacement vector rather than the incremental displacement vector as the updated Lagrange (U.L.) formulation does.

The main girders and towers of a cable-stayed bridge are often the structural members subjected to both the axial force and the bending moment. In the linear structural analysis, the axial stiffness and the flexural stiffness are considered to be uncoupled. However, if the deformations are no longer small, these structural members are subjected to an interaction between the axial force (tension or compression) and the bending moment. The additional bending moment would be caused by a simultaneously axial force applied due to the lateral deformation of a bending member and the flexural stiffness of the member would be altered. As a result, the effective bending stiffness of the member will decrease for a compressive axial force and increase for a tensile axial force. On the other hand, the presence of bending moments will affect the axial stiffness of the member due to an apparent shortening of the member caused by bending deformations. For the case of cable-stayed bridges, the large deformation may occur. The interaction between the axial force and the bending moment might be significant and should be considered. This effect can be included in the geometric stiffness matrix by using geometrically nonlinear analysis.

For a cable, supported at its ends and subjected to its own weight and an externally applied axial force, it sags into the shape of a catenarian. The axial stiffness of the cable varies nonlinearly as a function of cable tension force, which in turn changes with the distance of cable ends. For conventional truss members the sag due to self-weight can be ignored but for cable members this sag should be considered for the accurate analysis. Indeed, the sag phenomenon of individual cables results in geometrically nonlinear behavior of cable-stayed bridges. The sagging cable problem needs an explicit stress stiffness matrix included in the mathematical formulation to provide numerical stability. Basically, the cable sag effect can be included by introducing axial strains in the cables and running a static stress-stiffening analysis to determine an equilibrium configuration where the cables are “pre-stressed”.

The cable sag can be accounted for in the ANSYS by employing the tension-only truss element and utilizing its stress-stiffening capability in conjunction with a large deflection analysis. The stress stiffening is an effect that causes a stiffness change in the element due to the loading or stress within the element. The stress-stiffening capability is needed for the analysis of structures with a low or non-existent bending stiffness as is the case with cables. Physically, the stress-stiffening represents the coupling between the in-plane and transverse deflections within the structure. This coupling is the mechanism used by thin flexible structures to carry the lateral loads. As the in-plane tensile force increases, the capacity to assume the lateral loads increases. In other words, the transverse stiffness increases as the tensile stress increases. More details can be found in the ANSYS references.

The finite element model described previously is used here to reveal the large deflection effect on the structural behavior of the Owensboro cable-stayed bridge due to the dead load. Table 3.8 shows the comparison of the maximum deck deflection between small deflection analysis and large deflection analysis. It is clearly shown that the large deflection has almost no effect on the deck deflection due to dead load alone. This is consistent with the observation that the maximum deck deflection of the bridge is very limited (about 0.008 feet) due to introducing the pre-strain in the cables in which the bridge becomes quite stiffening. Further comparison between small deflection analysis and large deflection analysis without introducing the cable pre-strain, as shown in Table 3.8, has demonstrated that the large deflection does not change the deck deflection significantly even though the maximum deck deflection of the bridge is about 7 feet. Therefore, the large deflection analysis is not necessary in determining the initial equilibrium configuration of the bridge due to dead load and the small deflection analysis is enough in the current finite element model. But the stress stiffening must be always included in the static analysis of cable-supported bridges and hence the static analysis of a cable-stayed bridge is always geometrically nonlinear.

**Table 3.8** Comparison of Maximum Deflections (absolute value, ft)

Analysis type	With cable pre-strain	Without cable pre-strain
Small deformation	0.308001	6.874
Large deformation	0.315789	7.293

In the finite element modeling of a cable-stayed bridge, it is quite natural to discretize the cable between the tower and the girder into a single tension-only truss element (cable element). But two node cable elements, as we know, are relatively weak elements. However, since two end nodes of the cable element are connected with the beam elements of the tower and the girder, the nonlinear static analysis or the modal analysis can be carried out. Another key feature in the nonlinear structural analysis is the choice of convergence criterion to control the iteration procedure. The defaulted force convergence criterion in the ANSYS cannot provide an efficient iteration solution in the large deflection analysis of the Owensboro cable-stayed bridge. Sometimes the force convergence criterion results in the divergence especially when the structural deflection reaches slightly large. Instead, the displacement convergence criterion is very effective and always results in the convergent solution. In addition, as mentioned previously the stress stiffening plays an important role in the static analysis of cable-stayed bridges. The sagging of the cable requires the stress part in the stiffness matrix and results in the nonlinear analysis. Stress stiffening must be always used for sagging cable problem to provide numerical stability. Using a large deformation solution without the stress stiffening capability leads to an aborted run due to divergent oscillation.

### **3.4. Modal Analysis**

Cable-stayed bridges are more flexible than other structures because of large spans. One important aspect of such a flexible structure is a large displacement response of the deck when subject to dynamical loads. As a result, considerable amount of work has been conducted to study the dynamic behavior of cable-stayed bridges as a part of the design of wind and seismic resistance. The dynamic characteristics of a structure can be effectively analyzed in terms of natural frequencies and mode shapes. Modal analysis is needed to determine the natural frequencies and mode shapes of the entire cable-stayed

bridge. The natural frequencies and mode shapes of the Owensboro cable-stayed bridge are studied by using the current finite element model. Since the established model is a 3-D finite element model, a general modal analysis is capable to provide all possible modes of the bridge (transverse, vertical, torsion and coupled).

The modal analysis needs to solve the eigenvalue problem. The eigenvalue and eigenvector extraction technique used in the analysis is the Block Lanczos method. The Block Lanczos eigenvalue extraction method is available for large symmetric eigenvalue problems. Typically, this solver is applicable to the type of problems solved using the Subspace eigenvalue method, however, at a faster convergence rate. The Block Lanczos algorithm is basically a variation of the classic Lanczos algorithm, where the Lanczos recursions are performed using a block of vectors as opposed to a single vector. Additional theoretical details on the classic Lanczos method can be found in any textbooks on eigenvalue extraction.

#### **3.4.1. Effect of Initial Equilibrium Configuration**

As mentioned previously, the modal analysis of a cable-stayed bridge should include two steps: the static analysis loaded by the dead load and then followed by pre-stressed modal analysis. This kind of pre-stressed modal analysis is available in the ANSYS. In order to investigate the effect of initial equilibrium configuration due to the dead load and the pre-strain in the cables on the dynamic properties of the Owensboro cable-stayed bridge, the following three cases are considered:

- Case 1: the regular modal analysis without dead load effect where the modal analysis is starting from the undeformed configuration;
- Case 2: the pre-stressed modal analysis where the modal analysis follows a dead-load linear static analysis without the pre-strain in the cables;
- Case 3: the pre-stressed modal analysis where the modal analysis follows a dead-load linear static analysis with a pre-strain in the cables.

**Table 3.9** Comparison of Frequencies (Hz)

Mode Order	Case 1	Case 2	Case 3
1	0.28734	0.27731	0.29340
2	0.36567	0.34474	0.37361
3	0.52123	0.51331	0.52464
4	0.57663	0.55339	0.57900
5	0.66805	0.65227	0.67505
6	0.68444	0.67572	0.68530
7	0.70278	0.68387	0.71035
8	0.75283	0.73816	0.75806
9	0.76331	0.75064	0.76662
10	0.80528	0.78958	0.80814
11	0.81653	0.79268	0.81632
12	0.81871	0.81216	0.82163
13	0.90322	0.89117	0.90517
14	0.95013	0.91627	0.95383
15	0.95547	0.91843	0.95833
16	1.0843	1.0498	1.0873
17	1.1043	1.0746	1.1061
18	1.1425	1.1071	1.1381
19	1.1434	1.1078	1.1483
20	1.2276	1.1955	1.2283

The comparison results of frequencies among above three cases are summarized in Table 3.9. It is clearly shown that the beneficial effect of self-weight is used in improving stiffness. The cable-stayed bridge with sufficient amount of pre-strain in the cables is a highly pre-stressed structure. In the current case of the Owensboro cable-stayed bridge, the dead load effect will increase the natural frequency due to the stiffening of the structure. Therefore, the regular modal analysis without a dead-load static analysis will result in the under-estimation of the cable-stayed bridge capacity and consequently provides more safe evaluation of the bridge capacity.

Furthermore, compared with Case 2 and Case 3, the pre-strain in the cables increases the natural frequencies of the cable-stayed bridge if the pre-stressed modal analysis is used. It implies that it is the self-weight not the initial equilibrium configuration starting the vibration contributes the stiffness improvement because the pre-strain in the cables changes the initial equilibrium configuration and the distribution

of the pre-stress due to dead load. But the initial equilibrium configuration to start the vibration is obviously essential to the dynamic responses under wind or seismic loadings.

### **3.4.2. Modal Analysis Results**

To make the results close to the real situation, the pre-stressed modal analysis starting from the dead-load deformed equilibrium configuration with a pre-strain in the cables is performed here to evaluate the modal properties of the Owensboro cable-stayed bridge. The natural frequencies, mass distribution percentages and modal participation factors are summarized in Tables 3.10-11, respectively. The participation factor of particular mode demonstrates the importance of that mode. The mass fraction expresses the whole mass participation percentages before that mode. The table of the participation factor and mass distribution percentage is available in the ANSYS to provide the list of participation factors, mode coefficients and mass distribution percentages for each mode extracted. The participation factors and mode coefficients are calculated based on an assumed unit displacement spectrum in each of the global Cartesian directions.

In general, several modes of vibration contribute to the total dynamic response of the structure. For the purpose of directional uncertainty and the simultaneous occurrence of forces in the three orthogonal directions, coupling effects within each mode of vibration should be considered. Coupling effects, however, make it difficult to categorize the modes into simple vertical, transverse, or torsion, thus making comparisons with experimental measurements difficult. Most of studies are aimed to analyze the modal behavior of cable-stayed bridges in terms of pure vertical, transverse and torsion modes of vibration. Since the Owensboro cable-stayed bridge is modeled as a complete 3-D structure, all possible coupled modes can be obtained. It provides the full understanding of the dynamic behavior of the bridge.

The first ten sets of mode shapes are shown in Figures 3.6-3.15, respectively. All mode shapes are normalized to unity instead of mass matrix in order to check with the corresponding mode shapes obtained from the free vibration tests. The mode

classification can be identified by observing the mass distribution percentage, the modal participation factor and the animated mode shape and is listed in Table 3.11. It can be found that one dominated mode is always coupled with other modes. The vibration modes of the Owensboro cable-stayed bridge are complicated and coupled.

**Table 3.10** Natural Frequencies (Hz) and Mass Fraction

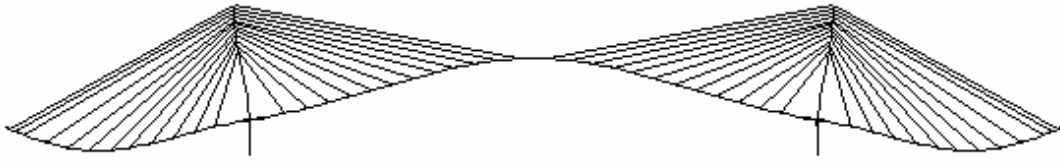
Frequency (Hz)	Mass Fraction					
	X	Y	Z	ROTX	ROTY	ROTZ
0.293403	0.80042E-23	0.104945	0.23984E-19	0.50462E-20	0.20665E-19	0.78601E-01
0.373609	0.176813	0.104945	0.25033E-19	0.59313E-20	0.21249E-19	0.119683
0.524643	0.176813	0.104945	0.221384	0.88676E-01	0.181743	0.119683
0.578998	0.176813	0.415541	0.221384	0.88676E-01	0.181743	0.352312
0.675054	0.176813	0.415541	0.221384	0.88676E-01	0.181995	0.352312
0.685296	0.176813	0.415541	0.511880	0.201439	0.420476	0.352312
0.710348	0.199770	0.415541	0.511880	0.201439	0.420476	0.511002
0.758056	0.199770	0.415541	0.511880	0.201439	0.444970	0.511002
0.766625	0.199770	0.415541	0.680656	0.236519	0.583526	0.511002
0.808145	0.199770	0.415541	0.915037	0.754355	0.775940	0.511002
0.816315	0.199770	0.415541	0.915037	0.754355	0.927145	0.511002
0.821629	0.199770	0.912095	0.915037	0.754355	0.927145	0.882910
0.905169	0.199770	0.912095	0.990145	0.994992	0.988804	0.882910
0.953834	0.381977	0.912095	0.990145	0.994992	0.988804	0.916995
0.958334	0.381977	0.912095	0.990145	0.994992	0.990562	0.916995
1.08725	0.381977	0.912095	0.990147	0.996652	0.990563	0.916995
1.10609	0.381977	0.912095	0.990147	0.996652	0.991272	0.916995
1.13813	0.381977	0.913580	0.990147	0.996652	0.991272	0.918108
1.14832	0.381977	0.913580	0.998979	0.998598	0.998522	0.918108
1.22834	0.589215	0.913580	0.998979	0.998598	0.998522	0.926461

**Table 3.11** Natural Frequencies (Hz) and Participation Factors

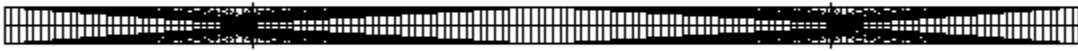
Frequency (Hz)	Participation Factor						Mode Classification
	X	Y	Z	ROTX	ROTY	ROTZ	
0.293403	-0.255E-08	272.33	-0.163E-06	-0.102E-04	0.187E-03	0.304E+06	Vertical
0.373609	380.27	0.234E-08	-0.342E-07	-0.427E-05	0.315E-04	-0.22E+ 06	Vertical
0.524643	-0.506E-08	0.161E-06	-497.36	-42806.	0.555E+06	0.194E-03	Transverse + Torsion
0.578998	0.801E-10	468.51	0.136E-06	0.157E-04	-0.176E-03	0.523E+06	Vertical

**Table 3.11 Continued** Natural Frequencies (Hz) and Participation Factors

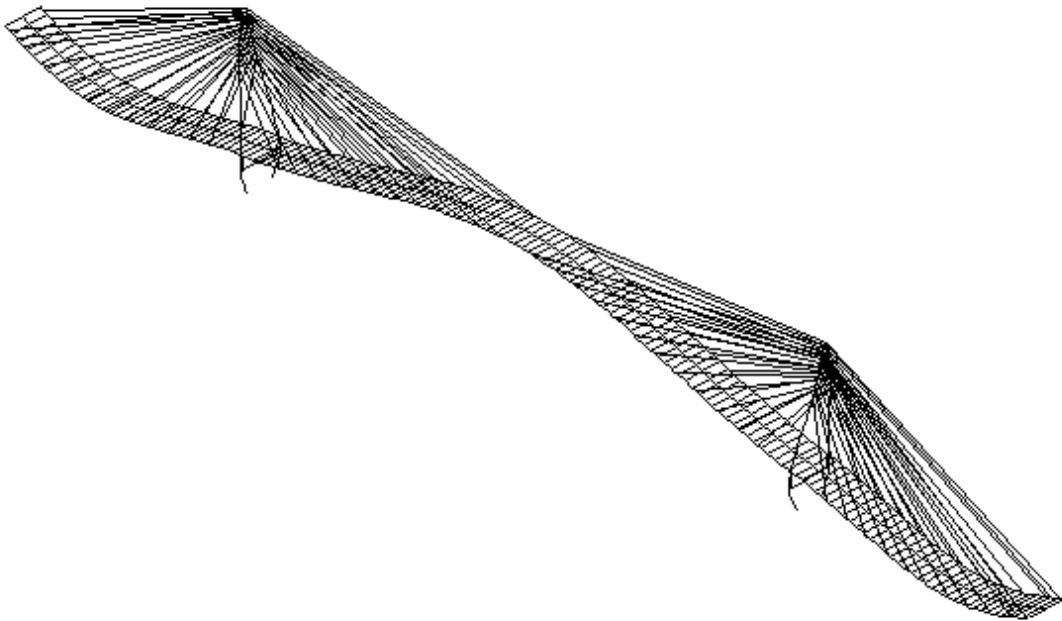
Frequency (Hz)	Participation Factor						Mode Classification
	X	Y	Z	ROTX	ROTY	ROTZ	
0.675054	-0.327E-08	-0.502E-07	0.227E-07	0.143E-05	20698.	-0.404E-04	Torsion
0.685296	0.662E-08	0.140E-06	569.73	48271.	-0.636E+ 06	0.152E-03	Transverse + Torsion
0.710348	-137.02	0.105E-08	-0.750E-08	0.486E-05	0.5209E-04	0.432E+06	Vertical
0.758056	0.797E-08	0.503E-07	0.511E-07	0.206E-05	0.204E+ 06	0.468E-04	Torsion
0.766625	-0.121E-07	0.786E-07	434.27	26924.	-0.485E+ 06	0.872E-04	Transverse + Torsion
0.808145	0.141E-07	0.340E-06	-511.76	-0.103E+ 06	0.571E+ 06	0.402E-03	Tower Sway + Torsion
0.816315	-0.272E-07	-0.188E-06	0.878E-07	0.141E-04	-0.506E+ 06	-0.193E-03	Tower Sway + Torsion
0.821629	0.931E-09	592.38	0.152E-06	0.405E-04	-0.328E-03	0.661E+06	Vertical
0.905169	-0.423E-07	0.609E-07	289.70	70515.	-0.323E+ 06	0.234E-04	Transverse + Torsion
0.953834	-386.03	0.1005E-08	-0.1105E-06	-0.176E-04	0.131E-03	-0.20E+ 06	Vertical
0.958334	0.867E-07	-0.556E-08	0.386E-08	-0.116E-05	-54653.	0.401E-04	Torsion
1.08725	0.241E-06	-0.229E-08	-1.4869	-5855.9	1661.6	0.254E-05	Torsion
1.10609	-0.164E-08	0.261E-07	-0.162E-08	0.105E-06	34699.	0.271E-04	Torsion
1.13813	0.693E-10	-32.402	-0.734E-08	0.284E-05	0.964E-05	-36209.	Vertical
1.14832	0.685E-07	0.943E-08	-99.338	6341.5	0.111E+ 06	0.181E-04	Torsion
1.22834	411.69	-0.324E-08	0.235E-07	0.367E-05	-0.261E-04	-99214.	Vertical



Elevation

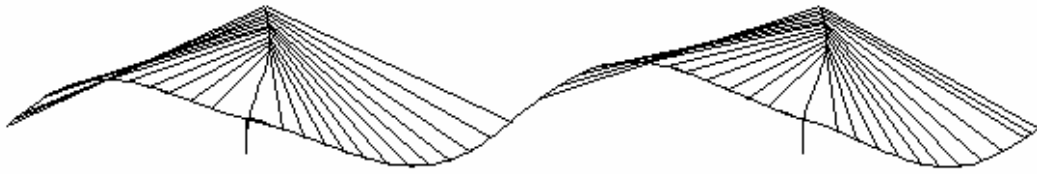


Plan



3-D View

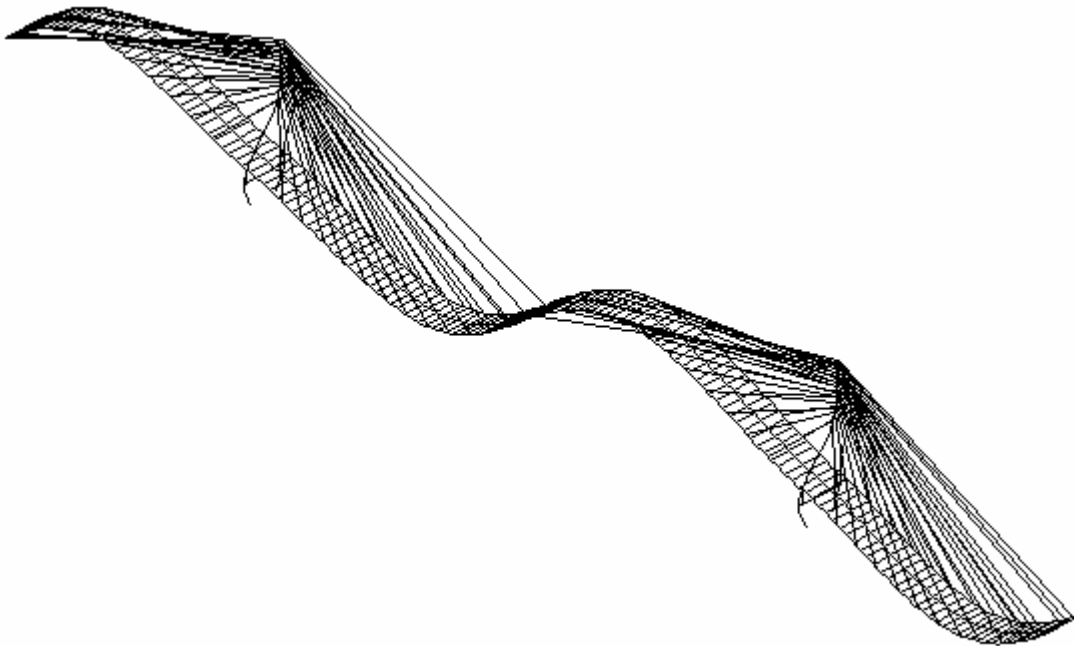
**Figure 3.6** 1st Mode Shape ( $f = 0.2934$  Hz, Vertical)



Elevation

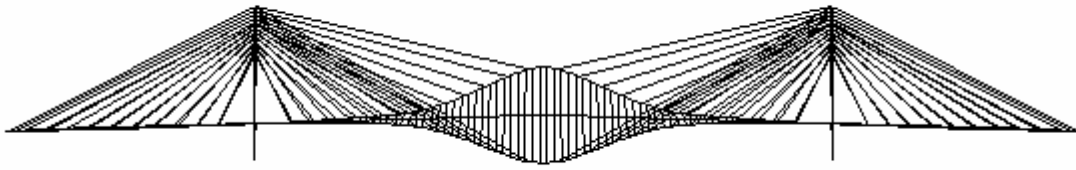


Plan



3-D View

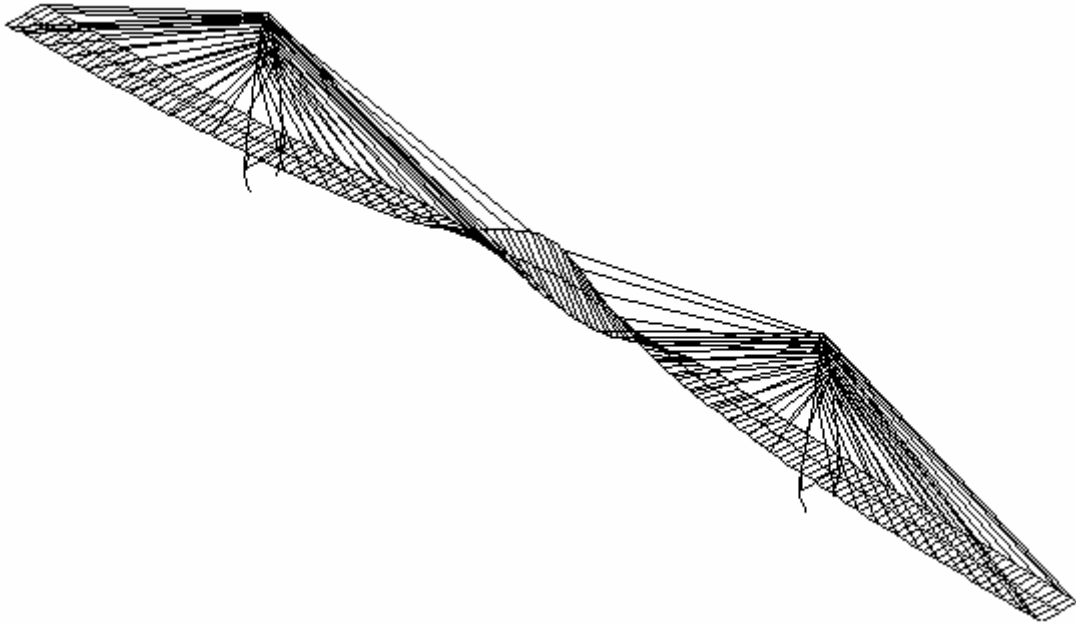
**Figure 3.7** 2nd Mode Shape ( $f = 0.3736$  Hz, Vertical)



Elevation

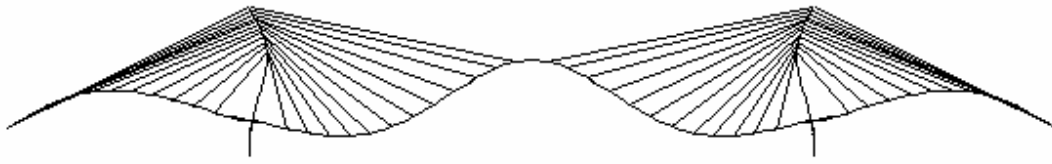


Plan

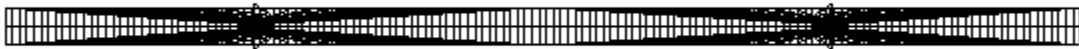


3-D View

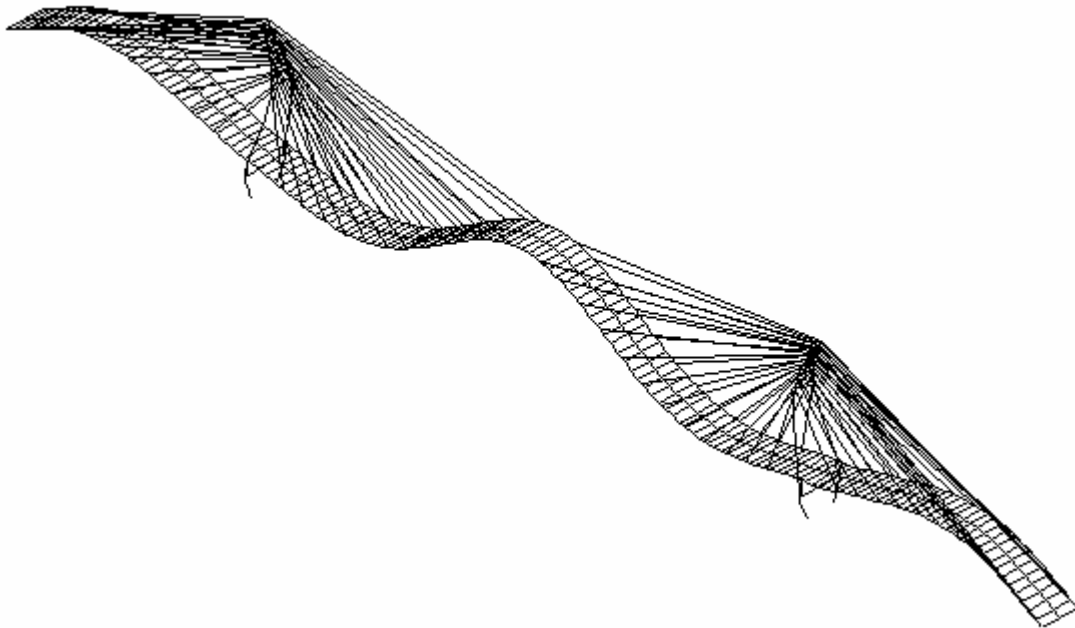
**Figure 3.8** 3rd Mode Shape ( $f = 0.5246$  Hz, Transverse + Torsion)



Elevation

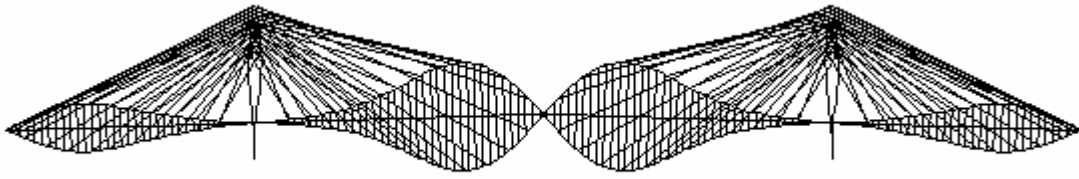


Plan



3-D View

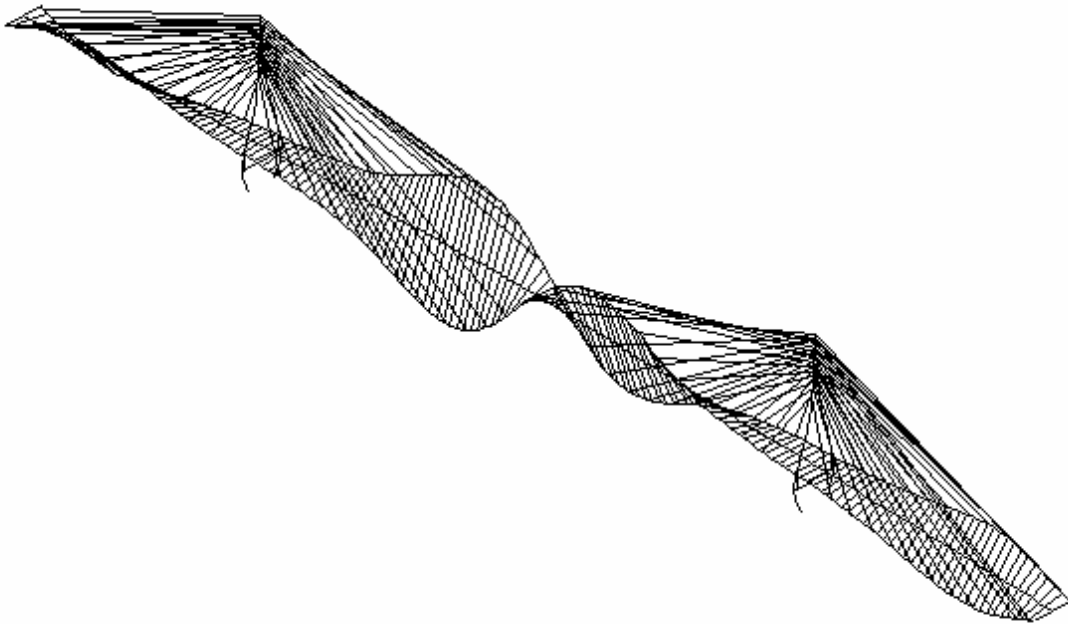
**Figure 3.9** 4th Mode Shape ( $f = 0.5790$  Hz, Vertical)



Elevation

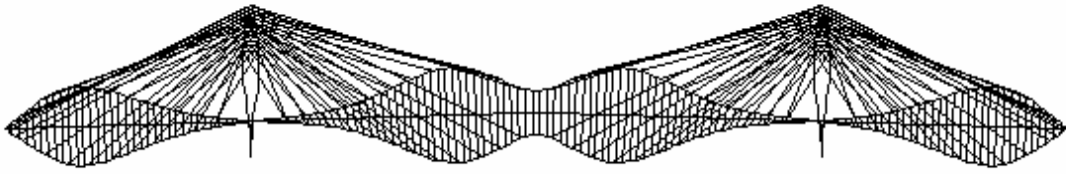


Plan



3-D View

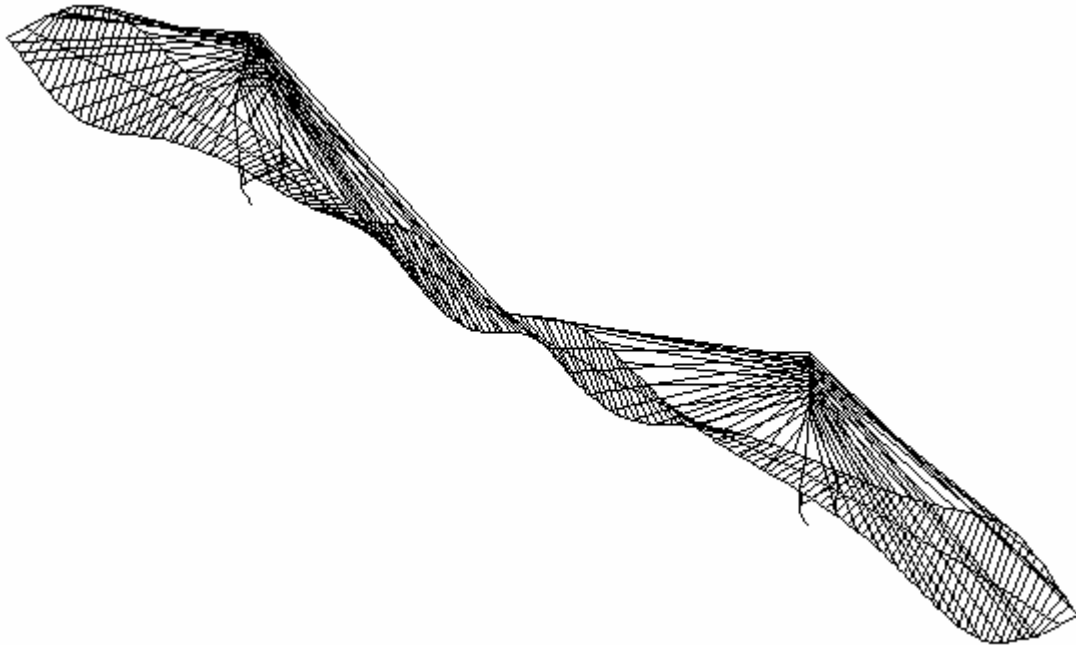
**Figure 3.10** 5th Mode Shape ( $f = 0.6751$  Hz, Torsion)



Elevation



Plan

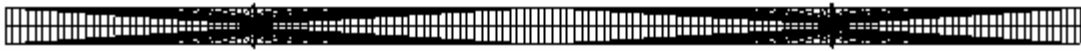


3-D View

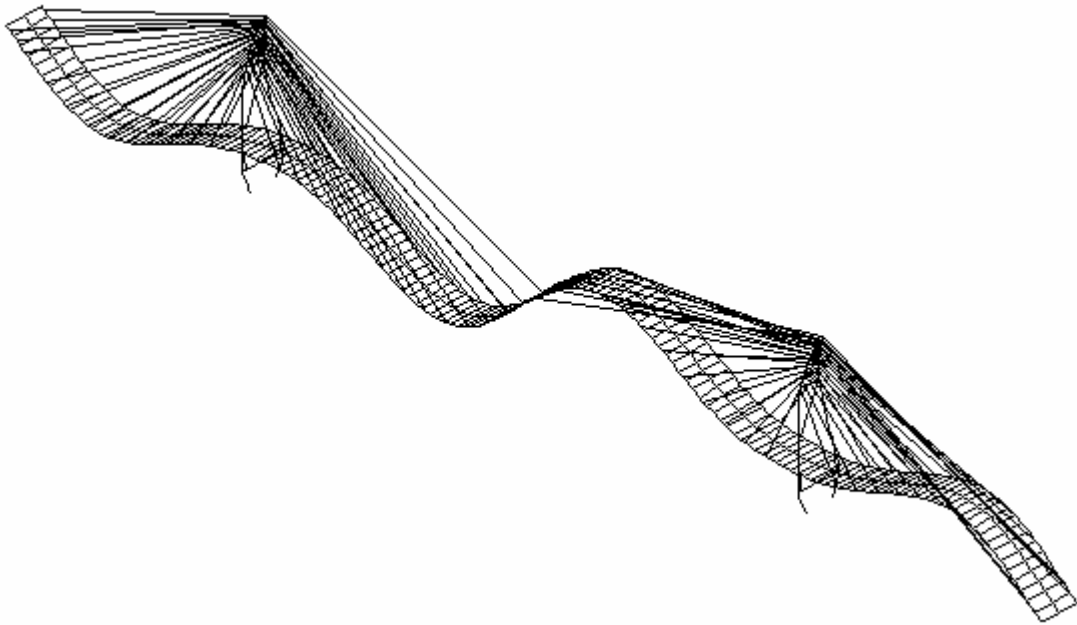
**Figure 3.11** 6th Mode Shape ( $f = 0.6853$  Hz, Transverse + Torsion)



Elevation

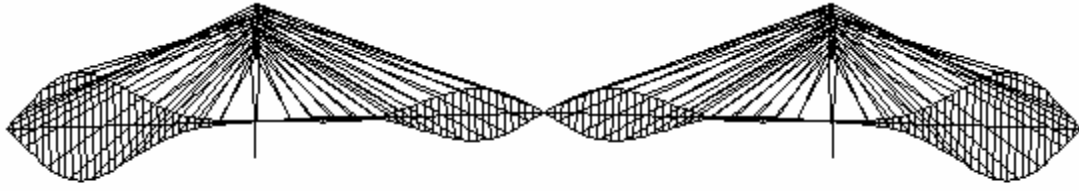


Plan



3-D View

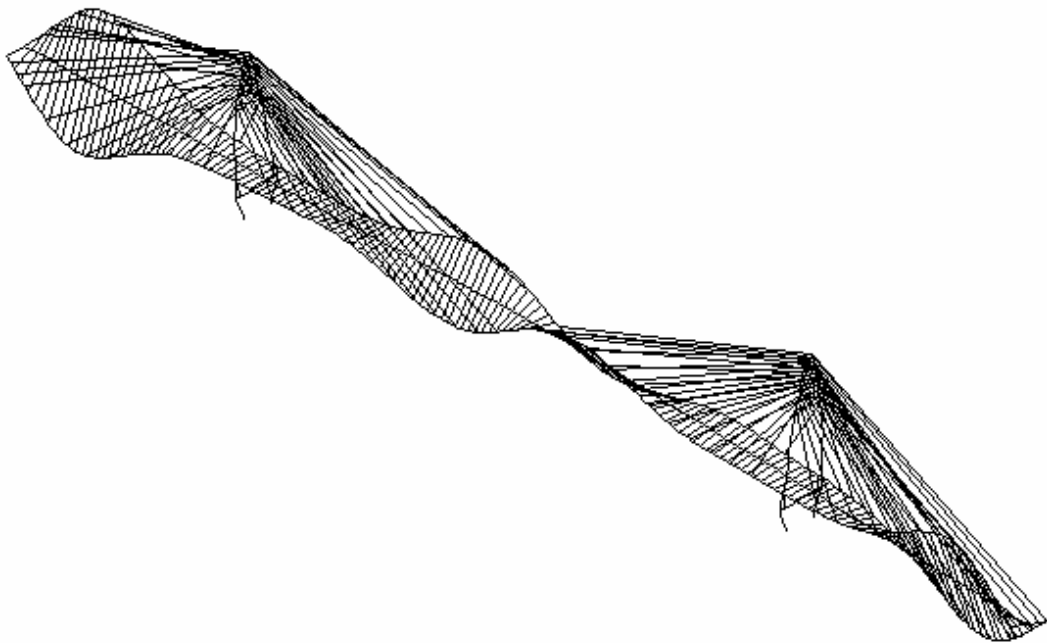
**Figure 3.12** 7th Mode Shape ( $f = 0.7103$  Hz, Vertical)



Elevation

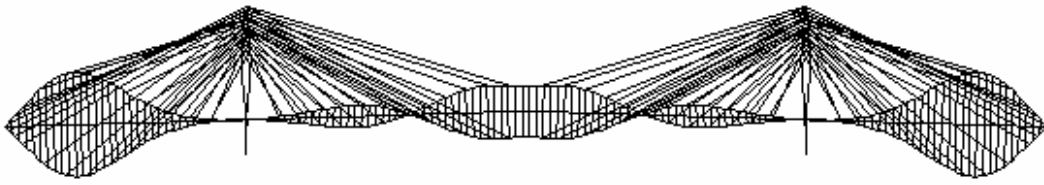


Plan



3-D View

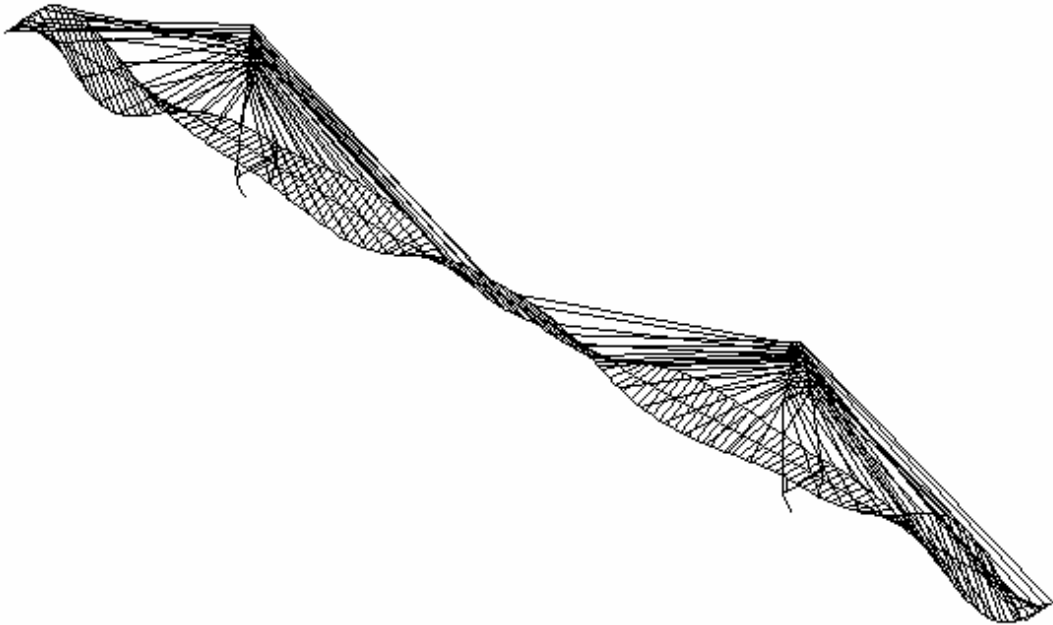
**Figure 3.13** 8th Mode Shape ( $f = 0.758$  Hz, Torsion)



Elevation

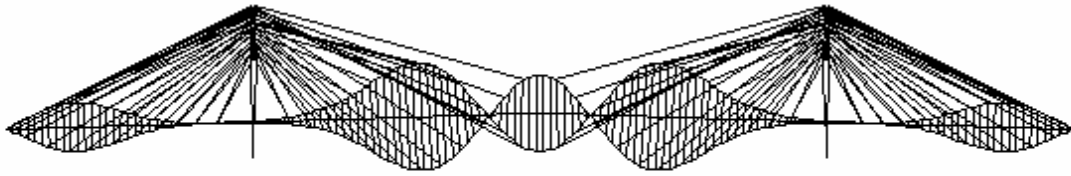


Plan



3-D View

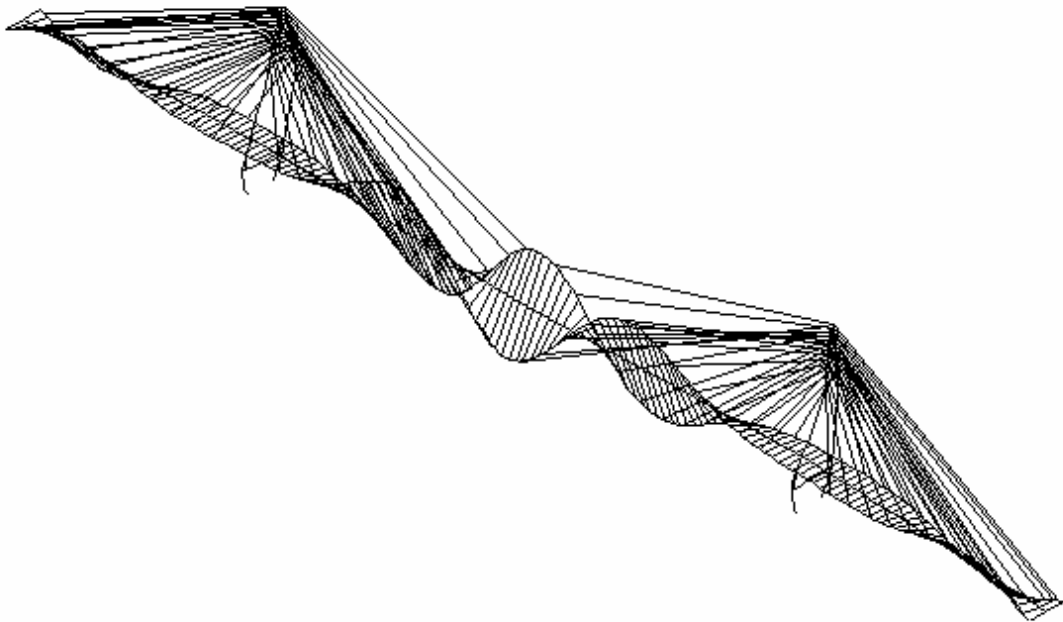
**Figure 3.14** 9th Mode Shape ( $f = 0.7666$  Hz, Transverse + Torsion)



Elevation



Plan



3-D View

**Figure 3.15** 10th Mode Shape ( $f = 0.8081$  Hz, Tower Sway + Torsion)

### 3.5. Parametric Studies

In order to calibrate the FE model of the Owensboro cable-stayed bridge with *in-situ* free vibration measurements in the sense of modal parameters, the structural and material parameters that may largely affect the modal properties of the bridge are supposed to be identified. This can be realized by the parametric studies. As mentioned previously, one of the most advantages of finite element modeling and analysis is to make the parametric studies possible. The parametric studies reported here not only prove the efficiency of the finite element methodology, but also demonstrate the extent and nature of variation in modal properties that a variation in the input parameters can cause. The FE model calibration can be conducted by adjusting these parameters to match the frequencies and mode shapes between testing and modeling. The calibrated FE model will be used as the base line for future structural evaluations of the bridge.

There are several structural and material parameters that would affect the modal behavior of the Owensboro cable-stayed bridge, such as the mass, the cable tension stiffness, the vertical and transverse bending stiffness of the deck. The effects of these parameters on the modal properties of the bridge are studied as follows.

#### 3.5.1. Deck Weight

The change of deck self weights is reflected by the relative mass density of edge girders and center beams that is defined by

$$\bar{\rho} = \frac{\rho}{\rho_0}$$

where  $\rho_0$  is the standard mass density of edge girders and center beams listed in Table 3.4. Frequencies for different deck mass density are summarized in Table 3.12. The variation of the first two frequencies with the relative mass density for the edge girders

and center beams is shown in Figure 3.16. From the Table 3.12 and Figure 3.16, it can be seen that the frequencies increase steadily with decreasing in the deck self weight.

**Table 3.12** Frequencies (Hz) for Different Deck Mass Densities

Mode order	Relative mass density $\bar{\rho} = \frac{\rho}{\rho_0}$ for the deck					
	0.0	0.25	0.5	1.0	1.5	2.0
1	0.58807	0.45698	0.37900	0.29340	0.24577	0.21433
2	0.64538	0.54422	0.46932	0.37361	0.31484	0.27403
3	0.81060	0.78892	0.70008	0.52464	0.43327	0.37607
4	0.82038	0.81688	0.74427	0.57900	0.48478	0.42169
5	1.2238	0.89530	0.81234	0.67505	0.55434	0.47901
6	1.5011	0.98511	0.82433	0.68530	0.57103	0.49699
7	1.6180	1.1963	0.92194	0.71035	0.58600	0.50731
8	1.6269	1.1993	0.95460	0.75806	0.62595	0.54092
9	1.7700	1.2248	0.96317	0.76662	0.63230	0.54759
10	1.8895	1.3912	1.0606	0.80814	0.67763	0.58574
11	1.8902	1.3946	1.0618	0.81632	0.69249	0.60110
12	2.1022	1.4059	1.1002	0.82163	0.77359	0.66762
13	2.1073	1.4140	1.1720	0.90517	0.80812	0.70423
14	2.2252	1.5996	1.2056	0.95383	0.80823	0.76242
15	2.4658	1.6635	1.3205	0.95833	0.84134	0.77113
16	2.7328	1.7188	1.3751	1.0873	0.89225	0.80128
17	2.9182	1.8664	1.4809	1.1061	0.90504	0.80129
18	2.9882	1.9620	1.5219	1.1381	0.93455	0.83245
19	3.0234	1.9802	1.5750	1.1483	0.97933	0.85859
20	3.0653	2.0183	1.5986	1.2283	1.0376	0.89784

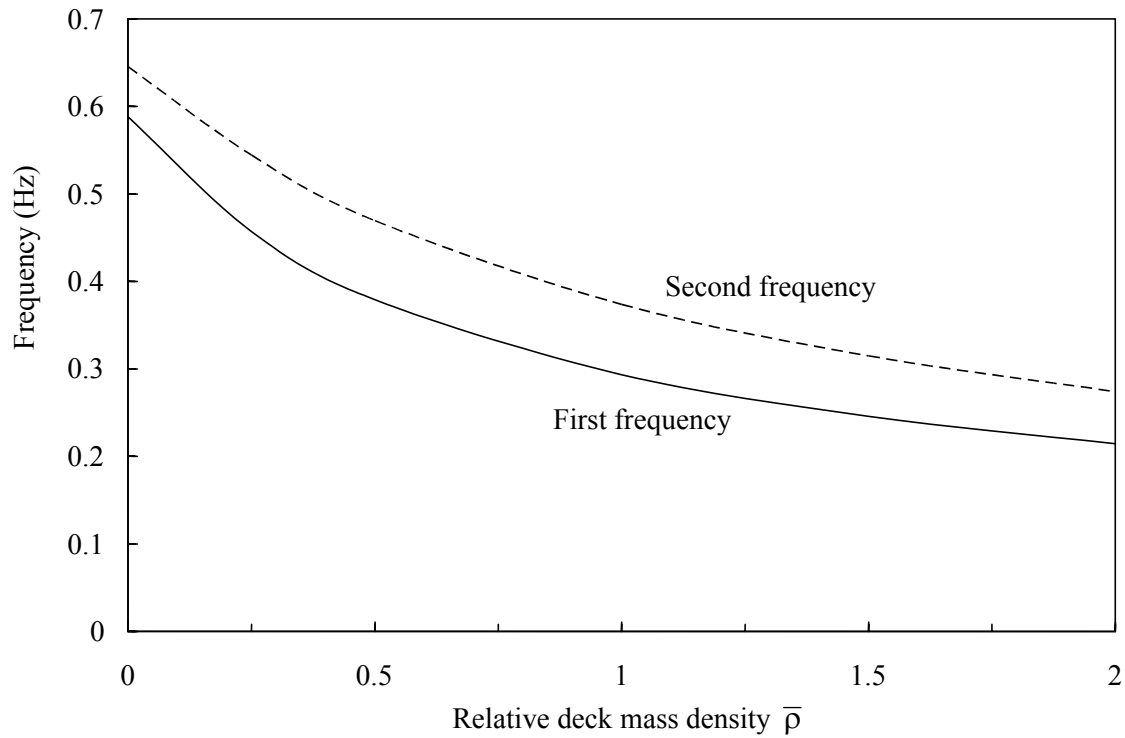


**Figure 3.16** Frequencies vs Deck Mass Density

### 3.5.2. Cable Stiffness

The tension stiffness of cables depends on the sectional area  $A$ , the elastic modulus  $E$  and the pre-strain. Because the initial tension force has been given in Table 3.7, we only study the effect of the sectional area  $A$  and elastic modulus  $E$  on the modal properties of the bridge, respectively in the following.

#### 3.5.2.1. Cable Sectional Area

The change of cable sectional areas is represented by the relative sectional area of cables that is defined by

$$\bar{A} = \frac{A}{A_0}$$

where  $A_0$  is the standard sectional area of cables given in Table 3.5. Frequencies for different cable area ratios are summarized in Table 3.13. The variation of the first two frequencies with the relative cable area is shown in Figure 3.17. It has been found that increasing the cable sectional area results in the increase of frequency values. Increasing the cable areas does result in larger tension stiffness, which is supposed to increase the frequencies, but at the same time cable weight increases with the increasing cable area, which results in reducing the frequencies. These two effects tend to compensate for each other resulting in the less increment of frequencies. It should be noted that the variation of cable areas does cause a reordering of the dominated mode shapes as they relate to the sequential natural frequency orders.

**Table 3.13** Frequencies (Hz) for Different Cable Areas

Mode order	Relative sectional area $\bar{A} = \frac{A}{A_0}$ for the cables					
	0.25	0.5	0.75	1.0	1.5	2.0
1	0.17038	0.23575	0.26902	0.29340	0.32934	0.35575
2	0.19581	0.30598	0.34735	0.37361	0.40732	0.42892
3	0.29844	0.41204	0.47855	0.52464	0.57819	0.60240
4	0.32266	0.47191	0.53568	0.57900	0.63700	0.67605
5	0.34132	0.50756	0.60508	0.67505	0.74022	0.78657
6	0.38688	0.54634	0.63949	0.68530	0.77130	0.79712
7	0.38738	0.55902	0.64218	0.71035	0.79854	0.83485
8	0.38983	0.57031	0.67846	0.75806	0.81510	0.84775
9	0.40988	0.60421	0.69966	0.76662	0.83712	0.88897
10	0.47933	0.65127	0.74696	0.80814	0.87821	0.95415
11	0.49993	0.70458	0.75728	0.81632	0.90903	1.0145
12	0.59557	0.73369	0.80973	0.82163	0.93987	1.0339
13	0.64588	0.81274	0.86491	0.90517	1.0074	1.0849
14	0.64671	0.83743	0.87765	0.95383	1.0251	1.1145
15	0.68308	0.84755	0.90650	0.95833	1.1029	1.2160
16	0.72434	0.87014	0.99317	1.0873	1.2255	1.2953
17	0.75644	0.87479	1.0023	1.1061	1.2302	1.3416
18	0.76933	0.91820	1.0420	1.1381	1.2679	1.3948
19	0.78683	0.97879	1.0778	1.1483	1.3197	1.4567
20	0.81680	1.0117	1.1427	1.2283	1.3552	1.4567

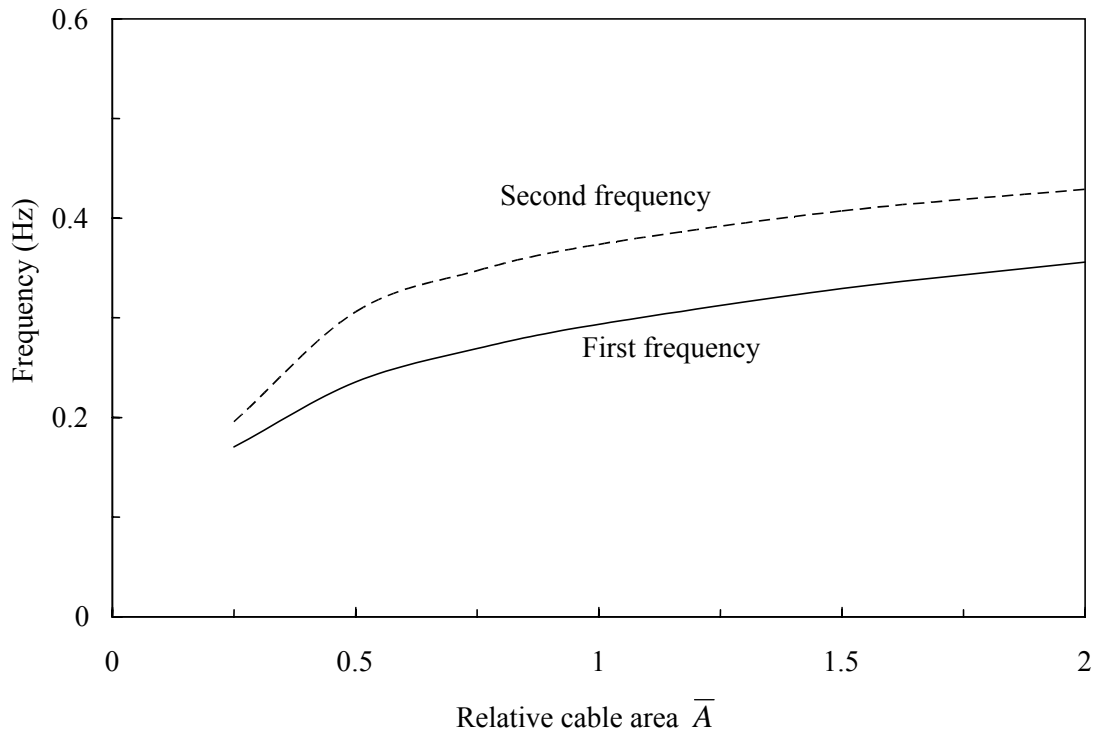


**Figure 3.17** Frequencies vs Cable Section Area

### 3.5.2.2. Cable Elastic Modulus

The variation of cable elastic modulus is represented by the relative cable elastic modulus that is defined by

$$\bar{E} = \frac{E}{E_0}$$

where  $E_0$  is the standard elastic modulus of cables defined in Table 3.4. Frequencies for different cable elastic modulus ratios are summarized in Table 3.14. The variation of the first two frequencies with the relative cable elastic moduli is shown in Figure 3.18. It has been observed that a variation in cable elastic modulus (cable tension stiffness) causes a reordering of the dominated mode shapes as they relate to the sequential order of natural

frequencies, especially for higher modes. The frequencies increase smoothly as the elastic modulus of cables increases in most cases.

**Table 3.14** Frequencies (Hz) for Different Cable Moduli

Mode order	Relative elastic modulus $\bar{E} = \frac{E}{E_0}$ for the cables						
	0.25	0.5	0.75	1.0	1.5	2.0	4.0
1	0.16678	0.23443	0.26836	0.29340	0.33072	0.35858	0.42746
2	0.18865	0.30432	0.34661	0.37361	0.40870	0.43164	0.47968
3	0.29302	0.40904	0.47692	0.52464	0.58153	0.60893	0.64187
4	0.31418	0.46975	0.53459	0.57900	0.63941	0.68114	0.78485
5	0.33510	0.50430	0.60335	0.67505	0.74439	0.79547	0.80680
6	0.38098	0.54420	0.63837	0.68530	0.77517	0.80440	0.85632
7	0.38104	0.55616	0.64063	0.71035	0.80218	0.84272	0.94243
8	0.38352	0.56732	0.67677	0.75806	0.81787	0.85371	0.97394
9	0.40171	0.60099	0.69790	0.76662	0.84032	0.89505	1.0646
10	0.47166	0.64873	0.74574	0.80814	0.88240	0.96399	1.2094
11	0.49008	0.70067	0.75526	0.81632	0.91370	1.0253	1.3085
12	0.58606	0.72984	0.80787	0.82163	0.94263	1.0400	1.3164
13	0.63742	0.80902	0.86286	0.90517	1.0122	1.0910	1.3532
14	0.63825	0.83434	0.87609	0.95383	1.0279	1.1255	1.4824
15	0.67434	0.84413	0.90508	0.95833	1.1079	1.2272	1.5297
16	0.71610	0.86662	0.99123	1.0873	1.2290	1.3028	1.5796
17	0.75083	0.87142	1.0004	1.1061	1.2352	1.3527	1.7021
18	0.76258	0.91395	1.0398	1.1381	1.2726	1.4055	1.7683
19	0.77351	0.97578	1.0764	1.1483	1.3247	1.4641	1.7861
20	0.81084	1.0084	1.1411	1.2283	1.3587	1.4678	1.8830

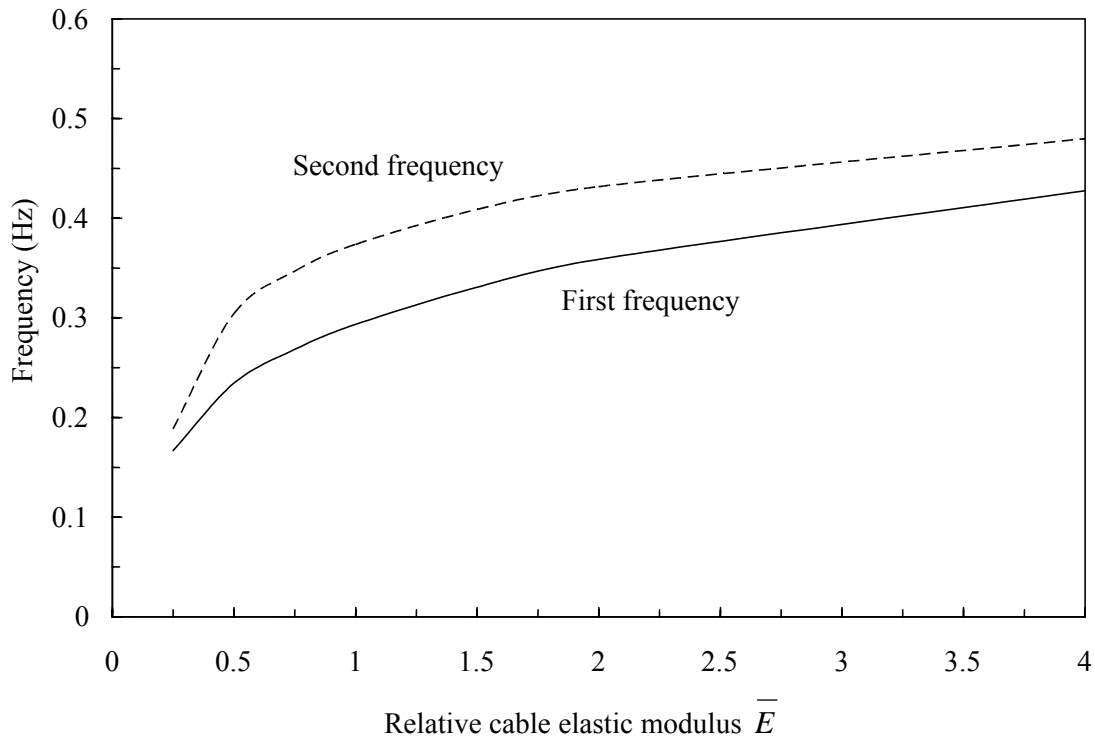


**Figure 3.18** Frequencies vs Cable Elastic Modulus

### 3.5.3. Deck Bending Stiffness

The deck system of the Owensboro cable-stayed bridge is modeled by the edge girders and center beams. A variation in the deck bending stiffness is then represented by the relative inertia moment of edge girders and center beams. They are changed by the same ratio. The vertical bending stiffness and lateral bending stiffness of edge girders and center beams are studied, respectively.

#### 3.5.3.1. Deck Vertical Bending Stiffness

The variation of the deck vertical bending stiffness is represented by the relative vertical inertia moment of edge girders and center beams that is defined by

$$\bar{I}_z = \frac{I_z}{I_{z0}}$$

where  $I_{z0}$  is the standard vertical inertia moment of edge girders and center beams defined in Table 3.5. Frequencies for different deck vertical bending stiffnesses are summarized in Table 3.15. The variation of the first two frequencies with the relative deck vertical bending stiffness is shown in Figure 3.19. The results show that the vertical frequencies increase smoothly as the deck vertical bending stiffness increases. However, the deck vertical bending stiffness has little effect on both transverse and torsion frequencies.

**Table 3.15** Frequencies (Hz) for Different Deck Vertical Stiffness

Mode order	Relative vertical bending stiffness $\bar{I}_z = \frac{I_z}{I_{z0}}$ for the deck					
	0.1	0.5	1.0	2.0	3.0	4.0
1	0.24060	0.27349	0.29340	0.31806	0.33468	0.34747
2	0.28418	0.33729	0.37361	0.42408	0.46201	0.49340
3	0.49848	0.51811	0.52464	0.53168	0.53581	0.53864
4	0.50570	0.54177	0.57900	0.63579	0.68122	0.70081
5	0.58818	0.66042	0.67505	0.69383	0.69862	0.71805
6	0.63845	0.66210	0.68530	0.69454	0.70724	0.72016
7	0.65053	0.67438	0.71035	0.77794	0.78998	0.79487
8	0.65506	0.73640	0.75806	0.78018	0.80783	0.82261
9	0.67795	0.74778	0.76662	0.79008	0.83282	0.84514
10	0.70073	0.75307	0.80814	0.82762	0.83927	0.85433
11	0.71108	0.78860	0.81632	0.82919	0.84102	0.88152
12	0.75765	0.81145	0.82163	0.92494	0.95733	0.98029
13	0.76131	0.83581	0.90517	0.93236	1.0094	1.0807
14	0.79427	0.88827	0.95383	1.0449	1.1105	1.1660
15	0.81586	0.89474	0.95833	1.0960	1.1659	1.2032
16	0.81601	0.98244	1.0873	1.2080	1.3043	1.3493
17	0.84848	1.0050	1.1061	1.2258	1.3155	1.3870
18	0.87157	1.0208	1.1381	1.2676	1.3215	1.4051
19	0.89410	1.0558	1.1483	1.2780	1.3838	1.4781
20	0.89449	1.0561	1.2283	1.3934	1.5236	1.6497

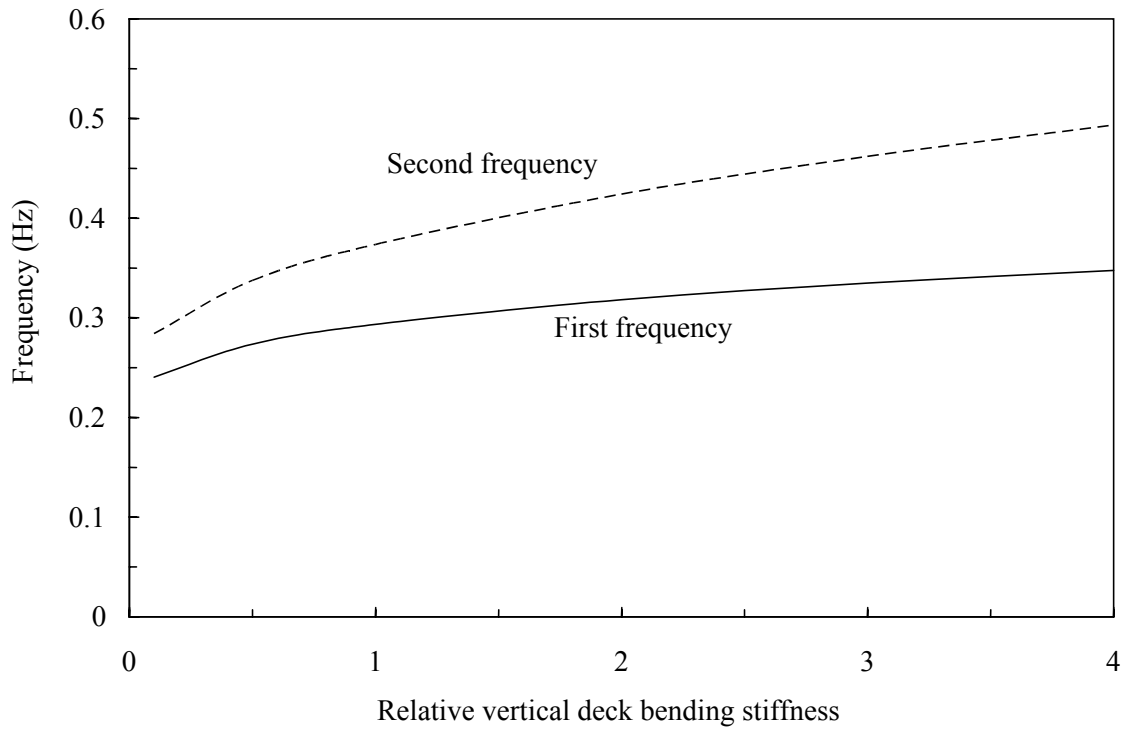


**Figure 3.19** Frequencies vs Deck Vertical Bending Stiffness

### 3.5.3.2. Deck Lateral Bending Stiffness

The variation of the deck lateral bending stiffness is represented by the relative lateral inertia moment of edge girders and center beams that is defined by

$$\bar{I}_y = \frac{I_y}{I_{y0}}$$

where  $I_{y0}$  is the standard lateral inertia moment of edge girders and center beams defined in Table 3.5. Frequencies for different deck lateral bending stiffness are summarized in Table 3.5. Frequencies for different deck lateral bending stiffness are summarized in Table 3.16. The variation of the first frequency and the third frequency with the relative deck lateral bending stiffness is shown in Figure 3.20. The results show that the increment of the deck lateral bending stiffness does affect on the transverse and torsion

frequencies but does not contribute to the vertical frequencies. It has been noted that increasing the deck lateral bending stiffness results in the warping of the deck and the variation of the deck lateral bending stiffness causes a reordering of the dominated mode shapes as they relate to the sequential order of natural frequencies.

**Table 3.16** Frequencies (Hz) for Different Lateral Deck Stiffness

Mode order	Relative lateral bending stiffness $\bar{I}_y = \frac{I_y}{I_{y0}}$ for the deck						
	0.1	0.25	0.5	0.75	1.0	1.5	2.0
1	0.29338	0.29339	0.29340	0.29340	0.29340	0.29340	0.29341
2	0.37358	0.37360	0.37360	0.37361	0.37361	0.37361	0.37361
3	0.47630	0.51037	0.52764	0.53019	0.52464	0.50299	0.47870
4	0.57894	0.57898	0.57899	0.57899	0.57900	0.57900	0.57065
5	0.71022	0.71030	0.71033	0.69744	0.67505	0.61638	0.57901
6	0.75169	0.73685	0.71329	0.71034	0.68530	0.65419	0.61526
7	0.80079	0.79914	0.75386	0.71131	0.71035	0.69519	0.64376
8	0.82045	0.80694	0.79877	0.78690	0.75806	0.71036	0.69016
9	0.82147	0.82157	0.82160	0.79830	0.76662	0.72753	0.71036
10	0.83959	0.82526	0.82685	0.82162	0.80814	0.76632	0.74901
11	0.92900	0.89336	0.84170	0.82368	0.81632	0.81079	0.79572
12	0.95375	0.92327	0.86688	0.82933	0.82163	0.82164	0.82165
13	0.96185	0.95380	0.95382	0.92379	0.90517	0.87495	0.82361
14	1.0649	1.0208	0.96276	0.95383	0.95383	0.90268	0.89250
15	1.1380	1.1381	1.0733	1.0109	0.95833	0.95384	0.93235
16	1.1998	1.1484	1.1381	1.1381	1.0873	0.99715	0.93828
17	1.2281	1.2283	1.2122	1.1445	1.1061	1.0080	0.95384
18	1.3120	1.2932	1.2283	1.1672	1.1381	1.0522	0.99283
19	1.3493	1.3257	1.2393	1.2105	1.1483	1.1381	1.0816
20	1.3762	1.3740	1.2848	1.2283	1.2283	1.1702	1.1381

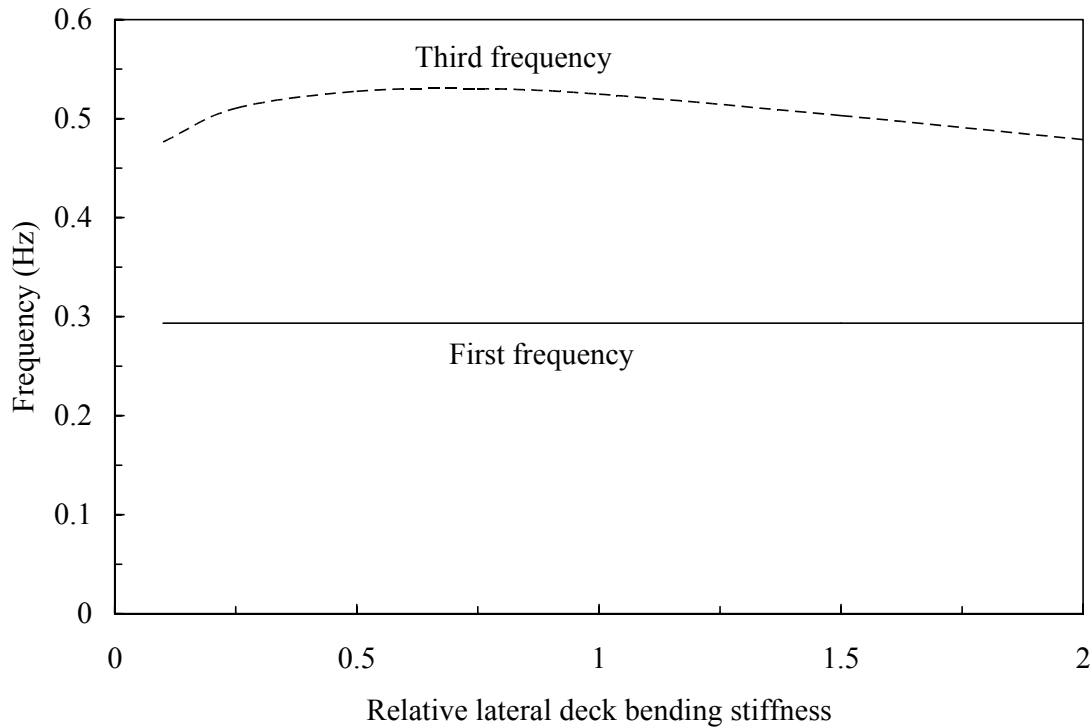


**Figure 3.20** Frequencies vs Deck Lateral Bending Stiffness

### 3.6. Finite Element Model Calibration

A realistic computation model, calibrated with the help of experimental measurements, can be a valuable tool in the efforts to preserve the bridge structural evaluation using dynamic-based methods. The process is required to combine the bridge analyses and experimental measurements. Confidence in using FE models for dynamic performance predictions of a structure is lacking owing to a relatively difference between experimental and analytical modes. The differences are not only from the modeling errors resulting from simplifying assumptions made in modeling the complicated structures but also from parameter errors due to structural defect and uncertainties in the material and geometric properties. Dynamic-based evaluation is therefore based on a comparison of the experimental modal analysis data obtained in *situ* field tests with the finite element predictions. The FE model of a real structure is then calibrated by using dynamic measurement results.

We have known the real dynamic properties of the bridge through field free vibration testing. And we have already known the structural or material parameters that may largely affect the modal properties of the bridge through parametric studies. The original finite element model can be calibrated by adjusting these parameters to match the frequencies and mode shapes best between testing and modeling. The updated structural and material parameters are summarized in Table 3.17 and Table 3.18, respectively.

**Table 3.17** Calibrated Real Constants

Type	Cross-section Area: (ft <sup>2</sup> )	Inertia moment: (ft <sup>4</sup> )		Initial strain	Structural member
		I <sub>zz</sub>	I <sub>yy</sub>		
1	3.33	35.031	0.25233	-	Edge girder
2	3.58	38.066	0.25288	-	Edge girder
3	2.7988	8.4107	0.25209	-	Edge girder
4	2.8508	8.5227	0.25222	-	Edge girder
5	2.7467	8.2983	0.25199	-	Edge girder
6	2.903	8.6344	0.25238	-	Edge girder
7	2.9264	8.8194	0.26226	-	Edge girder
8	2.7701	8.4879	0.26188	-	Edge girder
9	2.8743	8.7091	0.26211	-	Edge girder
10	2.8222	8.5986	0.26198	-	Edge girder
11	2.9264	9.164	0.31623	-	Edge girder
12	3.0774	10.123	0.39026	-	Edge girder
13	2.7232	8.1005	0.24211	-	Edge girder
14	2.7753	8.2152	0.24221	-	Edge girder
15	2.8274	8.3292	0.24233	-	Edge girder
16	2.8795	8.4427	0.24249	-	Edge girder
17	2.8222	8.7785	0.28901	-	Edge girder
18	2.9264	9.0061	0.28924	-	Edge girder
19	7.4139	98.031	5448.7	-	Center beam
20	0.3919	0.02483	1.6034	-	Floor beam
21	83	2486.3	2870.2	-	Tower (lower)
22	64.5	1894.4	638.6	-	Tower (upper)
23	58.5	613.9	1829.2	-	Tower (strut)
24	159.36	3399.7	1317.4	-	Tower (head)
25	142.72	3044.7	946.31	-	Tower (head)
26	128	2730.7	682.67	-	Tower (head)
27	126.72	2703.4	662.4	-	Tower (head)
28	122	2602.7	591.1	-	Tower (head)
29	121.28	2587.3	580.7	-	Tower (head)
30	52	69	732	-	Bearing
31	0.059722	-	-	3.6130E-03	Cables 1 & 49

**Table 3.17 Continued** Calibrated Real Constants

Type	Cross-section Area: (ft <sup>2</sup> )	Inertia moment: (ft <sup>4</sup> )		Initial strain	Structural member
		I <sub>zz</sub>	I <sub>yy</sub>		
32	0.058229	-	-	3.5285E-03	Cables 2 & 50
33	0.086597	-	-	3.7096E-03	Cables 3 & 51
34	0.044792	-	-	3.5552E-03	Cables 4 & 52
35	0.050764	-	-	3.6605E-03	Cables 5 & 53
36	0.047778	-	-	3.7440E-03	Cables 6 & 54
37	0.044792	-	-	3.6995E-03	Cables 7 & 55
38	0.041806	-	-	2.2396E-03	Cables 8 & 56
39	0.038819	-	-	1.8568E-03	Cables 9 & 57
40	0.035833	-	-	1.9514E-03	Cables 10 & 58
41	0.026875	-	-	2.0494E-03	Cables 11 & 59
42	0.037326	-	-	1.0586E-03	Cables 12 & 60
43	0.037326	-	-	1.1035E-03	Cables 13 & 61
44	0.026875	-	-	2.0226E-03	Cables 14 & 62
45	0.035833	-	-	2.0115E-03	Cables 15 & 63
46	0.037326	-	-	2.1107E-03	Cables 16 & 64
47	0.040313	-	-	2.1563E-03	Cables 17 & 65
48	0.043299	-	-	2.1790E-03	Cables 18 & 66
49	0.047778	-	-	2.4008E-03	Cables 19 & 67
50	0.050764	-	-	2.3303E-03	Cables 20 & 68
51	0.053750	-	-	2.0271E-03	Cables 21 & 69
52	0.058229	-	-	2.5415E-03	Cables 22 & 70
53	0.056736	-	-	3.3491E-03	Cables 23 & 71
54	0.074653	-	-	3.4066E-03	Cables 24 & 72
55	0.074653	-	-	3.4066E-03	Cables 25 & 73
56	0.056736	-	-	3.3491E-03	Cables 26 & 74
57	0.058229	-	-	2.5415E-03	Cables 27 & 75
58	0.053750	-	-	2.0271E-03	Cables 28 & 76
59	0.050764	-	-	2.3303E-03	Cables 29 & 77
60	0.047778	-	-	2.4008E-03	Cables 30 & 78
61	0.043299	-	-	2.1790E-03	Cables 31 & 79
62	0.040313	-	-	2.1563E-03	Cables 32 & 80
63	0.037326	-	-	2.1107E-03	Cables 33 & 81
64	0.035833	-	-	2.0115E-03	Cables 34 & 82
65	0.026875	-	-	2.0226E-03	Cables 35 & 83
66	0.037326	-	-	1.1035E-03	Cables 36 & 84
67	0.037326	-	-	1.0586E-03	Cables 37 & 85
68	0.026875	-	-	2.0494E-03	Cables 38 & 86
69	0.035833	-	-	1.9514E-03	Cables 39 & 87
70	0.038819	-	-	1.8568E-03	Cables 40 & 88
71	0.041806	-	-	2.2396E-03	Cables 41 & 89

**Table 3.17 Continued** Calibrated Real Constants

Type	Cross-section Area: (ft <sup>2</sup> )	Inertia moment: (ft <sup>4</sup> )		Initial strain	Structural member
		I <sub>zz</sub>	I <sub>yy</sub>		
72	0.044792	-	-	3.6995E-03	Cables 42 & 90
73	0.047778	-	-	3.7440E-03	Cables 43 & 91
74	0.050764	-	-	3.6605E-03	Cables 44 & 92
75	0.044792	-	-	3.5552E-03	Cables 45 & 93
76	0.086597	-	-	3.7096E-03	Cables 46 & 94
77	0.058229	-	-	3.5285E-03	Cables 47 & 95
78	0.059722	-	-	3.6130E-03	Cables 48 & 96

**Table 3.18** Calibrated Material Properties

Group No.	Young's modulus (lb/ft <sup>2</sup> )	Poisson's ratio	Mass density (lb/ft <sup>3</sup> )	Structural member
1	6.358×10 <sup>8</sup>	0.2	150	Towers
2	4.176×10 <sup>9</sup>	0.3	490	Cables
3	4.176×10 <sup>9</sup>	0.3	710.5	Edge girders
4	4.176×10 <sup>9</sup>	0.3	695.1	Edge girders
5	4.176×10 <sup>9</sup>	0.3	752.3	Edge girders
6	4.176×10 <sup>9</sup>	0.3	747.5	Edge girders
7	4.176×10 <sup>9</sup>	0.3	757.3	Edge girders
8	4.176×10 <sup>9</sup>	0.3	742.9	Edge girders
9	4.176×10 <sup>9</sup>	0.3	740.9	Edge girders
10	4.176×10 <sup>9</sup>	0.3	755.1	Edge girders
11	4.176×10 <sup>9</sup>	0.3	745.4	Edge girders
12	4.176×10 <sup>9</sup>	0.3	750.2	Edge girders
13	4.176×10 <sup>9</sup>	0.3	740.9	Edge girders
14	4.176×10 <sup>9</sup>	0.3	728.6	Edge girders
15	4.176×10 <sup>9</sup>	0.3	759.6	Edge girders
16	4.176×10 <sup>9</sup>	0.3	754.5	Edge girders
17	4.176×10 <sup>9</sup>	0.3	749.7	Edge girders
18	4.176×10 <sup>9</sup>	0.3	745	Edge girders
19	4.176×10 <sup>9</sup>	0.3	750.2	Edge girders
20	4.176×10 <sup>9</sup>	0.3	740.9	Edge girders
21	4.176×10 <sup>9</sup>	0.3	886.2	Center beam
22	4.176×10 <sup>12</sup>	0.3	490	Floor beams
23	4.176×10 <sup>9</sup>	0.3	490	Bearings

The several frequencies coming out of the system identification through the free vibration measurements and FEM predictions are summarized in Table 3.19. A good agreement of frequencies has been found between FE modeling and *in situ* vibration measurements. Since the floor beams in FEM are modeled as more rigid beams, its mode shape is transverse plus torsion. As mentioned previously, a dominated mode of the Owensboro cable-stayed bridge in 3-D FE modeling is always coupled with other mode shapes. The higher the dominated mode is, the more serious the coupling. Because the experimental modal properties of the bridge come from the free vibration measurements, the better matching for higher modes is not expected and not realistic.

**Table 3.19** Comparison of Frequencies

Mode	Test (Hz)	FE Model (Hz)	Mode classification
1	0.301667	0.293403	Vertical
2	0.388333	0.373609	Vertical
3	-	0.524643	Transverse + Torsion
4	0.601667	0.578998	Vertical
5	0.696667	0.675054	Vertical; Torsion for FEM
6	-	0.685296	Transverse + Torsion
7	0.74	0.710348	Vertical
8	-	0.758056	Torsion
9	-	0.766625	Transverse + Torsion
10	-	0.808145	Tower Sway + Torsion
11	-	0.816315	Tower Sway + Torsion
12	0.818333	0.821629	Vertical

The first two vertical mode shapes of both FE modeling and vibration testing are shown in Figures 3.21-3.22. The test mode shapes are directly obtained by picking up the magnitude values of each spectral diagram at the peak points from the moveable stations divided by those of each spectral diagram at the peak points from the base stations. The FE mode shapes have been normalized according to the maximum value (unity) of the test point. In fact, the mode shapes through free vibration are not always that good because the free excitation does not lend itself to frequency response functions (FRFs) or impulse response functions (IRFs) since the input force can not be measured. Peak

picking is always a subjective task. This is one of the drawbacks of structural system identification through free vibration measurements.

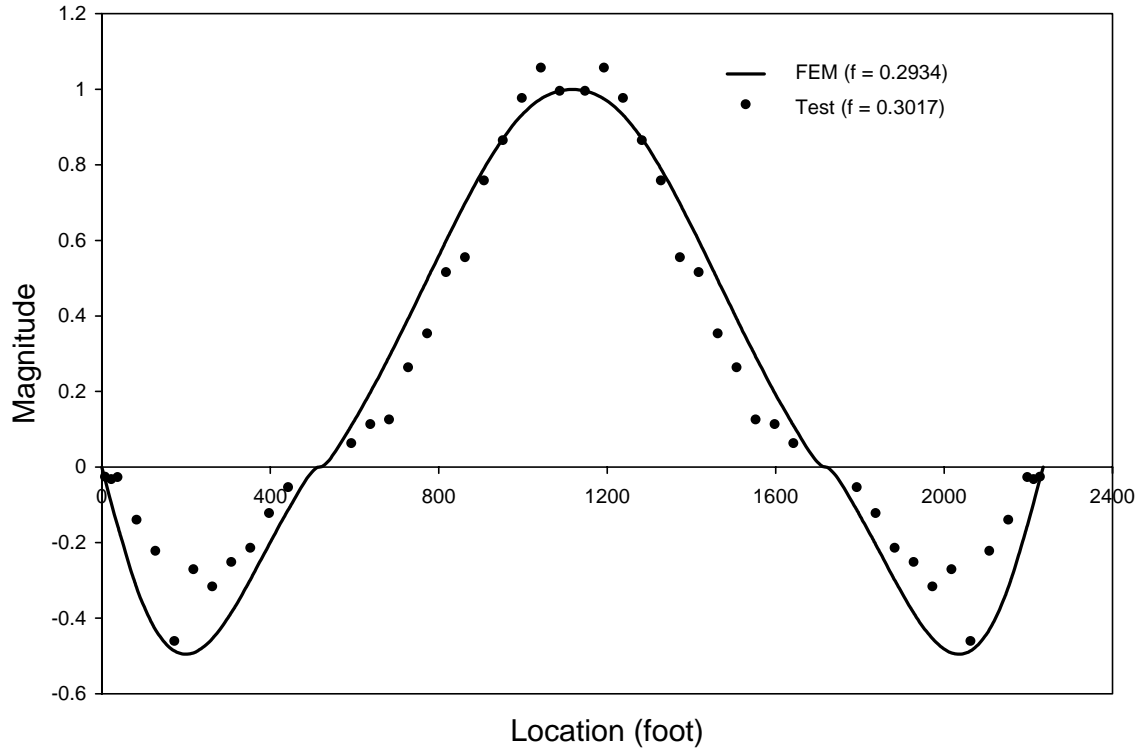
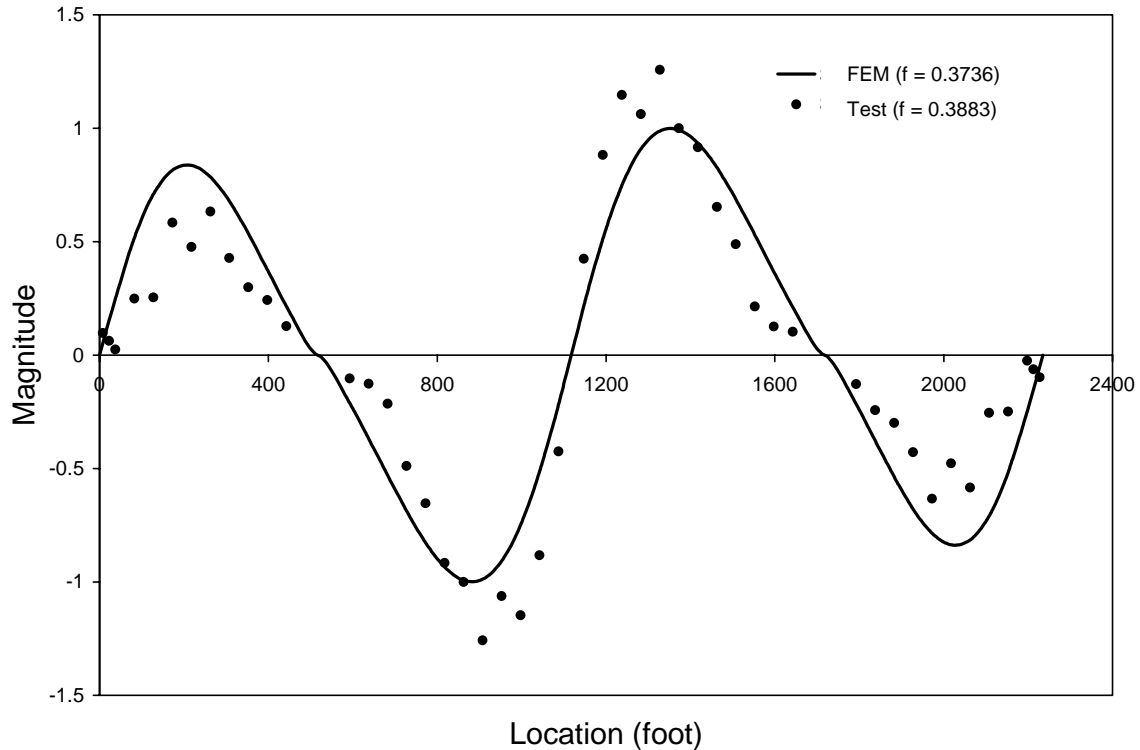


Figure 3.21 Comparison of First Vertical Mode Shape



**Figure 3.22** Comparison of Second Vertical Mode Shape

### 3.7. Remarks

A detailed 3-D finite element model has been developed for the Owensboro cable-stayed bridge in order to make a start toward the evaluation of this structure. From the static analysis due to dead loads, followed by pre-stressed modal analysis, parametric studies and FE Modeling calibration, the following observations and comments can be made:

1. It is natural to discretize the cable between the tower and the edge girder into a single tension-only truss element (cable element). Two node cable elements, however, are relatively weak elements. But, since two end nodes of the cable element are connected with the beam elements of the tower and the girder, sufficient constraints at each cable node are provided and then the nonlinear static analysis or the modal analysis can be carried out.

2. The completely 3-D nonlinear modeling of a cable-stayed bridge has proved to be difficult. The smaller discretization would be computationally very large and inefficient. Convergence of such a large number of nonlinear elements is not always guaranteed. The choice of convergent criterion to control the iteration procedure becomes essential. The common force convergent criterion defaulted in the ANSYS is not so effective in the nonlinear analysis of a cable-stayed bridge. Instead, the displacement convergence criterion has proved to be effective and often results in the convergent solution.
3. Due to the cable sagging, the static analysis of a cable-stayed bridge is always a geometric nonlinear. The stress stiffening of cable elements (cable sagging effect) plays an important role in both the static and dynamic analysis of a cable-stayed bridge. Nonlinear static analysis without the stress stiffening effect will lead to an aborted run due to the divergent oscillation even though the displacement convergence criterion is used.
4. The large deflection has been demonstrated to be the limited effect on the member forces and the deck deflection of the bridge under dead loads. After introducing enough amount of initial strain in the cables, the static analysis of the Owensboro cable-stayed bridge due to dead loads can be elastic and small deflection. The stress stiffening effect, however, is always required to ensure the convergent solution.
5. The initial strain in the cables is the key factor to control the initial equilibrium configuration under the dead load. For a completed bridge, the common fact is that the initial position of the cable and bridge is unknown. The initial geometry of the bridge which was modeled is really the deflected shape of the bridge loaded by the dead load. The initial equilibrium configuration of the bridge due to dead loads can be approximately achieved by referring to the bridge plans.
6. It is demonstrated that a cable-stayed bridge is a highly pre-stressed structure. The modal or any dynamic analysis must start from the initial equilibrium configuration

due to dead loads. This initial equilibrium configuration can be a small deflection static analysis because the large deflection can be ignored. The modal analysis of a cable-stayed bridge should include two steps: small deflection static analysis under the dead load and followed by pre-stressed modal analysis, so that the dead load effect on the stiffness can be included. In other words, the modal analysis of a cable-stayed bridge must be a pre-stressed modal analysis.

7. It is clearly shown that the self-weight can improve the stiffness of a cable-stayed bridge. In the case of the Owensboro cable-stayed bridge, the dead load effect increases the natural frequency of the bridge due to the stiffening of the structure. Therefore, the regular modal analysis without a dead-load static analysis will underestimate the stiffness of the cable-stayed bridge and consequently provide the more safe evaluation of the bridge.
8. It is observed that one dominated mode is always coupled with other modes. The dominated mode shapes of the Owensboro cable-stayed bridge in the low-frequency (0~1.0 Hz) range are mainly vertical direction. This reveals the fact that the lateral stiffness of the cable stayed bridge is stronger than that of the suspension bridge (Ren and Harik 2001).
9. From the parametric studies, it is found that the key parameters affecting the vertical modal properties are the mass, cable sectional area, cable elastic modulus and deck vertical bending stiffness. The key parameters affecting the transverse and torsion modal properties are the mass, cable sectional area, cable elastic modulus and deck lateral bending stiffness.
10. A good agreement of frequencies has been found between FE modeling and *in situ* free vibration testing. But the mode shapes are not too good as output-only measurement does not lend itself to frequency response functions (FRFs) or impulse response functions (IRFs) since the input force can not be measured. This is also one of the drawbacks of output-only measurements.

11. The better matching for higher modes is not expected and not realistic either, as the experimental modal properties of the bridge come from the output-only measurement.
12. The calibrated finite element model may be used as a baseline in the future structural analysis and monitoring of the Owensboro cable-stayed bridge.

## **4. CABLE TESTING AND MODELING**

### **4.1. General**

Many occurrences of wind-induced vibrations of bridge stay cables have been reported worldwide [Yoshimura, 1995; Hikami, 1988; Matsumoto, 1992]. Among these are instances of rain-wind vibrations occurring on other Ohio River crossings, including the East Huntington Bridge in West Virginia. Previous testing of the cable-stayed bridge in Maysville, Kentucky saw persistent rain-wind response of cables, but cross ties included in the Maysville design seemed to be effective in limiting the amplitude of the wind-induced response [Harik, 2005].

On some stay-cable bridges, retrofit designs have been required to mitigate large-amplitude wind-induced vibration. Consequently, separate cable modeling and testing was required. On other existing bridges, long-term cable condition assessment has been accomplished with cable modeling and testing. In this chapter, the bridge cables are considered separately to document baseline testing results and to create verified models.

Although researchers are investigating the causes and critical parameters associated with rain-wind vibration [Main, 2001; Flamand, 2001] and deck-induced cable motions [Caetano, 2000a; Caetano, 2000b], complete understanding of the physics behind these potentially damaging large-amplitude oscillations is not available. Recently, the FHWA released the report of its study of wind-induced oscillations of bridge stay cables including design strategies to mitigate stay cable oscillations. Some of these strategies, such as helical filets on the external surface of the stays and cross ties between the stay cables, are incorporated in the Owensboro stay cable design.

The objective of this effort was to develop detailed verified models of the Owensboro stay cable systems. In Kentucky, previous testing of the cables of the

Maysville bridge demonstrated the accuracy and utility of using short time record measurements of cable acceleration to determine cable fundamental frequencies for model verification. In Maysville, simultaneous recordings of the accelerations of the cable and deck anchor at the base of the cable enabled comparison of their motions. Similar testing procedures are applied in this effort to measure the dynamic response of the Owensboro cables and deck anchors. Observations of cable and cross-tie motion, along with their evaluation in the context of recent reports are also an objective.

It is important to note that identified frequencies for a cable may differ from field test to field test. In Maysville, differences seen in the identified fundamental cable frequencies of the longest cables were attributed to combined effects of temperature and use. The Owensboro cable modeling and testing effort did not include an objective to examine trends with temperature or use.

The ninety-six cables of the Owensboro Bridge are unique flexible structures whose dynamic response characteristics depend on material properties, tension, and possibly temperature. The Owensboro cables were constructed according to the plans with modifications as detailed in the as-built information provided by David McDowell ([David.McDowell@ky.gov](mailto:David.McDowell@ky.gov)) Transportation Engineer Supervisor, Kentucky Transportation Cabinet District Two - Madisonville. In the original plans, the ninety-six cables are nominally four sets of twenty-four cables. Each set is associated with either the Kentucky (South) or Ohio (North) tower and with the upstream (East) or downstream (West) side of the bridge as seen in the aerial photograph (Figure 4.1) and elevation drawing (Figure 4.2). Cables are numbered from 1 to 48 from Kentucky.

To bring the bridge deck into alignment side-to-side as the constructed sections met in the center and to smooth the vertical deck profile, cable design tensions were adjusted from those listed in the original plans. Several “as-built” cable tensions differed considerably from the tensions listed on the bridge plans with an average tension change of 24% (decrease) from the bridge plans. Some tensions decreased by as much as 70 % (maximum tension decreases: 72.1% for Cable 36E, 71.9% for Cable 12E and 70.0% for

Cables 37W and 37E). For a few cables, the “as-built” tensions increased from those on the bridge plans (maximum tension increases: 17.8% for Cable 6E, 17.5% for Cable 7E and 17.3% for Cable 37W). Changes to all design dead load tensions are presented graphically in Figure 4.3. Note that the largest as-built tension increases occurred for the longest cables at the ends of the span while the largest tension decreases occurred for the shortest cables at the towers.



Figure 4.1 Aerial and Approach Views of the Owensboro Bridge

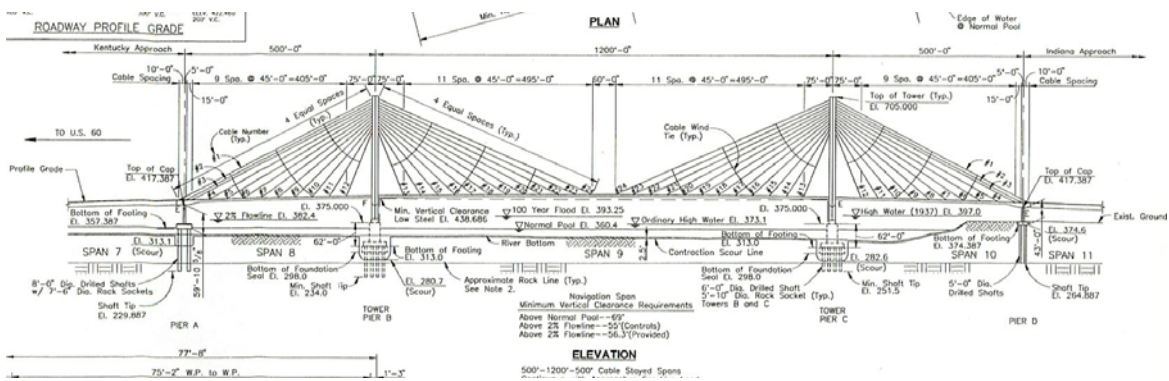
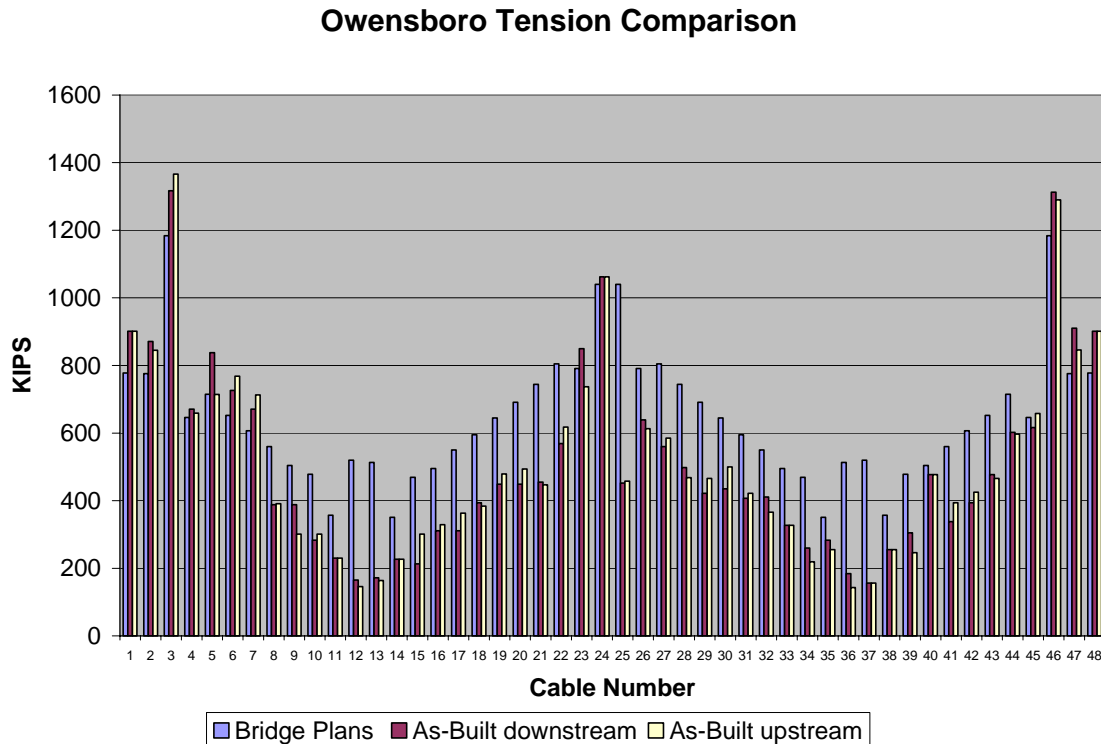


Figure 4.2 Elevation Drawing of the Owensboro Bridge



**Figure 4.3** Recorded Changes to Design Tensions for Alignment and Profile Adjustment

Assuming linear response, development of correlated finite element models of the cables requires field tests. Two different field tests of the Owensboro cables were conducted to support development of accurate finite element models. This chapter presents the field-testing and test results, the modeling approaches and analysis results, observations of the cables and cross-ties and then closes with summarizing remarks.

## 4.2. Field Testing of the Owensboro Bridge Stay Cables

Two field survey tests were conducted of the Owensboro cables as follows:

1) October 15-16, 2002 – Prior to opening the bridge, loaded trucks were run to excite dynamic response of the bridge, including the cables. It was found that wind-induced motion of the cables was also sufficient for fundamental frequency identification. Acceleration responses of cables and their corresponding deck anchors were recorded. The height of the anchors of the Owensboro Bridge required the use of a man-lift vehicle

for accelerometer placement on the cable. Figure 4.4 is a typical run of the loaded trucks exciting the bridge motion. Dr. Suzanne Weaver Smith, with graduate students Jennie Campbell, Matt Hayden and Philip Jean conducted the test.



**Figure 4.4** Field Tests of the Owensboro Bridge Conducted with Loaded Trucks

2) August 4-5, 2003 – Acceleration responses of the 48 upstream cables (cables 1E-48E) and 24 downstream cables (1W-24W) and their deck anchors were recorded as typical light and moderate traffic traveled the bridge. Accelerometers were placed at several locations on the deck anchors for use in model verification, if required. Dr. Suzanne Smith, Jennie Campbell, Michiko Usui, Justin Kearns and Dr. John R. Baker (UK Paducah Engineering) conducted the test.



**Figure 4.5** Typical Traffic Including Heavy Trucks During Test on August 4-5, 2003

#### 4.2.1. First Field Test, October 15-16, 2002

The first field test and results are summarized in Figures 4.6 through 4.15. The bridge was closed to traffic for the field tests, with excitation provided by two loaded trucks driven in tandem. A few of the test runs occurred coincident with those reported in Chapter 2, but differences in testing approaches (record lengths, for example) and no simultaneous measurement capability precluded synchronized testing of the cables with the superstructure.

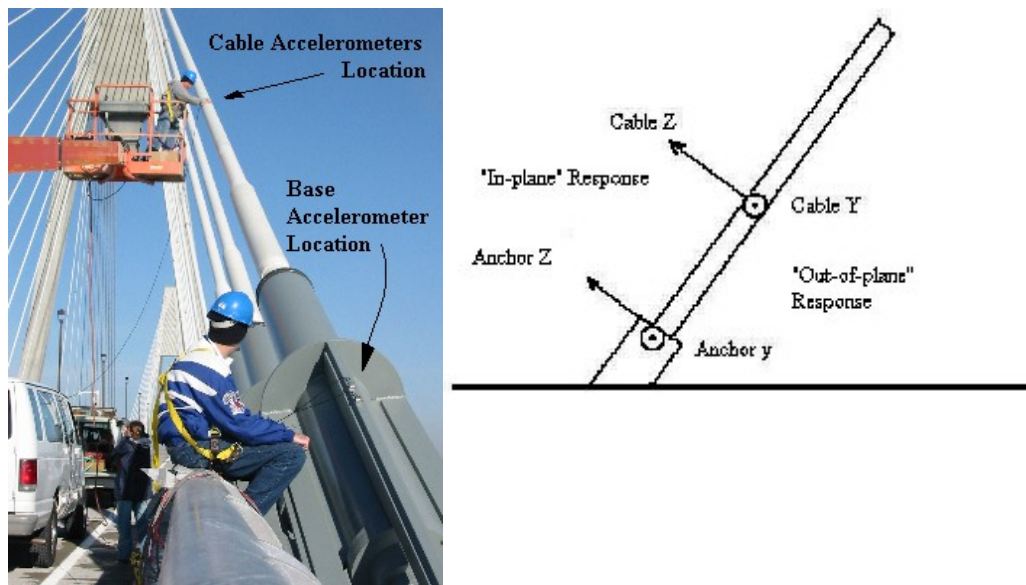


**Figure 4.6** Triaxial Accelerometer Placement and Coordinate Definition

Cable response measurement proceeded as with previous successful tests of cables of the Maysville bridge. Triaxial accelerometers (PCB Piezotronics, Inc. model 3703G3FD3G) were used to measure three-dimensional accelerations of each cable and anchor (representing the motion of the deck); voltage signals were recorded for 60 seconds at a sampling rate of 200 Hz to a notebook PC using Iotech's Wavebook/512 12-bit, 1 MHz Data Acquisition System. Redundant accelerometers were mounted to provide alternate records in case a channel failed during the testing. The first pair of accelerometers was placed on the above-the-deck anchor, representing the motion of the deck as seen in Figure 4.7. The second pair of accelerometers was mounted securely to the cable using a lift to reach a mounting location above the anchor. All accelerometers were oriented with respect to primary directions of the cable as shown in Figure 4.6 with the x-axis parallel to the longitudinal cable axis, the y-axis

transverse to the cable horizontally for out-of-plane motion (this is lateral with respect to the bridge deck), and the z-axis transverse to the cable in the vertical plane of static equilibrium. Simultaneous measurement of tower anchor motion for each cable was not possible. However, note that previous superstructure testing of other bridges (e.g., the Maysville bridge) showed tower motion to be one to two orders of magnitude smaller than deck motions.



**Figure 4.7** Typical Anchor Accelerometer Mounting



**Figure 4.8** Typical Cable Accelerometer Mounting



**Figure 4.9** Cable Cross Ties (Restrainers)



**Figure 4.10** Additional Images of October 2002 Testing



**Figure 4.11** Additional Images of the Owensboro Bridge

#### **4.2.2. Cepstrum Signal Processing for Frequency Identification**

The signal processing approach used to identify the fundamental frequency of each cable from the recorded short time-record accelerations is the same as that used to date for testing over 800 cables on four bridges in Texas and Kentucky, including the previous Maysville bridge cable testing effort. Modern-design cable-stayed bridges have from dozens to hundreds of cables. Of primary interest is determination of the cable fundamental frequency, typically in the range of 0.5 to 3.0 Hz. Identification of deck modal frequencies in this same low-frequency bandwidth usually involves signal processing of time records often 15-minutes in length or longer. Based on experience from field testing, acquiring data records of this length for all 96 cables of the Owensboro Bridge would require more than 5 days of testing time on the bridge.

However, cables have unique frequency response characteristics including harmonics, enabling a more efficient field testing approach for condition monitoring. Signal processing techniques have been developed for rotating machinery to identify the underlying frequency of the harmonic family. This paper presents this “cepstrum” approach applied to bridge stay cables. With this approach, short time records 45 to 60 seconds in length are able to be used to determine the fundamental cable frequency. Consequently, field survey testing of 72 cables of the Owensboro bridge was accomplished in only 1.5 days. Further, the approach is easily automated to enable processing of the resulting data in less than half a day. Therefore, with this approach, periodic field testing can be efficiently conducted of cable-stayed bridges for condition monitoring and for model validation.

In applications involving rotating machinery or gear systems, cepstrum analysis has been used for over a decade to detect families of uniformly spaced harmonics that appear in the measured signal when faults occur in the system [Shock and Vibration Handbook, 1996]. A family of uniformly-spaced harmonics is also seen in inclined bridge stay cable response (Figure 4.12). Therefore, cepstrum analysis was applied for automation of the data analysis to determine the fundamental frequency of the cables.

In essence, one finds the “spectrum of the spectrum.” First the frequency content of the time history (time-domain) data is determined using a discrete Fourier transform spectral analysis. Treating the spectrum (frequency-domain) data as a signal, a second spectral analysis finds the “frequency” of the peaks in the cable response spectrum. The second Fourier transform returns the result to the time domain. The first, largest peak of the cepstrum occurs at a time that is the period associated with frequency spacing of the peaks in the spectrum of the recorded data.

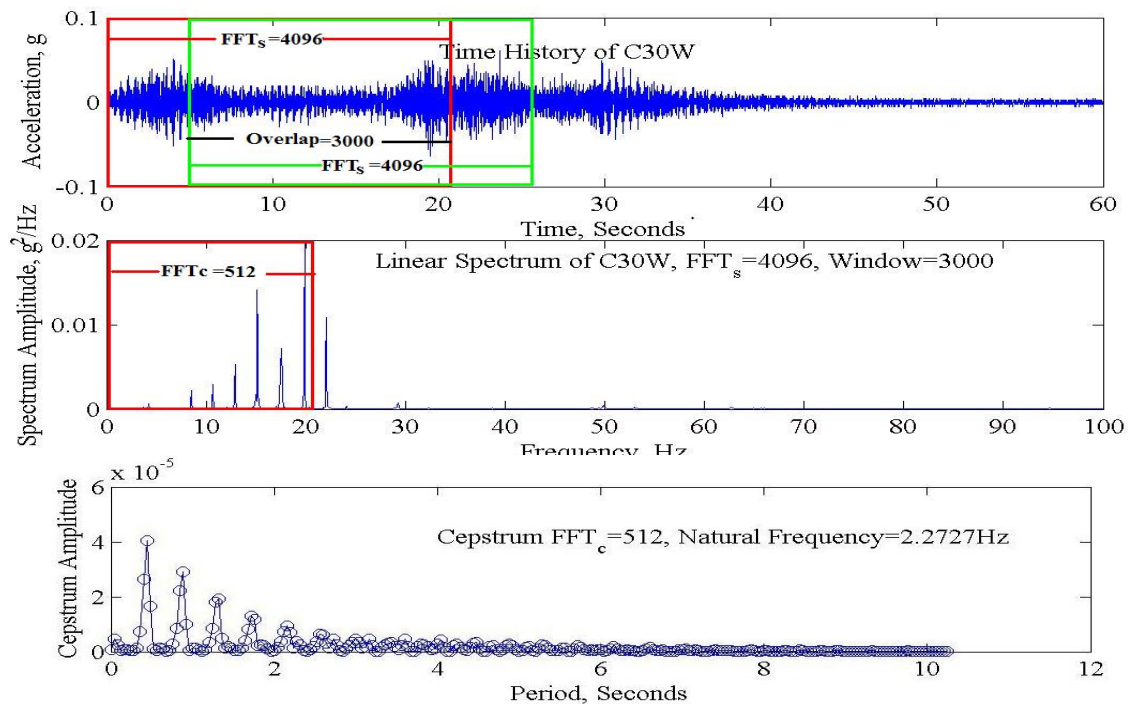


**Figure 4.12** Typical Cable Time-History Data, Corresponding Spectrum and Cepstrum

Herein, a slight variation of the typical cepstrum analysis is used. In other applications the spectrum is used on a log scale which magnifies subtle features of the response. In this application, we want to deemphasize noise and other subtle effects, so the spectrum is used on a linear scale. Note that for a distinct peak in the cepstrum, one must have a “reasonable number of adequately resolved” members of the harmonic family in the spectrum [Shock and Vibration Handbook, 1996]. For most inclined bridge stay cables, ambient excitation of cable-stayed bridges from passing traffic or wind satisfies this requirement.

For the typical example (Figure 4.12) above, a 60-second time record was recorded with a 200-Hz sample rate; corresponding spectra were computed using a 4096-point Fast Fourier Transform (FFT) and 3000-point overlap averaging. The FFT length to compute the Cepstrum was 512 points.

A study was performed under this effort to understand the impact of selecting different FFT sizes to compute the Cepstrum. As seen in Figures 4.13 and 4.14, the Cepstrum FFT size, along with the bandwidth of the excited modes, may lead to zero-padding in the FFT computation. With larger FFT sizes, a near-zero peak appears in the Cepstrum. Parameters are selected for optimal automated identification of the cable frequencies and may be different for each test depending on the excited bandwidth and the desired resolution of the identification. The resulting time-domain resolution is  $\Delta t$  seconds. Since the dominant period is the inverse of the fundamental frequency, this time-domain resolution gives a variance of the identified frequency results for the longest cables (with fundamental frequency near 0.5 Hz) and for the shortest cables (with fundamental frequency near 2.0 Hz). The resolution of the identified frequency of a shorter cable is larger than that for longer cables.

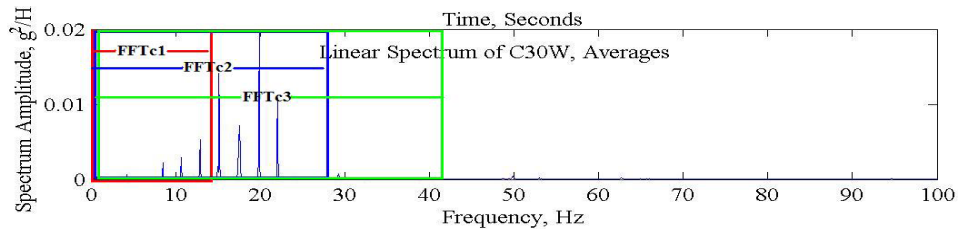


**Figure 4.13** Typical Cable Spectrum and Three Possible FFT Lengths for Cepstrum

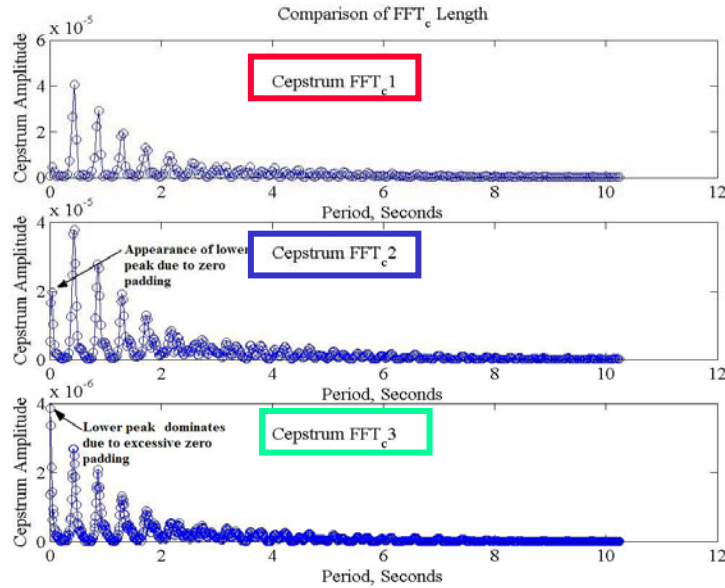


**Figure 4.14** Resulting Cepstra Using Three FFT Lengths

Results of the field survey testing and Cepstrum analyses are tabulated later in the section on finite element modeling. However, a quick look at the identified frequency results is presented in Figure 4.15. Here the upstream cable data sets were processed automatically using the Cepstrum approach. The horizontal axis is the data set number, rather than the cable number. For about five cables, multiple recorded time histories were used, so instead of 48 cables, this preliminary result shows 53 results. The vertical axis is the fundamental frequency, in Hz. Each result uses two different FFT sizes to automatically compute the Cepstrum, and shows that for most of the cables, the results are identical. These are compared to fundamental frequencies determined from the as-built specifications using a taut-string model:

$$f = \frac{1}{2L} \sqrt{\frac{T}{m}}$$

where  $f$  is the fundamental frequency in cycles per second,  $L$  is the free length in feet,  $T$  is the tension in lbs, and  $m$  is the mass per unit length of the string in lbs-s<sup>2</sup>/ft<sup>2</sup>. Comparison of the field test frequencies to taut-string frequencies shows that they correlate well, within the resolution of the method. Note that with this method, there is a larger resolution for higher-frequency, shorter cables (see, for example, Cable 16 compared to Cable 7 in Figure 4.15).

As is typical with this approach for field testing and signal analysis, occasionally with the smaller FFT size some frequencies are identified incorrectly as compared to the frequency of a taut string. For this small number of cables, the data can be examined and processed by hand to select different processing parameters to improve the result. From these preliminary results of the first field survey test, the cables of the Owensboro bridge are seen to be adequately excited by traffic or wind for frequency identification.

One additional result from the first field survey test of the Owensboro cables was that some of the cross ties (restrainers) were visibly moving. This is a concern as persistent excessive flexing of the cross ties may lead to problems with positioning or fatigue.

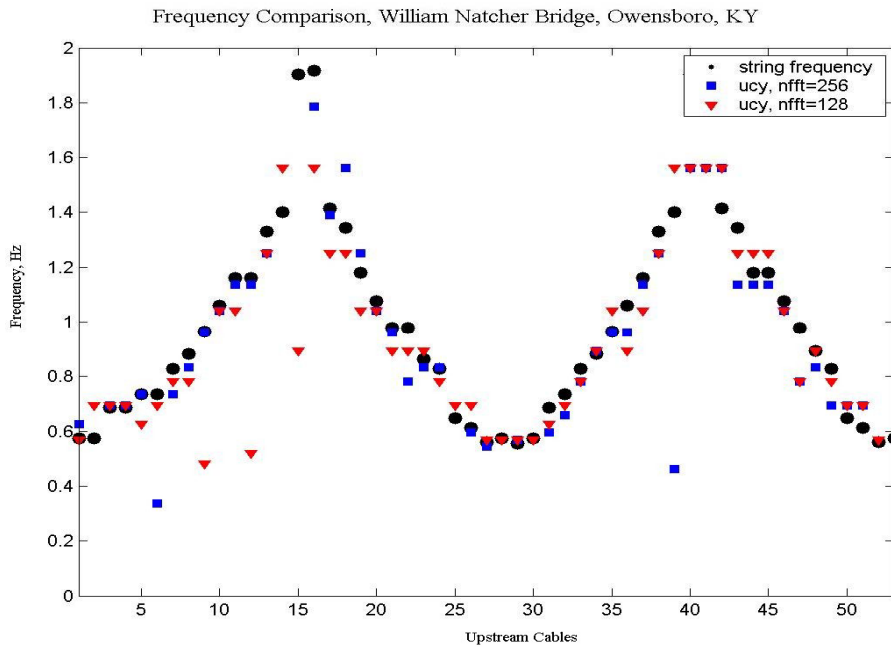


**Figure 4.15** Preliminary Frequency Results Compared to Taut-String Model Frequencies

#### 4.2.3. Second Field Test, August 4-5, 2003

The second field test and results are summarized in Figures 4.16 through 4.17. The bridge was open to traffic for the field tests, with excitation provided by traffic and ambient wind. Field testing and data analysis proceeded as described above for the first test with a few exceptions. No problems were experienced with instrumentation used for the first test, so it was concluded that there is no need for redundant sensors at each location. The available

accelerometers were placed at additional locations on the deck anchors to enable verification of detailed anchor models. Accelerometer mounting locations are seen in Figure 4.16.

Comparison of the spectra of the deck and the cable can reveal frequency relationships indicating deck excited motions of the cables. Figure 4.17 presents a plot of the deck and cable spectra for 48 upstream cables of the Owensboro bridge. For each line plotted, the dark (blue) spectrum is of the anchor motion and the light (green) spectrum is for the cable motion. No relationship is seen between the deck motion and that of the cables for the Owensboro bridge. Note that for the Maysville bridge a 2:1 relationship is seen between the deck spectrum and the corresponding cable spectrum, indicating the possibility of parametric (axial) excitation of the cable resulting from deck motion.



**Figure 4.16** Typical Accelerometer Placement and Mounting for Second Field Survey Test

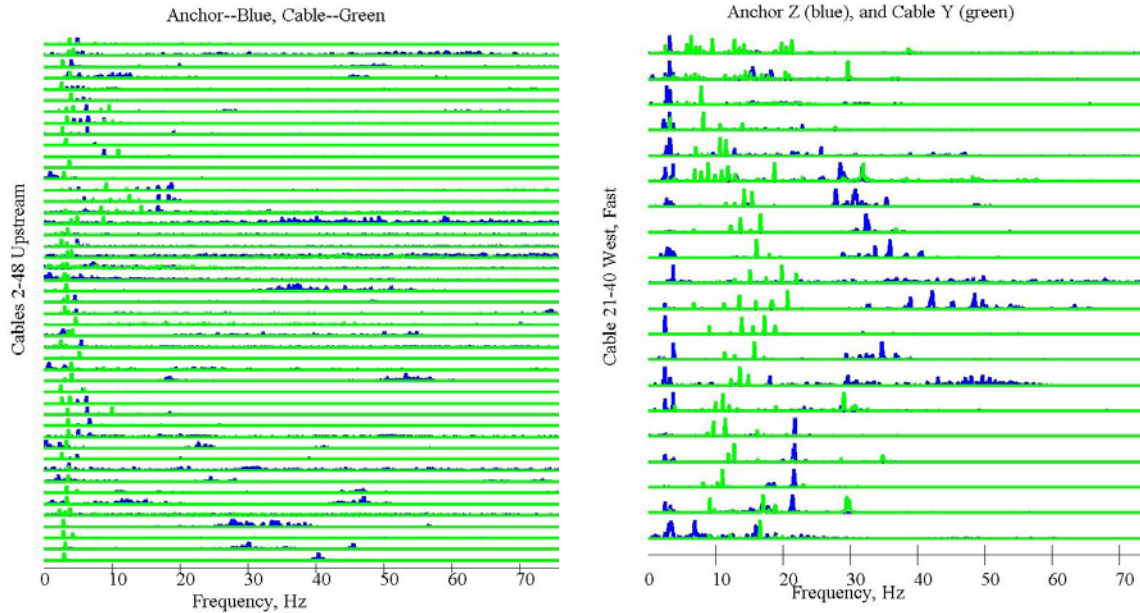


**Figure 4.17** Cable to Anchor Comparison for Owensboro (left) and Maysville (right) for Anchor Y (In-Plane) to Cable Z (Out-of-Plane) Spectra

### 4.3. Finite Element Analysis

Finite element (FE) models were developed for the Owensboro Bridge cables using cable properties from the original drawings and as-built information provided after the construction was completed. This section describes the development of the FE models of a set of 12 unrestrained cables, and comparison of the results to those of the field survey experiments. Cable models were developed using ANSYS finite element software.

The Owensboro Bridge includes 96 cables in eight sets of 12 cables. Two planes of cables, designated “upstream” and “downstream” include cables numbered from 1 to 48 from the Kentucky to the Indiana side of the bridge. To describe the development of an FE model of a representative set of twelve cables, upstream cables 1 to 12 will be the focus of the discussion. Data to enable development of similar models of all 96 cables is included.

Each cable model is developed using three-dimensional beam elements (ANSYS Beam Element Type 4). Prior experience modeling bridge stay cables indicated that bending effects should be included for correlated models of some cables, so beam elements were used

herein. Each cable is modeled with 35 nodes, with nodes 1 and 35 respectively at the coordinates specified as Work Points  $B_1$  and  $T_1$  in Figure 4.18, and the others equally spaced between the endpoints.

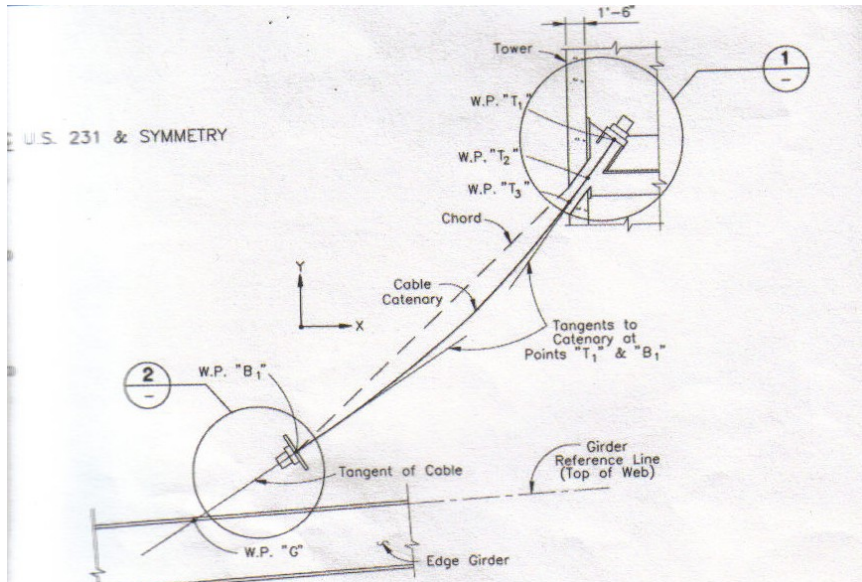


**Figure 4.18** Cable Workpoints shown on the Bridge Plans

Thirty-four beam elements are defined between each consecutive pair of end points. Representing fixed boundary conditions, all six degrees-of-freedom (DOFs) are restrained for the two endpoints of each cable. The cable tension was incorporated in the analysis by first performing a static analysis to prestress the cables. A block Lanczos modal analysis was run to determine the fundamental frequencies of the cables.

Varying cable geometry and material properties necessary to develop FE models of each individual cable include diameter, Young's modulus, mass density and initial strain. These properties are summarized, along with coordinates of the endpoints of the cables, in Table 4.1. Endpoints of the cables were defined as Work Points  $B_1$  and  $T_1$  of the drawings. As has been used on prior cable-stayed bridge projects, the effective Young's moduli were computed using Kollbruner's relation (Kollbruner, 1980). The mass densities were computed using the cable fabricated length, weight per unit length and cross section area. Also in the models, two additional properties were specified for all cables: Poisson's ration and modal

damping. Poisson’s ratio was specified as 0.30. Modal damping was specified to be one quarter of one percent, 0.0025. Note that modal damping does not enter into the normal modes computation performed with these models. Figure 4.19 presents the finite element model mesh with boundary conditions indicated. Table 4.2 and Figure 4.20 present the computed fundamental frequencies compared to experimental results. Tables 4.3 and 4.4 present the complete geometry and properties for all cables.

**Table 4.1:** Cable Geometry and Material Properties of Upstream Cables 1-12

CABLE NUMBER	COORDINATE POINTS						PE PIPE DIAMETER	EFFECTIVE YOUNG'S MODULUS	DENSITY	INITIAL STRAIN
	WORK POINT B <sub>i</sub>			WORK POINT T <sub>i</sub>						
	X	Y	Z	X	Y	Z				
	FT	FT	FT	FT	FT	FT				
1	-1101.042	435.122	36.951	-604.167	698.000	4.440	8.625	27423.27	0.000238	0.000562
2	-1086.058	435.572	36.951	-604.167	690.500	5.165	8.625	27372.86	0.000236	0.000528
3	-1071.180	436.022	36.951	-604.167	683.000	5.890	8.625	27713.58	0.000270	0.000844
4	-1026.752	437.372	36.951	-604.167	675.500	6.616	6.625	27661.22	0.000252	0.000691
5	-982.379	438.721	36.951	-604.167	668.000	7.341	6.625	27728.00	0.000269	0.000747
6	-938.005	440.027	36.951	-604.167	660.000	8.115	6.625	27844.60	0.000263	0.000800
7	-893.691	441.272	36.951	-604.417	652.000	8.888	6.625	27869.89	0.000257	0.000742
8	-848.801	442.957	36.881	-604.667	643.500	9.710	6.625	27598.55	0.000251	0.000411
9	-804.678	444.081	36.881	-604.667	635.000	10.951	6.625	27522.70	0.000245	0.000317
10	-760.190	445.644	36.810	-604.917	625.500	11.869	6.625	27735.66	0.000240	0.000315
11	-716.179	446.896	36.775	-605.167	616.000	12.788	6.625	27795.55	0.000222	0.000240
12	-672.319	448.338	36.705	-605.167	606.000	13.755	6.625	27633.66	0.000243	0.000153

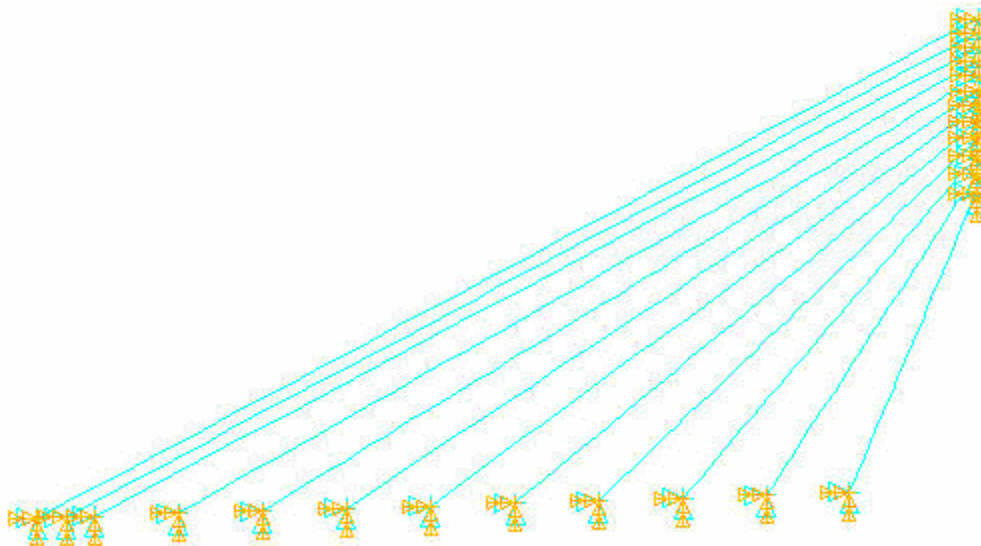


**Figure 4.19** Finite Element Model of Twelve Unrestrained Cables of the Owensboro Bridge

**Table 4.2:** Finite Element Model Fundamental Frequency Results Compared with Test Frequencies and String Model Frequencies

upstream cable #	Field (Hz)	String (Hz)	ANSYS (Hz)	ANSYS restrained
1	0.5682	0.5550	0.6133	0.61113
2	0.625	0.5740	0.6158	0.60756
3	0.6944	0.6850	0.7522	0.73727
4	0.6944	0.7350	0.7641	0.74542
5	0.7813	0.8280	0.8456	0.82347
6	0.8333	0.8840	0.9824	0.95452
7	0.9615	0.9640	1.074	1.041
8	0.8929	1.0600	0.9257	0.89452
9	1.0417	1.1620	0.9523	0.92366
10	1.25	1.3300	1.133	1.083
11	1.25	1.4010	1.242	1.178
12	1.5625	1.9030	1.178	1.127

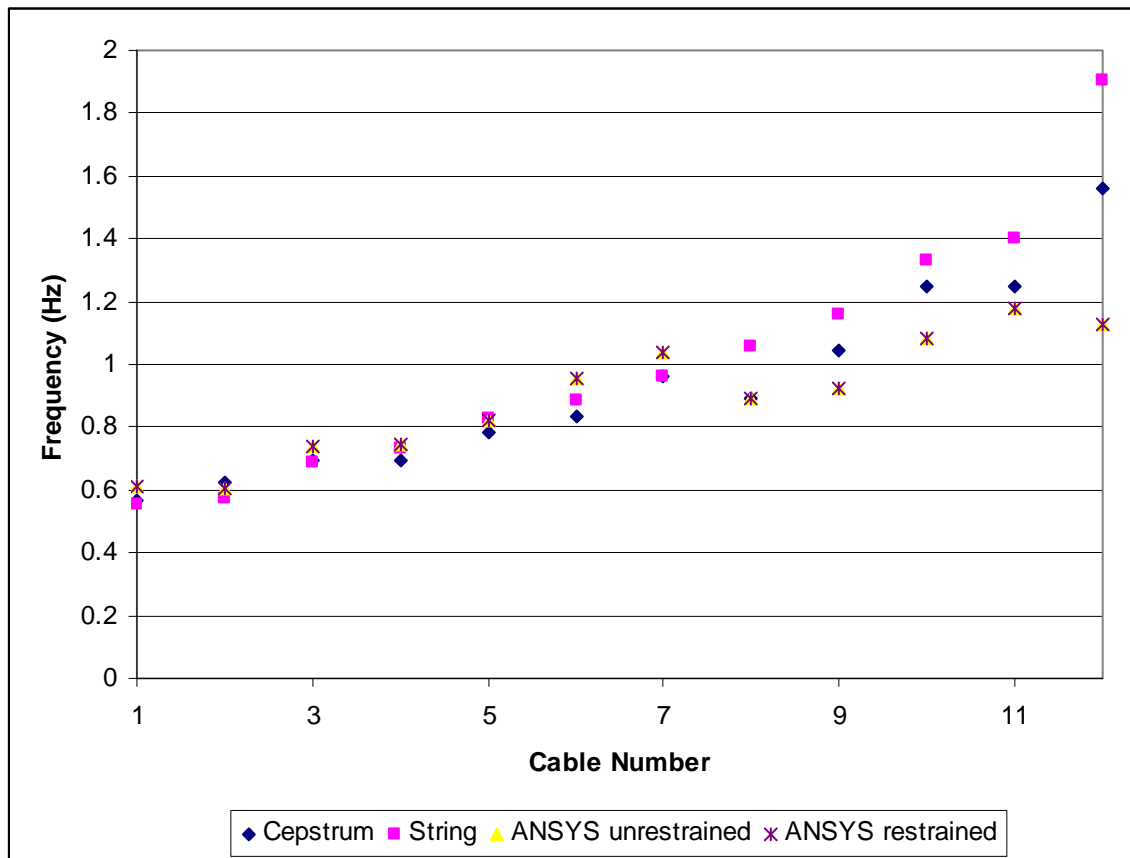


**Figure 4.20** Comparison of Finite Element Model Fundamental Frequency Results for Cables 1-12 E to Experimental and String Model Frequencies

To add restrainers to a model of a set of twelve cables, additional beam elements connect the nodes of the cables closest to the restrainer locations. Note that the restrainers were installed without specific locations indicated in the drawings relative to the work points that define the cable lengths. Restrainer locations in the model were established using the geometry indicated on the drawings and observations of the installed restrainers. Note also that the restrainers are a system including the following (as seen in Figure 4 above): an elastic interface between the cable and the collar (cable band), the collar, threaded stud welded to the cable and screwed into the collar, and two criss-crossing cable ties (bridge wires). Past experience has identified that the cross-ties are the dominant component in this system, therefore the cross-ties are modeled as single cables, with a cross-sectional area equivalent to the two criss-crossing cables, connecting at the appropriate nodes.



**Figure 4.21** Photograph of Restrainers on the Owensboro Bridge

Properties of the cross ties are as follows: cross-section diameter = 0.707 inches, Young's modulus =  $20 \times 10^6$  psi, density = 0.01826 slugs/in<sup>3</sup>, Poisson's ratio = 0.3 and modal

damping ratio = 0.0025. Two lines of restrainers are installed for each set of ten cables. The restrainer locations for the model are specified by listing a cable number (in this set the cables are numbered from 1 through 12 with 1 being the longest and 12 being the shortest) with a node number (nodes are numbered from 1 to 35 from the deck to the tower). The first restrainer line connects the following cable-nodes: 1-10, 2-9, 3-9, 4-7, and 5-4. The second restrainer line connects the following cable-nodes: 1-17, 2-17, 3-16, 4-15, 5-14, 6-12, 7-10, 8-7, and 9-4. The third restrainer line connects the following cable-nodes: 1-26, 2-26, 3-26, 4-26, 5-25, 6-24, 7-23, 8-22, 9-21, 10-20, 11-19, and 12-18. For the restrainers, tension-only elements are used rather than beam elements. The model mesh is presented in Figure 4.22. Fundamental frequency results of the restrained cable model are included above in Table 4.4. As noted in the field test results, the out-of-plane response of the cables is not appreciably affected by the restrainers, so the fundamental cable frequencies from the restrained cable model are only slightly lower than that of the unrestrained cable model.

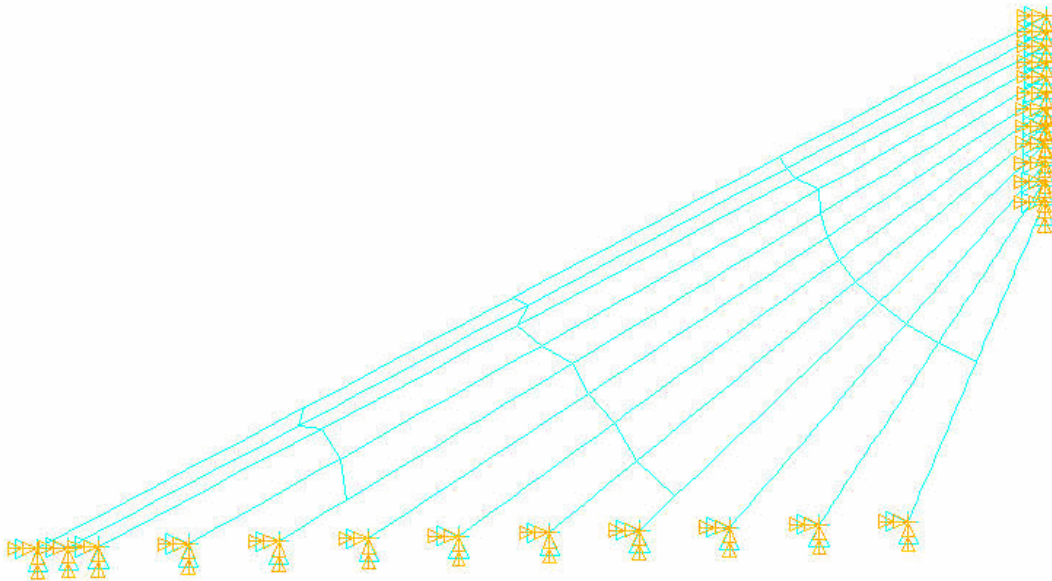


**Figure 4.22:** Finite Element Model of Twelve Restrained Cables of the Owensboro Bridge

Finally, unrestrained models of upstream cables 1-48 and downstream cables 1-24 of the Owensboro Bridge were constructed in sets of 12 as described above and using the as-built information provided in Tables 4.3 and 4.4. The fundamental frequencies resulting from these models were compared to the field test results. Field tests were not performed in August 2003

on downstream cables 25-48, therefore no FE models were constructed and no comparisons were made for these cables. The results of these comparisons are presented in Figure 4.23. There is reasonable correlation to the field test data with larger discrepancies in shorter cables.

**Table 4.3** Cable Geometry and Material Properties for Upstream Cables 1-48

CABLE NUMBER	COORDINATES						PE PIPE DIAMETER INCHES	EFFECTIVE YOUNG'S MODULUS KSI	DENSITY SLUGS/IN3	INITIAL STRAIN
	WORK POINT B1			WORK POINT T1						
	X FT	Y FT	Z FT	X FT	Y FT	Z FT				
1	-1101.042	435.122	-36.951	-604.167	698	-4.44	8.625	27423.27	0.0002377	0.000562
2	-1086.058	435.572	-36.951	-604.167	690.5	-5.165	8.625	27372.86	0.0002359	0.000528
3	-1071.18	436.022	-36.951	-604.167	683	-5.89	8.625	27713.58	0.0002695	0.000844
4	-1026.752	437.372	-36.951	-604.167	675.5	-6.616	6.625	27661.22	0.0002521	0.000691
5	-982.379	438.721	-36.951	-604.167	668	-7.341	6.625	27728.00	0.0002688	0.000747
6	-938.005	440.027	-36.951	-604.167	660	-8.115	6.625	27844.60	0.0002628	0.000800
7	-893.691	441.272	-36.951	-604.417	652	-8.888	6.625	27869.89	0.0002568	0.000742
8	-848.801	442.957	-36.881	-604.667	643.5	-9.71	6.625	27598.55	0.0002508	0.000411
9	-804.678	444.081	-36.881	-604.667	635	-10.951	6.625	27522.70	0.0002449	0.000317
10	-760.19	445.644	-36.81	-604.917	625.5	-11.869	6.625	27735.66	0.0002395	0.000315
11	-716.179	446.896	-36.775	-605.167	616	-12.788	6.625	27795.55	0.0002215	0.000240
12	-672.319	448.338	-36.705	-605.167	606	-13.755	6.625	27633.66	0.0002426	0.000153
13	-527.726	451.038	-36.705	-594.833	606	-13.755	6.625	27761.57	0.0002426	0.000171
14	-483.918	451.216	-36.775	-594.833	616	-12.788	6.625	27805.25	0.0002215	0.000237
15	-439.97	451.584	-36.81	-595.083	625.5	-11.869	6.625	27747.07	0.0002395	0.000315
16	-395.536	451.641	-36.881	-595.333	635	-10.951	6.625	27651.19	0.0002418	0.000345
17	-351.49	452.137	-36.881	-595.333	643.5	-9.71	6.625	27558.57	0.0002479	0.000382
18	-306.645	452.072	-36.951	-595.583	652	-8.888	6.625	27409.05	0.0002538	0.000406
19	-261.999	452.197	-36.986	-595.833	660	-8.115	6.625	27491.88	0.0002629	0.000505
20	-217.671	452.511	-36.986	-595.833	668	-7.341	6.625	27346.65	0.0002688	0.000524
21	-172.932	452.514	-37.021	-595.833	675.5	-6.616	8.625	25781.67	0.0002306	0.000297
22	-128.52	452.706	-37.021	-595.833	683	-5.89	8.625	26662.79	0.0002359	0.000397
23	-84.108	452.838	-37.021	-595.833	690.5	-5.165	8.625	27016.33	0.0002341	0.000467
24	-39.564	452.909	-37.021	-595.833	698	-4.44	8.625	27356.68	0.0002554	0.000664
25	39.564	452.909	-37.021	595.833	698	-4.44	8.625	22994.70	0.0002554	0.000341
26	84.108	452.838	-37.021	595.833	690.5	-5.165	8.625	26421.54	0.0002341	0.000397
27	128.52	452.706	-37.021	595.833	683	-5.89	8.625	26464.67	0.0002359	0.000378
28	172.932	452.514	-37.021	595.833	675.5	-6.616	8.625	26013.02	0.0002306	0.000308
29	217.671	452.511	-36.986	595.833	668	-7.341	6.625	27241.79	0.0002688	0.000496
30	261.999	452.197	-36.986	595.833	660	-8.115	6.625	27545.32	0.0002629	0.000527
31	306.645	452.137	-36.951	595.583	652	-8.888	6.625	27535.87	0.0002538	0.000445
32	351.49	452.072	-36.881	595.333	643.5	-9.71	6.625	27567.76	0.0002479	0.000385
33	395.536	451.641	-36.881	595.333	635	-10.951	6.625	27645.71	0.0002418	0.000343
34	439.97	451.584	-36.81	595.083	625.5	-11.869	6.625	27420.30	0.0002395	0.000232
35	483.918	451.216	-36.775	594.833	616	-12.788	6.625	27855.88	0.0002215	0.000266
36	527.726	451.038	-36.705	594.833	606	-13.755	6.625	27668.69	0.0002426	0.000150
37	672.319	448.338	-36.705	605.167	606	-13.755	6.625	27687.18	0.0002426	0.000163
38	716.179	446.896	-36.775	605.167	616	-12.788	6.625	27843.22	0.0002215	0.000266
39	760.19	445.644	-36.81	604.917	625.5	-11.869	6.625	27562.75	0.0002395	0.000259
40	804.678	444.081	-36.881	604.667	635	-10.951	6.625	27854.14	0.0002449	0.000497
41	848.801	442.957	-36.881	604.667	643.5	-9.71	6.625	27606.34	0.0002508	0.000414
42	893.691	441.272	-36.951	604.417	652	-8.888	6.625	27481.81	0.0002568	0.000449
43	938.005	440.027	-36.951	604.167	660	-8.115	6.625	27408.69	0.0002628	0.000493
44	982.379	438.721	-36.951	604.167	668	-7.341	6.625	27558.96	0.0002688	0.000628
45	1026.752	437.372	-36.951	604.167	675.5	-6.616	6.625	27659.81	0.0002521	0.000690
46	1071.18	436.022	-36.951	604.167	683	-5.89	8.625	27665.60	0.0002695	0.000798
47	1086.058	435.572	-36.951	604.167	690.5	-5.165	8.625	27374.82	0.0002359	0.000529
48	1101.042	435.122	-36.951	604.167	698	-4.44	8.625	27423.27	0.0002377	0.000562

**Table 4.4** Cable Geometry and Material Properties for Downstream Cables 1-24

CABLE NUMBER	COORDINATES						PE PIPE DIAMETER INCHES	EFFECTIVE YOUNG'S MODULUS KSI	DENSITY SLUGS/IN3	INITIAL STRAIN
	WORK POINT B1			WORK POINT T1						
	X	Y	Z	X	Y	Z				
	FT	FT	FT	FT	FT	FT				
1	-1101.042	435.122	36.951	-604.167	698	4.44	8.625	27423.27	0.000238	0.000562
2	-1086.058	435.572	36.951	-604.167	690.5	5.165	8.625	27421.22	0.000236	0.000544
3	-1071.18	436.022	36.951	-604.167	683	5.89	8.625	27683.79	0.000270	0.000814
4	-1026.752	437.372	36.951	-604.167	675.5	6.616	6.625	27677.53	0.000252	0.000703
5	-982.379	438.721	36.951	-604.167	668	7.341	6.625	27824.80	0.000269	0.000874
6	-938.005	440.027	36.951	-604.167	660	8.115	6.625	27818.73	0.000263	0.000757
7	-893.691	441.272	36.951	-604.417	652	8.888	6.625	27846.40	0.000257	0.000699
8	-848.801	442.957	36.881	-604.667	643.5	9.71	6.625	27590.56	0.000251	0.000408
9	-804.678	444.081	36.881	-604.667	635	10.951	6.625	27749.62	0.000245	0.000406
10	-760.19	445.644	36.81	-604.917	625.5	11.869	6.625	27691.24	0.000240	0.000296
11	-716.179	446.896	36.775	-605.167	616	12.788	6.625	27795.55	0.000222	0.000240
12	-672.319	448.338	36.705	-605.167	606	13.755	6.625	27726.67	0.000243	0.000173
13	-527.726	451.038	36.705	-594.833	606	13.755	6.625	27787.66	0.000243	0.000180
14	-483.918	451.216	36.775	-594.833	616	12.788	6.625	27805.25	0.000222	0.000237
15	-439.97	451.584	36.81	-595.083	625.5	11.869	6.625	27400.88	0.000240	0.000226
16	-395.536	451.641	36.881	-595.333	635	10.951	6.625	27597.42	0.000242	0.000327
17	-351.49	452.137	36.881	-595.333	643.5	9.71	6.625	27480.04	0.000248	0.000328
18	-306.645	452.072	36.951	-595.583	652	8.888	6.625	27515.10	0.000254	0.000415
19	-261.999	452.197	36.986	-595.833	660	8.115	6.625	27400.00	0.000263	0.000475
20	-217.671	452.511	36.986	-595.833	668	7.341	6.625	27177.89	0.000269	0.000479
21	-172.932	452.514	37.021	-595.833	675.5	6.616	8.625	26358.84	0.000231	0.000295
22	-128.52	452.706	37.021	-595.833	683	5.89	8.625	26991.17	0.000236	0.000378
23	-84.108	452.838	37.021	-595.833	690.5	5.165	8.625	27479.99	0.000234	0.000529
24	-39.564	452.909	37.021	-595.833	698	4.44	8.625	27356.68	0.000255	0.000664

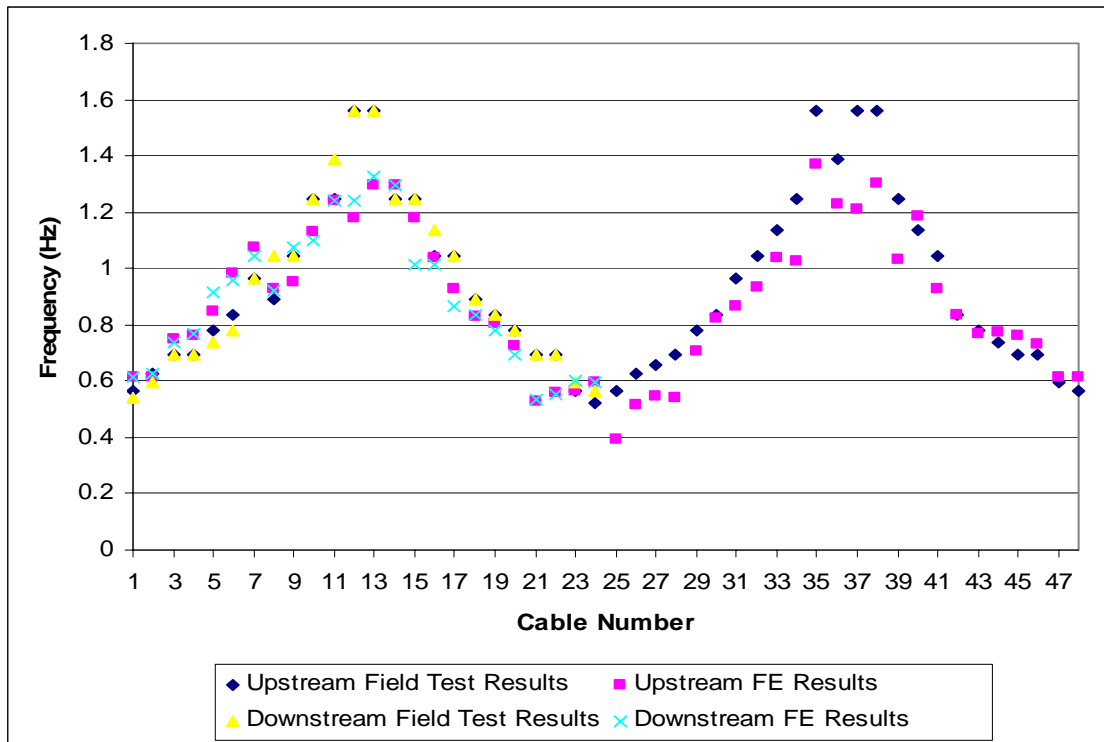


**Figure 4.23** Comparison of Finite Element Frequency Results and Field Test Results

These results provided reasonable model correlation, with larger differences in shorter cables. As part of this effort and described above under the testing section, a study was undertaken to examine signal processing parameter selection with the goal of reducing the shorter cable resolution. Although the resolution can be improved (decreased) slightly, other issues such as zero-padding effects may arise.

Another, and more critical, question was whether the above-the deck anchors needed to be modeled in detail for analysis of the cable instead of as providing a fixed end condition. A FE study using inclined cable models with springs in the transverse directions at their base illustrated the change in fundamental frequency that occurs with reduced stiffness at the anchor. Figure 4.24 presents an illustration of this trend, along with a definition of critical stiffness – the anchor stiffness required to result in a cable fundamental frequency in that direction that is 95% of the fixed boundary condition frequency.

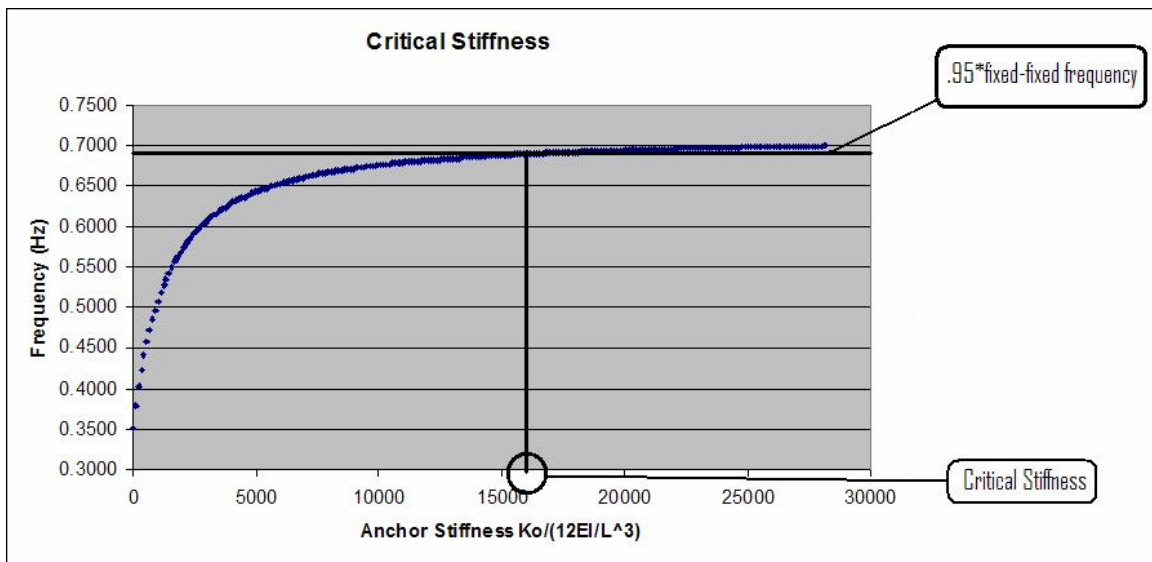


**Figure 4.24** Cable Frequency Trend vs. Anchor Stiffness and Definition of Critical Stiffness

To evaluate the necessity for including a detailed model of the anchor to improve correlation, a detailed finite element model of the deck anchorages was constructed with mesh as presented in Figure 4.25. The model was developed so that the geometry for different cable anchors could be used to create a detailed model of each cable anchor. A selection of these anchor models were studied with transverse forces applied to represent the loading of the

anchor due to motion of the cable. As seen in Figures 4.26 and 4.27, deflections of the anchors under various loadings were computed and used to determine the anchor stiffness in the two transverse (axial stiffness was not a consideration here) directions.

The result of this study was that the in-plane (vertical) transverse direction had a stiffness that was much higher than the critical stiffness value as expected by looking at the anchor dimensions at the deck. However, in the out-of-plane (lateral) transverse direction, the stiffness approached the critical stiffness defined for fixed-fixed modeling boundary conditions. The lateral stiffness was slightly higher than critical, though, so a fixed boundary condition is appropriate for the Owensboro cables.

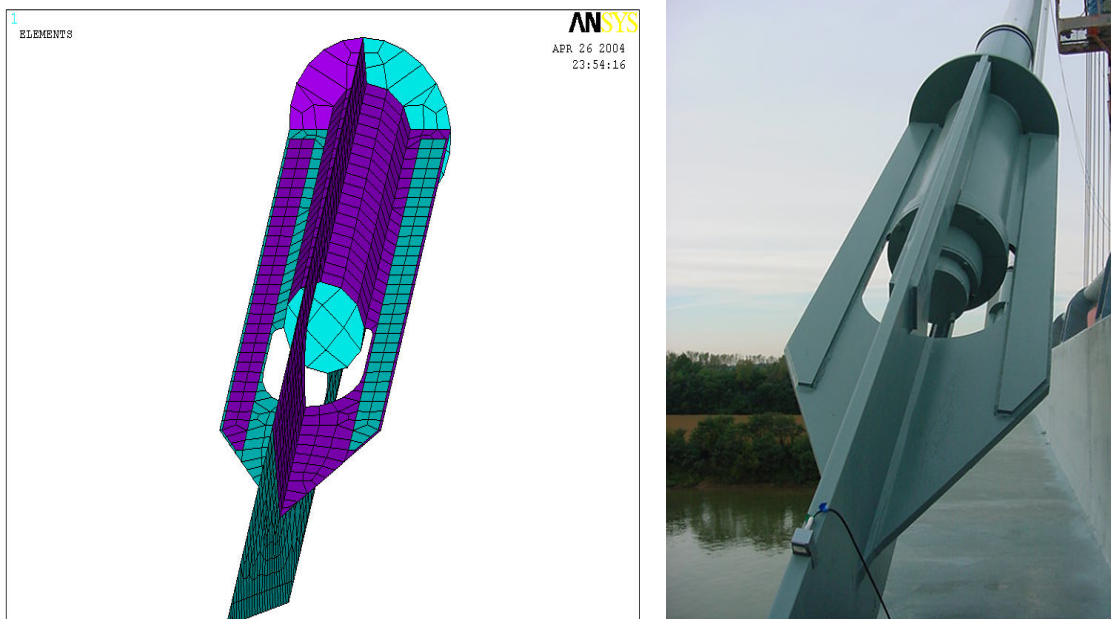


**Figure 4.25** FE model of the Owensboro anchor along side anchor picture

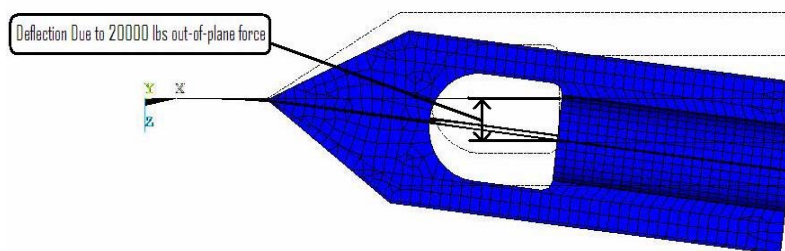


**Figure 4.26** Deflected FE Model with Transverse Loading Applied from Cable

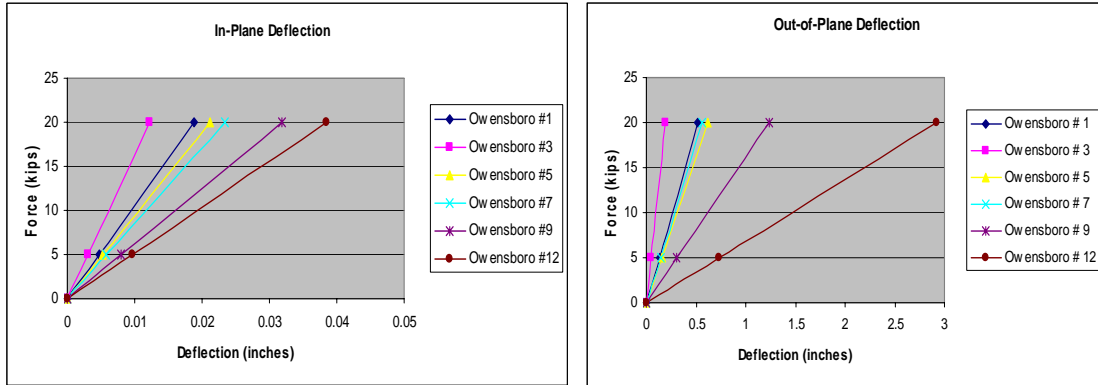


**Figure 4.27** Anchor Force-Deflection Plots for Selected Owensboro Anchor Geometries: In-Plane (left) and Out-of-Plane (right)

For improved correlation with the fixed boundary condition, additional parameter studies were performed to identify the properties of the cable that have the most significant effect on the frequency of the cable. Since the geometry of the cable, length and diameter, are known to a high degree of certainty, they were not included in the parameter study. This study showed that the tension in the cable had a much greater effect on the frequency than the Elastic Modulus, or the density.

Discrepancies in the as-built tensions and the actual tension in the cables does not seem entirely unlikely because of the drastic differences between the original bridge plan tension values and the as-built tension values. Adjusting the initial strain in upstream cable 12 from .000153 to .000300 results in a well correlated frequency value. This corresponds to a tension increase of 146 kips to 286 kips. Though this seems like a large adjustment, the original bridge plans specify a tension load of 520 kips for upstream cable 12. Consequently, this adjustment is well within the original tension specification. Results for upstream cables 1 through 12 are included in Table 4.5. There are no known methods for directly measuring the tension of cables that have been installed on the bridge without built-in instrumentation.

Therefore, to this point, the as-built load values provided are the best information available. However, tensions are expected to change with deck creep and other use-life factors, and with temperature. Consequently, a periodic survey of frequencies may be useful for comparison with design predictions of tension changes. The FE models using the as-built load values provide reasonable correlation, and no further modifications will be performed. Tables 4.6 and 4.7 present the frequency results for the models and field tests.

**Table 4.5** Tension Adjustments for Model Correlation of Upstream Cables 1-12

Cable Number	Field Test Frequency (Hz)	As-Built Frequency (Hz)	As-Built Tension (lbs)	Adjusted Model Tension (lbs)	Adjusted Model Frequency (Hz)	Original Plans Tension (lbs)
1	0.5682	0.6133	901	777	0.571	778
2	0.625	0.6158	845	865	0.6231	776
3	0.6944	0.7522	1366	1166	0.6961	1184
4	0.6944	0.7641	659	548	0.6985	646
5	0.7813	0.8456	714	602	0.7782	715
6	0.8333	0.9824	768	550	0.8353	652
7	0.9615	1.074	713	570	0.9631	607
8	0.8929	0.9257	391	360	0.8896	560
9	1.0417	0.9523	301	365	1.043	504
10	1.25	1.133	301	373	1.2505	478
11	1.25	1.242	230	235	1.253	357
12	1.5625	1.178	146	286	1.568	520

**Table 4.6** Downstream Cable Frequency Results

Cable Number	Field (Hz)	String (Hz)	ANSYS (Hz)	ANSYS restrained	% Difference Field vs ANSYS
1	0.5435	0.5550	0.6133	0.6098	-12.84
2	0.5952	0.5740	0.6253	0.6184	-5.06
3	0.6944	0.6850	0.7386	0.7274	-6.37
4	0.6944	0.7350	0.7708	0.7486	-11.00
5	0.7353	0.8280	0.9147	0.8899	-24.40
6	0.7813	0.8840	0.9559	0.9294	-22.35
7	0.9615	0.9640	1.0420	1.0110	-8.37
8	1.0417	1.0600	0.9223	0.8927	11.46
9	1.0417	1.1620	1.0740	1.0350	-3.10
10	1.25	1.3300	1.1000	1.0570	12.00
11	1.3889	1.4010	1.2420	1.1580	10.58
12	1.5625	1.9030	1.2420	1.2070	20.51
13	1.5625	1.9180	1.3250	1.2800	15.20
14	1.25	1.4150	1.2980	1.2030	-3.84
15	1.25	1.3430	1.0110	0.9541	19.12
16	1.1364	1.1810	1.012	0.9808	10.95
17	1.0417	1.0770	0.8644	0.8418	17.02
18	0.8929	0.9770	0.8372	0.8137	6.24
19	0.8333	0.8940	0.7789	0.7574	6.53
20	0.7813	0.8270	0.6927	0.6754	11.34
21	0.6944	0.6480	0.5347	0.5256	23.00
22	0.6944	0.6120	0.5501	0.5412	20.78
23	0.5952	0.5620	0.6031	0.5949	-1.33
24	0.5628	0.5730	0.5959	0.59	-5.88

**Table 4.7** Upstream Cable Frequency Results

Cable Number	Field (Hz)	String (Hz)	ANSYS (Hz)	ANSYS restrained	% Difference Field vs ANSYS
1	0.5682	0.5550	0.6133	0.61113	-7.94
2	0.625	0.5740	0.6158	0.60756	1.47
3	0.6944	0.6850	0.7522	0.73727	-8.32
4	0.6944	0.7350	0.7641	0.74542	-10.04
5	0.7813	0.8280	0.8456	0.82347	-8.23
6	0.8333	0.8840	0.9824	0.95452	-17.89
7	0.9615	0.9640	1.074	1.041	-11.70
8	0.8929	1.0600	0.9257	0.89452	-3.67
9	1.0417	1.1620	0.9523	0.92366	8.58
10	1.25	1.3300	1.133	1.083	9.36
11	1.25	1.4010	1.242	1.178	0.64
12	1.5625	1.9030	1.178	1.127	24.61
13	1.5625		1.297		16.99
14	1.25		1.298		-3.84
15	1.25		1.182		5.44
16	1.0417		1.039		0.26
17	1.0417		0.9303		10.69
18	0.8929		0.8268		7.40
19	0.8333		0.8036		3.56
20	0.7813		0.7258		7.10
21	0.6944		0.5305		23.60
22	0.6944		0.5598		19.38
23	0.5682		0.5629		0.93
24	0.5208		0.5959		-14.42
25	0.5682		0.3953		30.43
26	0.625		0.5147		17.65
27	0.6579		0.5447		17.21
28	0.6944		0.5422		21.92
29	0.7813		0.7054		9.71
30	0.8333		0.8212		1.45
31	0.9615		0.866		9.93
32	1.0417		0.9339		10.35
33	1.1364		1.036		8.83
34	1.25		1.023		18.16
35	1.5625		1.367		12.51
36	1.3889		1.228		11.58
37	1.5625		1.211		22.50
38	1.5625		1.301		16.74
39	1.25		1.033		17.36
40	1.1364		1.184		-4.19
41	1.0417		0.929		10.82

**Table 4.7 Continued** Upstream Cable Frequency Results

Cable Number	Field (Hz)	String (Hz)	ANSYS (Hz)	ANSYS restrained	% Difference Field vs ANSYS
42	0.8333		0.8365		-0.38
43	0.7813		0.7705		1.38
44	0.7353		0.7746		-5.34
45	0.6944		0.7635		-9.95
46	0.6944		0.7312		-5.30
47	0.5952		0.6164		-3.56
48	0.5682		0.6133		-7.94

#### 4.4. Remarks

Cable testing and modeling for the Owensboro bridge included two field tests of the cables (October 2002 and August 2003). The first of these was just before the bridge opened with excitation provided by loaded trucks. The second used ambient (typical traffic and wind) excitation. Signal processing analysis of the recorded acceleration time histories identified fundamental frequencies of the cables. Finite element models were developed for all cables using the as-built cable properties and compared to field test results showing good correlation.

Notable results include the following:

1) A critical stiffness value for the anchor was defined as the stiffness required for the cable frequency to be 95% of the fixed-boundary frequency. A detailed model of each Owensboro bridge anchor was constructed to determine its influence on the cable response. Although the lateral stiffness approaches the critical value for the anchor design, it is larger. Therefore, the cables can be modelled as fixed to the deck and detailed models of the anchors are not required.

2) Signal processing was performed to identify the fundamental cable frequency from each cable record. The cable transverse direction response (perpendicular to the vertical plane containing the parallel cables and restrainers) enabled identification of the unrestrained fundamental frequency for each cable. The Cepstrum signal processing approach, developed at the University of Kentucky for a previous cable-stayed bridge

project, allowed automated processing of the data records. Studies were conducted to improve understanding of the FFT parameters specified for the analyses.

3) Using short time records with Cepstrum analysis enables testing of all bridge stay cables in 1.5 days (facilitating periodic visits for cable monitoring). Periodic monitoring may be useful for the cables of the Owensboro bridge to understand tension changes as the bridge is in use.

4) Field tests of the cables on both occasions resulted in consistent fundamental frequencies.

5) Excessive motion of the cable cross ties (restrainers) was observed during both field tests. This raises concerns suggesting close inspection of the cross ties in case fatigue becomes a problem.

6) Eight technical papers and theses related to the Owensboro bridge testing and nonlinear modeling of cables (not in the scope of this project and under separate support) have been completed from 2003 through 2005 and are included in the references.

Finally, note that the cable testing and modeling effort could not have been accomplished without the assistance of many colleagues and capable students who helped with the bridge testing, data analysis and model verification. Their careful attention to detail contributed to the excellent results seen herein.

## **5. CONCLUSIONS AND RECOMMENDATIONS**

### **5.1. General**

Owensboro cable-stayed bridge, dedicated as the William H. Natcher Bridge, was completed in 2002. It connects Owensboro (Daviness County), Kentucky and Rockport (Spencer County), Indiana over the Ohio River. Since the main span length was increased and more shallow and slender stiffness girders were used in modern cable-stayed bridges, the safety of the whole bridges under service loadings and environmental dynamic loadings presents increasingly important concerns in design, construction and service. It has become essential to synthetically understand and realistically predict their response to these loadings. The present study focuses on the baseline modeling of the Owensboro cable-stayed bridge. It has been demonstrated that the dynamics-based structural evaluation method provides a 'global' way to evaluate the structural state and safety of the bridge. The dynamics-based structural evaluation requires improvements in instrumentation for sensing and recording, data acquisition, algorithms for system identification, model updating and structure evaluation. The finite element model calibration through the field dynamic testing plays an important role in the dynamics-based structural evaluation. The calibrated finite element model can be used as a baseline for health assessments of the bridge structure in the future.

### **5.2. Finite Element Modeling and Dynamic Properties**

The complete 3-D nonlinear modeling of a cable-stayed bridge has proved to be difficult. The smaller discretization would be computationally very large and inefficient. Convergence of such a large number of nonlinear elements is not always guaranteed. The displacement convergence criterion is effective and often results in the convergent solution. Due to the cable sagging, the static analysis of a cable-stayed bridge is always a geometric nonlinear. The stress stiffening of cable elements plays an important role in both the static and dynamic analysis. Nonlinear static analysis without the stress stiffening effect will lead to an aborted run due to the divergent oscillation even though the displacement convergence criterion is used. Large deflection has been demonstrated

to be the limited effect on the member forces and deck deflection of the bridge under dead loads. After introducing enough amount of initial strain in the cables, the static analysis of the Owensboro cable-stayed bridge due to dead loads can be elastic and small deflection. However, the stress stiffening effect is always required to ensure the convergent solution.

The initial strain in the cables is the key factor to control the initial equilibrium configuration under the dead load. For a complete bridge, the common fact is that the initial position of the cable and bridge is unknown. The initial geometry of the bridge which was modeled is really the deflected shape of the bridge loaded by the dead load. The initial equilibrium configuration of the bridge due to dead loads can be approximately achieved by referring to the bridge plans.

It is demonstrated that a cable-stayed bridge is a highly pre-stressed structure. The self-weight effect can significantly improve the stiffness of a cable-stayed bridge. The modal or any dynamic analysis must start from the initial equilibrium configuration due to dead loads. This initial equilibrium configuration can be a small deflection static analysis because the large deflection can be ignored. The modal analysis of a cable-stayed bridge should include two steps: small deflection static analysis under the dead load and followed by pre-stressed modal analysis, so that the dead load effect on the stiffness can be included. In other words, the modal analysis of a cable-stayed bridge must be a pre-stressed modal analysis.

It is observed that one dominated mode of the Owensboro cable-stayed bridge is always coupled with other modes. The dominated mode shapes of the Owensboro cable-stayed bridge in the low-frequency (0~1.0 Hz) range are mainly vertical direction. This reveals the fact that the lateral stiffness of the cable stayed bridge is stronger than that of the suspension bridge (Ren and Harik 2001). From the parametric studies, it is found that the key parameters affecting the vertical modal properties are the mass, cable sectional area, cable elastic modulus and deck vertical bending stiffness. The key parameters

affecting the transverse and torsion modal properties are the mass, cable sectional area, cable elastic modulus and deck lateral bending stiffness.

### **5.3. Free Vibration Testing and Model Calibration**

On site free vibration testing provides a fast way to obtain the real dynamic properties of a structure. The modal parameters can be effectively extracted from output-only dynamic testing by using the frequency domain based peak picking (PP) method. The peak picking identification is very fast and efficient since no model has to be fitted to the data. For real applications, the peak picking method could be used on site to verify the quality of the measurements. But the mode shapes for the transverse direction did not match well since the bridge is very stiff in the transverse direction and the transverse excitation data could not be filtered from the noise data.

A good agreement of frequencies has been found between the results of the calibrated finite element model and in *situ* free vibration testing results. The identified frequencies from the high-speed measurements are quite stable. The better matching for higher modes is not expected and not realistic either, as the experimental modal properties of the bridge come from the output-only measurement. The calibrated finite element model may be used as a baseline in the future structural analysis and monitoring of the Owensboro cable-stayed bridge.

### **5.4. Cable Testing and Modeling**

A critical stiffness value for the anchor was defined as the stiffness required for the cable frequency to be 95% of the fixed boundary frequency. Detailed models of the anchors were constructed to determine whether they had to be included in the cable models. Although the lateral stiffness approaches the critical value, it is larger. Therefore, the cables can be modelled as fixed to the deck and detailed models of the anchors are not required.

Signal processing was performed to identify the fundamental cable frequency from each cable record. Field tests of the cables on both occasions resulted in consistent fundamental frequencies. The cable transverse direction response (perpendicular to the vertical plane containing the parallel cables and restrainers) enabled identification of the unrestrained fundamental frequency for each cable. Excessive motion of the cable cross ties (restrainers) was observed during both field tests. This raises concerns suggesting close inspection of the cross ties in case fatigue becomes a problem.

The Cepstrum signal processing approach, developed at the University of Kentucky for a previous cable-stayed bridge project, allowed automated processing of the data records. Using short time records with Cepstrum analysis enables testing of all bridge stay cables in 1.5 days. Periodic monitoring may be useful for the cables of the Owensboro bridge to understand tension changes as the bridge is in use.

## REFERENCES

- Abdel-Ghaffar, A.M. (1980). "Vertical vibration analysis of suspension bridges." *Journal of Structural Engineering*, ASCE, 106(10), 2053-2075.
- Abdel-Ghaffar, A.M. and Rubin, L.I. (1983). "Vertical seismic behavior of suspension bridges." *Earthquake Engineering and Structural Dynamics*, 11, 1-19.
- Abdel-Ghaffar, A.M. and Nazmy A.S. (1987) "Effects of three-dimensionality and nonlinearity on the dynamic and seismic behavior of cable-stayed bridges." *Proceedings of the Structures Congress (Bridges and Transmission Line Structures)*, ASCE, New York, 389-404.
- Abdel-Ghaffar, A.M. and Nazmy, A.S. (1991a). "3-D nonlinear seismic behavior of cable-stayed bridges." *Journal of Structural Engineering*, ASCE, 117(11), 3456-3476.
- Abdel-Ghaffar, A.M. and Khalifa, M.A. (1991b) "Importance of cable vibration in dynamics of cable-stayed bridges." *Journal of Engineering Mechanics*, ASCE, 117(11), 2571-2589.
- Abdel-Ghaffar, A.M. and Scanlan, R. H. (1985). "Ambient vibration studies of Golden Gate Bridge. I: suspended structure." *Journal of Engineering Mechanics*, ASCE, 111(4), 463-482.
- Andersen, P., Brincker, R. and Kirkegaard, P.H. (1996). "Theory of covariance equivalent ARMAV models of civil engineering structures." *Proceedings of IMAC14, the 14th International Modal Analysis Conference*, Dearborn, MI, 518-524.
- ANSYS5.6 (1999). *User's manual*, Swanson Analysis System, USA.
- Au, F.T.K., Cheng, Y.S., Cheung, Y.K. and Zheng, D.Y. (2001). "On the determination of natural frequencies and mode shapes of cable-stayed bridges." *Applied Mathematical Modeling*, 25, 1099-1115.
- Baker, J.R. and Smith, S.W. (2002) "Simulation of parametric response of bridge stay cables." *Proceedings of the International Modal Analysis Conference*, Los Angeles, California.
- Bathe, K.J. (1982). *Finite element procedures in engineering analysis*. Prentice-Hall, Inc., Englewood Cliffs, New Jersey.
- Bendat, J.S. and Piersol, A.G. (1993). *Engineering applications of correlation and spectral analysis*. 2nd edition, John Wiley & Sons, New York.

- Boonyapinyo, V., Miyata, T. and Yamada, H. (1999). "Advanced aerodynamic analysis of suspension bridges by state-space approach." *Journal of Structural Engineering*, ASCE, 125(12), 1357-1366.
- Boonyapinyo, V., Yamada, H. and Miyata, T. (1994). "Wind-induced nonlinear lateral-torsional buckling of cable-stayed bridges." *Journal of Structural Engineering*, ASCE, 120(2), 486-506.
- Bracewell, R.N. (2000). *The fourier transform and its applications*. Third edition, McGraw Hill.
- Brownjogn, J.M.W. and Xia, P.Q.(2000). "Dynamic assessment of curved cable-stayed bridge by model updating." *Journal of Structural Engineering*, ASCE, 126(2), 252-260.
- Brownjohn, J.M.W., Dumanoglu, A.A. and Severn, R.T. (1992). "Ambient vibration survey of the Faith Sultan Mehmet (Second Bosphorus) suspension bridge." *Earthquake Engineering and Structural Dynamics*, 21, 907-924.
- Caetano, E., Cunha, A. and Taylor, C.A. (2000a) "Investigation of dynamic cable-deck interaction in a physical model of a cable-stayed bridge, part I: modal analysis." *Earthquake Engineering and Structural Dynamics*, 29(4), 481-498.
- Caetano, E., Cunha, A. and Taylor, C.A. (2000b) "Investigation of dynamic cable-deck interaction in a physical model of a cable-stayed bridge, part II: seismic response." *Earthquake Engineering and Structural Dynamics*, 29(4), 499-521.
- Campbell, J.E. and Smith, S.W. (2003) "Comparison of field survey test results of four cable stayed bridges: deck/cable response and controlled/ambient traffic excitation." *Proceedings of the Fifth International Symposium on Cable Dynamics*, Santa Margarita Ligure, Italy, 517-524.
- Campbell, J.E., Baker, J.R. and Smith, S.W. (2004) "Simulations and tests of bridge stay-cable dynamics based on experimental deck motion measurements." *Proceedings of the International Modal Analysis Conference*, Detroit, Michigan.
- Casas, J.R. and Aparicio, A.C. (1994). "Structural damage identification from dynamic-test data." *Journal of Structural Engineering*, ASCE, 120(8), 2437-2450.
- Chang, C.C., Chang, T.Y.P. and Zhang, Q.W. (2001). "Ambient vibration of long-span cable-stayed bridge." *Journal of Bridge Engineering*, ASCE, 6(1), 46-53.
- Chen, H.L., Spyrakos, C.C. and Venkatesh, G. (1995). "Evaluating structural deterioration by dynamic response." *Journal of Structural Engineering*, ASCE, 121(8), 1197-1204.

Cunha, A., Caetano, E. and Delgado, R. (2001). "Dynamic tests on large cable-stayed bridge." *Journal of Bridge Engineering*, ASCE, 6(1), 54-62.

DADiSP (1996). *User Manual, DADiSP Worksheet, Data Analysis and Display Software*. DSP Development Corporation, Cambridge, Massachusetts.

De Roeck, G. and Peeter, B. (1999). *MACCEC2.0 – Modal Analysis on Civil Engineering Constructions*, Department of Civil Engineering, Catholic University of Leuven, Belgium.

De Roeck, G., Peeters, B. and Ren, W.X. (2000). "Benchmark study on system identification through ambient vibration measurements." *Proceedings of IMAC-XVIII*, the 18<sup>th</sup> International Modal Analysis Conference, San Antonio, Texas, 1106-1112.

Doebbling, S.W., Farrar, C.R., Prime, M.B. and Shevitz, D.W. (1996). "Damage identification and health monitoring of structural and mechanical systems from changes in their vibration characteristics: A literature review." *Research report LA-13070-MS, ESA-EA*, Los Alamos National Laboratory, New Mexico, USA.

Ewins, D.J. (1986). *Modal testing: theory and practice*. Research Studies Press Ltd., England.

Flamand, O., Peube, J. and Papanikolas, P. (2001) "An Explanation of the Rain-Wind Induced Vibration of Inclined Stays," in *Proceedings of the Fourth International Symposium on Cable Dynamics*, Montreal, Canada, May 28-30, 2001.

Fleming, J.F. and Egeseli, E.A. (1980). "Dynamic behavior of a cable-stayed bridge." *Earthquake Engineering and Structural Dynamics*, 8, 1-16.

Friswell, M.I. and Mottershead, J.E. (1995). *Finite element model updating in structural dynamics*, Kluwer Academic Publishers, Netherlands.

Fujina, Y., Warnitchai, P. and Pacheco, B.M. (1993) "An experimental and analytical study of autoparametric resonance in a 3dof model of a cable-stayed beam," *Nonlinear Dynamics*, 4, 111-138.

Gagel, J.C., Baker, J.R. and Smith, S.W. (2005), "Simulations of cable/anchor designs for cable-stayed bridges," *Proceedings of IMAC-XXIII*, the 23<sup>rd</sup> International Modal Analysis Conference, Kissimmee, FL.

Gagel, J.C. (2005), "Dynamic simulations of interactions between stay cables and cable-to-deck anchorages for the William H. Natcher bridge," *Masters Thesis, University of Kentucky*.

Gupta, A.K. (1992). *Response Spectrum Method in Seismic Analysis and Design of Structures*, CRC Press, Ann Arbor, Michigan.

Harik, I.E., Allen, D.L., Street, R.L., Guo, M., Graves, R.C., Harrison, J. and Gawry, M.J. (1997). "Free and ambient vibration of brent-spence bridge." *Journal of Structural Engineering*, ASCE, 123(9), 1262-1268.

Harik, I.E., Allen, D.L., Street, R.L., Guo, M., Graves, R.C., Harrison, J. and Gawry, M.J. (1997). "Seismic evaluation of brent-spence bridge." *Journal of Structural Engineering*, ASCE, 123(9), 1269-1275.

Harik, I.E., Hu, J.D., Smith, S.W., Ren, W.X., Zhao, T., Campbell, J.E. and Graves, R.C. (2005). "Baseline modeling of the Maysville cable-stayed bridge over the Ohio River" *Research Report KTC-05-10*, Kentucky Transportation Center, University of Kentucky.

Harik, I.E., Vasudevan, K., Madasamy, C., Chen, D., Zhou, L., Sutterer, K., Steet, R. and Allen, D.L. (1999). "Seismic evaluation of the US41 Southbound bridge over the Ohio River at Henderson, KY." *Research Report KTC-99-17*, Kentucky Transportation Center, University of Kentucky.

Harris, C.M., ed. (1996) *Shock and Vibration Handbook, Fourth Edition*, McGraw-Hill, New York, 14.34-14.37.

Hearn, G. and Testa, R.B. (1991). "Modal analysis for damage detection in structures." *Journal of Structural Engineering*, ASCE, 117(10), 3042-3063.

Hikami, Y. and Shiraishi, N. (1988) "Rain-wind induced vibrations of cables in cable stayed bridges." *J. Wind Engineering and Industrial Aerodynamics*, 29, 409-418.

James III, G.H., Carne, T.G. and Lauffer, J.P. (1995). "The natural excitation technique (NExT) for modal parameter extraction from operating structures." *International Journal of Analytical and Experimental Modal Analysis*, 10(4), 260-277.

Jean, D.P., Baker, J.R., Smith, S.W. and Li J. (2003) "Phased development of nonlinear finite element simulations of deck-excited response of sagged bridge stay cables." *Proceedings of the Fifth International Symposium on Cable Dynamics*, Santa Margarita Ligure, Italy, 173-180.

Jean, D.P., Baker, J.R. and Smith, S.W. (2003) "Nonlinear finite element simulations of sagged bridge stay cables." *Proceedings of the International Modal Analysis Conference*, Kissimmee, Florida.

Jean, D.P. (2003) "Nonlinear finite element simulations of large oscillations of flexible structures with applications to bridge stay cables." *Masters Thesis, University of Kentucky*.

Johnson, M.L. (1999) "Vibration reduction for rain-wind induced vibrations of the stay cables of the Fred Hartman bridge." *Masters Thesis, University of Kentucky*.

- Juneja, Y., Haftka, R.T. and Cudney, H.H. (1997). "Damage detection and damage detectability - analysis and experiments." *Journal of Aerospace Engineering*, ASCE, 10(4), 135-142.
- Kollbruner, C., Hajdin, N. and Stipanis, B. (1980) "Contribution to the analysis of cable-stayed bridges." *Institut Fuer Bauwissenschaftliche Forsch Publikation* (Switzerland), 48, 1-45.
- Kumarasena, T., et. al., (2005) "Wind-Induced Vibration of Stay Cables," Interim Final Report, FHWA RDT 05-004, RI 98-034.
- Lall, J. (1992). "Analytical modelling of the J.A. Roebling suspension bridge." A thesis submitted to the Department of Civil and Environmental Engineering, University of Cincinnati in partial fulfillment of the requirements for the degree of Master of Science.
- Lilen, J.L. and Pinto da Costa, A. (1994) "Amplitudes caused by parametric excitations on cable stayed structures." *Journal of Sound and Vibration*, 174(1), 64-90.
- Liu, P.L. (1995). "Identification and damage detection of trusses using modal data." *Journal of Structural Engineering*, ASCE, 121(4), 599-608.
- Ljung, L. (1987). *System identification: theory for the user*. Prentice-Hall Inc., Englewood Cliffs, New Jersey.
- Maia, N.M.M. and Silva, J.M.M. Edited. (1997). *Theoretical and experimental modal analysis*. Research Studies Press Ltd., England.
- Main, J.A. and Jones, N.P. (1999) "Full-scale measurements of stay cable vibration." *Proceedings of the 10th International Conference on Wind Engineering*, Copenhagen, Denmark.
- Main, J.A. and Jones, N.P. (2001) "Characterization of rain-wind induced stay-cable vibrations from full-scale measurements." *Proceedings of the Fourth International Symposium on Cable Dynamics*, Montreal, Canada, 235-242.
- Matsumoto, M., Shiraishi, N. and Shirato, H. (1992) "Rain-wind induced vibration of cables of cable stayed bridges." *J. Wind Engineering and Industrial Aerodynamics*, 2011-2022.
- Mazurek, D.F. and Dewolf, J.T. (1990). "Experimental study of bridge monitoring technique." *Journal of Structural Engineering*, ASCE, 116(9), 2532-2549.
- Nazmy, A.S. and Abdel-Ghaffar, A.M. (1990). "Three-dimensional nonlinear static analysis of cable-stayed bridges." *Computers and Structures*, 34(2), 257-271.

- Okauchi, I., Miyata, T., Tatsumi, M. and Sasaki, N. (1997). "Field vibration test of a long span cable-stayed bridge using large exciters." *Journal of Structural Engineering /Earthquake Engineering*, Tokyo, 14(1), 83-93.
- Peeters, B. and De Roeck, G. (2000). "Reference based stochastic subspace identification in civil engineering." *Inverse Problems in Engineering*, 8(1), 47-74.
- Peeters, B., et al. (2003) "Continuous monitoring of the Oresund Bridge: system and data analysis." *Proceedings of International Modal Analysis Conference*, Kissimmee, FL.
- Pinto da Costa, A., et. al. (1996) "Oscillations of bridge stay cables induced by periodic motions of deck and/or towers," *Journal of Engineering Mechanics*, 122(7), 613-622.
- Podolny, W. and Fleming, J.F. (1972). "History development of cable-stayed bridges." *J. Strut. Div.*, ASCE, 98(9), 2079-2095.
- Ren, W.X. (1999). "Ultimate behavior of long span cable-stayed bridges." *Journal of Bridge Engineering*, ASCE, 4(1), 30-37.
- Ren, W.X., Harik, I.E. and Blandford, G.E. (2001). *Structural evaluation of the John A. Roebling suspension bridge over the Ohio river*. Kentucky Transportation Center Research Report KTC- - . University of Kentucky, Lexington, Kentucky.
- Ren, W.X., Harik, I.E., Lenett, M. and Basehearh, T. (2001). "Modal properties of the Roebling suspension bridge – FEM modeling and ambient testing." *Proceedings of IMAC-XX: A Conference on Structural Dynamics*, Kissimmee, Florida, February 5-8, 1139-1145.
- Ren, W.X. and Obata, M. (1999). "Elastic-plastic seismic behavior of long span cable-stayed bridges." *Journal of Bridge Engineering*, ASCE, 4(3), 194-203.
- Ren, W.X., Shen, J.Y. and De Roeck, G. (2000c). "Structural Stiffness Matrix Identification with Maximum Likelihood Estimation Method." *Proceedings of IMAC-XVIII, the 18<sup>th</sup> International Modal Analysis Conference*, San Antonio, Texas, 418-423.
- Ren, W.X. and Chen, G. (2003) "Experimental modal analysis of bridge stay cables." *Proceedings of International Modal Analysis Conference*, Kissimmee, Florida.
- Salawu, O.S. (1997). "Detection of structural damage through changes in frequency: a review." *Engineering Structures*, 19(9), 718-723.
- Schrader, M.D. (1999) "Stay Cable Properties for vibration analysis model comparisons: Veterans Memorial and Maysville bridges." *Masters Thesis, University of Kentucky*.
- Smith, S.W. and Campbell, J.E. (2005), "Short-time record analysis for condition monitoring of bridge stay cables," *Proceedings of the 12<sup>th</sup> International Conference on Sound and Vibration*, Lisbon, Portugal.

- Smith, S.W. and Johnson, M.L. (1998) "Field test to determine frequencies of bridge stay cables." *Proceedings of the 17<sup>th</sup> International Modal Analysis Conference*, Kissimmee, Florida.
- Smith, S.W., Johnson, M.L. and Schrader, M.D. (2000) "Correlation of bridge stay cable models using short time record data." *Proceedings of the AIAA Dynamics Specialists Conference*, Atlanta, Georgia, USA.
- Smith, S.W. and Baker, J.R. (2001) "Toward simulating parametric response of bridge stay cables resulting from motion of the deck and tower." *Proceedings of the Fourth International Symposium on Cable Dynamics*, Montreal, Canada, 361-368.
- Smith, S.W. and Campbell, J.E. (2002) "Testing and model verification of the Maysville Kentucky bridge stay cables." *Proceedings of the International Modal Analysis Conference*, Los Angeles, California.
- Spyrakos, C.C., Kemp, E.L. and Venkatareddy, R. (1999). "Validated analysis of Wheeling suspension bridge." *Journal of Bridge Engineering*, ASCE, 4(1), 1-7.
- Stubbs, N., Sikorsky, C., Park, S., Choi, S. and Bolton, R. (1999). "A methodology to nondestructively evaluate the structural properties of bridges." *Proceedings of IMAC17, the 17th International Modal Analysis Conference*, 1260-1268, Kissimmee, Florida, USA.
- Van der Auweraer, H. and Hermans, L. (1999). "Structural modal identification from real operating conditions." *Sound and Vibration*, 33(1), 34-41.
- Van Overschee, P. and De Moor, B. (1996). *Subspace identification for linear systems: theory, implementation and applications*, Kluwer Academic Publishers, Dordrecht, Netherlands.
- West, H.H., Suhoski, J.E. and Geschwindner Jr., L.F. (1984). "Natural frequencies and modes of suspension bridges." *Journal of Structural Engineering*, ASCE, 110(10), 2471-2486.
- Wilson, J.C. and Gravelle, W. (1991). "Modeling of a cable-stayed bridge for dynamic analysis." *Earthquake Engineering and Structural Dynamics*, 20, 707-721.
- Wilson, J.C. and Liu, T. (1991). "Ambient vibration measurements on a cable-stayed bridge." *Earthquake Engineering and Structural Dynamics*, 20, 723-747.
- Xu, Y.L., Ko, J.M. and Zhang, W.S. (1997). "Vibration studies of Tsing Ma Suspension Bridge." *Journal of Bridge Engineering*, ASCE, 2, 149-156.
- Yang, F.H. and Fonder, G.A. (1998). "Dynamic response of cable-stayed bridges under moving loads." *Journal of Engineering Mechanics*, ASCE, 124(7), 741-747.

Yang, Y.B. and McGuire, W. (1986). "A stiffness matrix for geometric non-linear analysis." *Journal of Structural Engineering, ASCE*, 112(4), 853-877.

Yang, Y.B. and McGuire, W. (1986). "Joint rotations and geometric non-linear analysis." *Journal of Structural Engineering, ASCE*, 112(4), 879-905.

Yoshimura, T., Savage, M.G. and Tanaka, H. (1995) "Wind-induced vibrations of bridge stay cables." *Proceedings of the International Symposium on Cable Dynamics, A.I.M., Liege, Belgium*, 437-444.

Zhang, Q.W., Chang, T.Y.P. and Chang, C.C. (2001). "Finite-element model updating for the Kap Shui Mun cable-stayed bridge." *Journal of Bridge Engineering, ASCE*, 6(4), 285-293.

Zhu, L.D., Xiang, H.F. and Xu, Y.L. (2000). "Triple-girder model for modal analysis of cable-stayed bridges with warping effect." *Engineering Structures*, 22, 1313-1323.